2012

Laboratory Methods for the Advancement of Wastewater Treatment Modeling

Holly E. Gray
Wilfrid Laurier University, gray1010@mylaurier.ca

Laboratory Methods for the Advancement of Wastewater Treatment Modeling

Holly E. Gray

Bachelor of Science, Honours Biology and Chemistry, Wilfrid Laurier University, 2009

THESIS

submitted to the Department of Chemistry

in partial fulfillment of the requirements for

the degree of Master of Science

Wilfrid Laurier University

Waterloo, Ontario, Canada

Abstract

To achieve the low levels of total phosphorus required in wastewater treatment plant effluent all chemical forms of phosphorus should be removed. The most refractory phosphorus in terms of removal is so-called "organic phosphorus". This thesis explores potential relationships between dissolved organic matter and organic phosphorus and methods of removing organic phosphorus from waste water. This thesis also investigates current limitations of pH simulation in the wastewater treatment process. In order to optimize any type of nutrient removal pH simulation must be as advanced as the wastewater treatment technologies. This thesis is divided into three experimental sections; each section is discussed further below.

I

The first study in this thesis represents an effort to probe the relationship between organic phosphorus removal and the molecular nature of dissolved organic matter in wastewater. The results obtained by fluorescence characterization of dissolved organic matter (DOM) in 44 wastewater samples collected from 12 wastewater treatment plants and several different technologies are presented. Samples within treatment plants at various steps in the treatment process allow for the observation of the effects of treatment processes on DOM and phosphorus. PARAllel FACtor analysis (PARAFAC) was used to resolve the fluorescence spectra into three components. It was found that proteinaceous fluorophores, tyrosine (Tyr) and tryptophan (Trp), correlate well with nonreactive phosphorus (nRP) removal. The correlation between Trp, or Tyr, and nRP improved with use of biological treatment. The steepest correlation was determined to be between Trp and nRP for a plant using tertiary biological treatment (R^2=.810, r =.900, p<0.01).

Secondary biological treatment plants have a more moderate slope and a correlation coefficient R^2=0.642, p<0.01 for nRP and Trp. Humic substances (HS) fluorescence was found to have no correlation with nRP removal. It was found that as nRP decreased, HS fluorescence stays relatively the same. It is known that natural HS contain phosphorus; the inability to remove HS may represent a limit of technology on total phosphorus removal.

II

In hopes of achieving low level phosphorus in effluents, wastewater treatment plants are potentially interested in implementing advanced oxidative processes (AOPs) to break down non-reactive (or organic) phosphorus to reactive phosphorus which is easier to remove. Chapter 4 explores six wastewater treatment processes in hopes to discover methods of breaking down non-reactive phosphorus. These methods have been used in the past for wastewater disinfection but have never been tested for phosphorus removal. These treatments included AOPs hydrogen peroxide (H_2O_2), ultraviolet (UV) photolysis, ferrate (FeO_4^{2-}), ozone (O_3) and combined H_2O_2 and UV photolysis. Absorption chemistry was also investigated using activated carbon, which was discovered to be a source of phosphorus and thus not useful for nRP removal. Changes in non-reactive phosphorus were observed in all AOP treatments except ozone where no change occurred. When used separately, UV photolysis was found to decrease non-reactive phosphorus by approximately 26%. In the combined UV/H_2O_2 treatment, non-reactive phosphorus was decreased by 18%. Ferrate, the final AOP investigated in this study, was found to decrease total phosphorus by approximately 35%. With the exception of activated carbon, the different treatments investigated show promise of conversion of

non-reactive to reactive phosphorus. Ferrate treatment could be very useful due to it being a combination treatment, combining oxidation and chemical phosphorus precipitation.

III

The final chapter of this thesis focuses on the improvement of a pH prediction model for wastewater. Simulation of pH is very important for almost all wastewater treatment processes. Current modeling determines pH based on the concentrations of strong base cations, strong acid anions, weak acids and ammonia. This causes an underestimation of pH because the modeling does not take into account positively charged surface reactive sites in wastewater solids. The effect on proton concentration can be seen in the following rearranged electroneutrality equation: $[H^+] = \sum$[Strong acid anions] - $\sum$[Strong base cations] + $\sum$[Weak acid anions] - $\sum$**[positive surface sites]**. Characterization of the terms highlighted in bold could lead to the improvement of phosphorus removal modeling. Acid base titrations are an excellent method to probe surface reactivity in terms of proton binding affinities (pK_a) and capacities. For each type of reactive surface group, proton binding affinity and ionizable site concentrations are unique. Data obtained from acid-base titrations can be used to determine reactive site concentrations at certain pK_a values. This study uses linear programming to calculate reactive site concentrations at various pK_a values. A synthetic wastewater recipe was used since characterization of surface reactive sites would lead to an improvement in wastewater treatment modeling. High solid titration data agreed with the model after the addition of two positively charged surface reactive sites to the pH modeling. The first positively charged site had a pK_a of around 8 while the second site had a pK_a around

10.2. The pK_a value of 8 agreed with pK_as found for hydrous ferric oxides in literature as well as the pK_a spectra calculated using titration data and discrete site analysis for the high solids system.

Acknowledgements

First and foremost, I would like to thank my wonderful supervisor Dr. Scott Smith for the support and guidance that he has given me throughout my time working in his lab. Thank you for putting up with my inherent stubbornness and my blank stares. It has been a privilege to work under your supervision. Thank you to Dr. Lillian DeBruin, Dr. Vladimir Kitaev and Dr. Jim McGeer for graciously lending their time to be on my committee. Thank you for coming to my meetings, reading my thesis and for all your input.

I have to thank Rachael Diamond, for whom I have absolutely no words, Pedro Diogo, for being around some of the time and letting me be productive for the rest. Many thanks need to go to the many students in the Science Research Building; you have made the Research building an awesome place to be. Thank you members (past and present) of the Smith lab, you guys always made life interesting. A huge thank you to Ashtina Appadu, Amanda Johnston, Petrease Patton and Tara Tait, you guys always knew how to cheer me up when I needed it.

I would like to thank my parents for all the support they have given me over the last 27 years. I couldn't have done this without you. Thank you to my Fiji, the cat that could operate his own wastewater treatment plant.

Finally, I would like to thank the various funders of my projects: EnviroSim Associates Ltd., Water Environment Research Foundation (WERF), Trojan Technologies, Ferrate Treatment Technologies LLC and NSERC who help make this research possible.

Table of Contents

List of Abbreviations and Symbols

AHP – Acid Hydrolysable Phosphorus

ANC – Acid Neutralizing Capacity

ANOVA – ANalysis Of VAriance

AOP – Advanced Oxidative Process

BNR – Biological Nutrient Removal

C_{anc} – Acid Neutralizing Capacity Initial Concentration

C_a – Concentration of Acid

C_b – Concentration of Base

COD – Chemical Oxygen Demand

DIP – Dissolved Inorganic Phosphorus

DISI – Discrete Site Analysis

DOM – Dissolved Organic Matter

DOP – Dissolved Organic Phosphorus

EBPR – Enhanced Biological Phosphorus Removal

FEEM – Fluorescence Excitation Emission Matrix

HFO – Hydrous Ferric Oxide

HS – Humic Substances

K_a – Acid Dissociation Constant

LM – Luther Marsh Organic Matter Isolate

mtAHP – Measured Total Acid Hydrolysable Phosphorus

MWCO – Molecular Weight Cut Off

nRP – Non-reactive Phosphorus

OP – Organic Phosphorus

PAO – Phosphorus Accumulating Organism

PARAFAC – PARAlell FACtor Analysis

pK_a – Negative Log of the Acid Dissociation Constant

PWQO – Provincial Water Quality Objectives

RO – Reverse Osmosis

RP – Reactive Phosphorus

sAHP – Soluble Acid Hydrolysable Phosphorus

smAHP – Measured Soluble Acid Hydrolysable Phosphorus

snRP – Soluble Nonreactive Phosphorus

sRP – Soluble Reactive Phosphorus

sTP – Soluble Total Phosphorus

tAHP – Total Acid Hydrolysable Phosphorus

tnRP – Total Nonreactive Phosphorus

tOP – Total Organic Phosphorus

TP – Total Phosphorus

Trp – Tryptophan

tRP – Total Reactive Phosphorus

Tyr – Tyrosine

WWTP – Wastewater Treatment Plant

List of Figures

List of Tables

Chapter 1: Introduction

1.1 Phosphorus in the Environment

Addition of nutrients, such as phosphorus and nitrogen, to an aquatic system causes a response in algae and aquatic plant organisms to increase growth. This effect is called eutrophication (vanLoon and Duffy, 2000). Over time, nutrients and decaying organic matter enter the water system from the surrounding environment. With the supply of nutrients, algae and aquatic plants grow and use photosynthesis to convert carbon dioxide into sugars and generate oxygen (Love et al., 2010). Under natural conditions, algal growth is moderate and usually benefits aquatic biota. When excess nutrients are introduced from anthropogenic sources, the resulting algae and plant growth increases exponentially. As a result of such rapid growth, the bloom quickly uses up limiting nutrient supplies causing the algal bloom to die and begin to decompose (Spivakov et al., 1999). During the process of decomposition, dissolved oxygen is consumed and carbon dioxide is released into the water. The resulting anoxic, and slightly acidic, conditions are detrimental to the development of higher forms of aquatic life and causes reduced diversity in the water system (vanLoon and Duffy, 2000; Love et al., 2010).

Due to the threat of eutrophication, one of the major anthropogenic risks to water quality is municipal wastewater treatment plant (WWTP) discharge. Wastewater effluent is a point source for nutrients. The presence of phosphorus, an essential nutrient, aids in the growth of aquatic plant species. Phosphorus is the limiting nutrient in many freshwater and estuarine systems; concentrations exist in the lowest amount relative to the other nutrients an organism needs. Since the amount of phosphorus present in the

system often limits the extent of eutrophication, eutrophic conditions can be prevented by controlling the quantity of phosphorus in WWTP output (vanLoon and Duffy, 2000). Phosphorus concentration in wastewater effluent is highly regulated. However, in order to remove phosphorus from waste water effluent, the composition of phosphorus in waste water has to be understood.

1.2 Phosphorus in Waste Water

Total phosphorus (TP) in wastewater effluents is made up of dissolved and particulate phosphorus. The separation of total phosphorus into the dissolved and particulate phosphorus species is defined by the ability to pass through a membrane filter with an undefined pore size (often 0.2 or 0.45 μm). The fraction of total phosphorus which passes through the filter is operationally defined as dissolved phosphorus, while the remaining fraction is called particulate phosphorus (Spivakov, 1999). Figure 1.1 summarizes the breakdown of total phosphorus found in waste water. Particulate, or insoluble, phosphorus can be found adsorbed to particles or as part of amorphous and crystalline materials. Particulate phosphorus can be introduced into a system as a result of weathered materials, incorporated in biological mater or direct precipitation of inorganic phosphorus (Mayer and Woo, 1998).

The dissolved phosphorus fraction consists of a variety of phosphorus species including orthophosphate (PO_4^{3-}), inorganic condensed phosphates (such as pyrophosphate) and phosphorus which is bound covalently to organic matter (organic condensed and organic phosphorus) (Maher and Woo, 1998). Organic phosphorus species are species in which phosphate is bound to an organic molecule through an ester bond (Maher and Woo, 1998). This should not be confused with phosphorus that has been adsorbed non-

covalently to organic matter. The two important forms of phosphorus in wastewater are dissolved inorganic phosphorus (DIP) and dissolved organic phosphorus (DOP) (Dupuis et al., 2010).

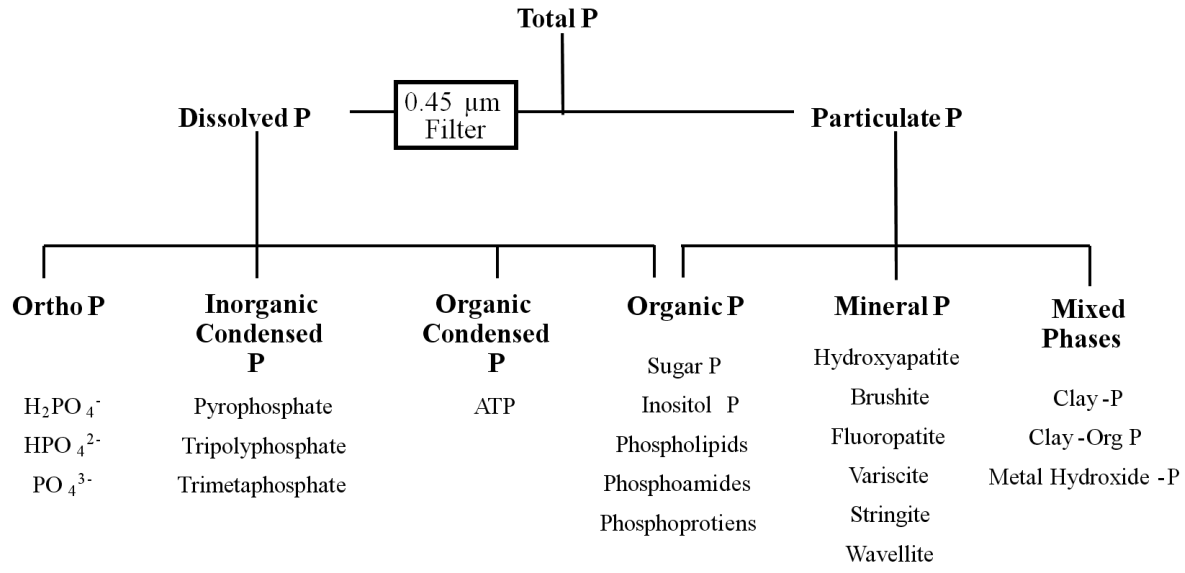

Figure 1.1: **Breakdown of total phosphorus in waste water and subsequent organization into subgroups (Maher and Woo, 1998).**

Dissolved inorganic phosphorus is found in various orthophosphate forms. Figure 1.2 illustrates orthophosphate in various protonated and deprotonated states. Around pH 1, the most prevalent species of orthophosphate is phosphoric acid, H_3PO_4 (magenta), while the dominant species of orthophosphate around pH 5 is $H_2PO_4^-$ (green). The last two species of orthophosphate, HPO_4^{2-} (blue) and PO_4^{3-} (red), are dominant around pH 10 and 13, respectively (Harris, 2007). The most prevalent orthophosphate species in freshwater systems, which typically have a pH lower than 8.2, is $H_2PO_4^-$ (Love et al., 2010). Dissolved organic phosphorus is a designation given to a diverse collection of phosphorus containing compounds. DOP groups in waste water include phosphonates,

phosphate mono- and diesters, orthophosphate and condensed phosphates (Maher and Woo, 1998; Love et al., 2010). When trying to achieve low phosphorus levels in wastewater effluent, DOP is important. This is because reactive phosphorus is easy to remove, and once reactive phosphorus has been removed DOP still remains in effluent. In order to achieve high levels of removal, focus must be placed on removing DOP from the wastewater.

The main contributing species to total phosphorus in municipal wastewater influents are organic and inorganic phosphorus. Inorganic phosphorus, typically in the form of orthophosphate, accounts for approximately 75% of total phosphorus concentrations (Love et al., 2010). While exact wastewater influent composition for individual treatment plants is unique, depending on location, season and service load, average phosphorus concentrations of the different species can be estimated. Love et al. (2010) identified inorganic phosphorus as the main soluble species in influent with concentrations ranging of 3 – 10 mg P/L. Particulate species, usually present in the form of organic phosphorus, were found to have concentrations in the range of 1 – 5 mg P/L. Organic phosphorus was also be found in influent in the soluble form; however, its contribution to total phosphorus concentration is very minor (Love et al., 2010).

As with wastewater influent, effluent composition depends on individual wastewater treatment plants and the different nutrient removal technologies in operation. Treatment plants which implement removal processes that do not use enhanced nutrient removal have typical effluent total phosphorus concentrations in the range of 1 – 5 mg P/L. When chemical removal is being used, either alone or in combination with enhanced removal, effluent concentrations can be lower than 0.01 mg P/L (Love et al., 2010).

Regulation of total phosphorus in effluent is dependent on the local policies implemented to protect the body of water in effect (Dupuis et al., 2010).

Individual wastewater treatment plants have different total phosphorus compliance limits dependent on incoming treatment volumes; however, there are specific guidelines for each province. The Ontario Provincial Water Quality Objectives (PWQO) has set a limit for total phosphorus entering streams and lakes from wastewater treatment. To protect surface water, total phosphorus effluent limits for streams are 30 µg/L while lakes have a limit of 20 µg/L in lakes (Ontario Ministry of the Environment, 1994). The protection of Canadian surface water is also largely dependent on U.S. water protection policies, especially due to the sharing of the Great Lakes Watershed. In 1978, the United States and Canada signed the Great Lakes Water Quality Agreement which was followed by the agreement of both countries to the Phosphorus Load Reduction Supplement in

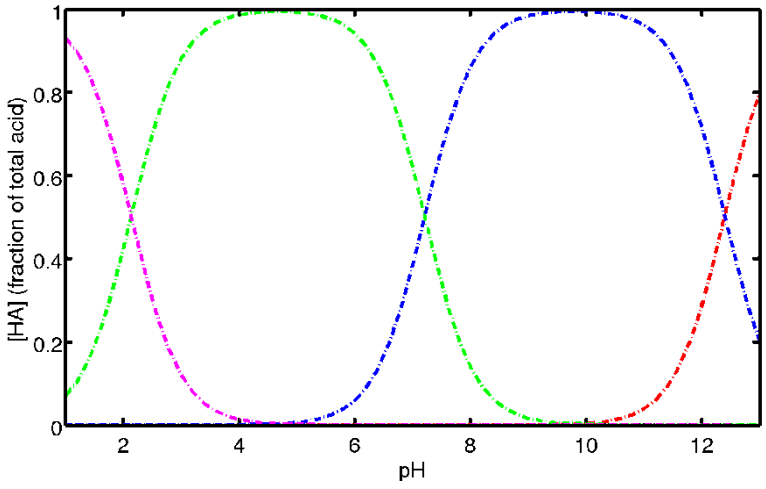

Figure 1.2: Distribution of orthophosphate over pH. Phosphoric acid (H_3PO_4) distribution is shown in magenta, $H_2PO_4^-$ is shown in green, HPO_4^{2-} is shown in blue and PO_4^{3-} is shown in red. The pk_as of for orthophosphate are 2.15, 7.20 and 12.33 for pK_{a1}, pK_{a2} and pK_{a3}, respectively.

1983. The agreement placed a total phosphorus discharge limit of 1.0 mg P/L for all municipal wastewater treatment plants discharging more than 3.8 ML/d (Dupuis et al., 2010). Monitoring and assessment of discharge into the Great Lakes is constant; assessment is constant due to further interest in forming reduced phosphorus loading goals (Dupuis et al., 2010).

1.3 Methods of Phosphorus Removal

While wastewater treatment plants utilize various technologies in the treatment process, most plants have the same series of steps. A basic overview of the steps of wastewater treatment is shown in Figure 1.3. In brief, a WWTP combines preliminary treatment with primary, secondary and tertiary clarification, and then finishes the process with disinfection. To prevent damage to equipment down the line, preliminary treatment removes large grit and solids prior to the water entering the primaries. During primary treatment the larger particles settle and move to sludge digesters. Scum is also removed from the surface. In the secondary stages, an activated sludge is formed through aeration. The biologically activated sludge makes use of the natural behavior of microorganisms to disinfect the water (Hammer and Hammer, 2001). The remaining sludge from primary and secondary treatment processes is removed to landfill. Tertiary treatment, also referred to as advanced treatment, is a broad term used for any treatment process following the primary and secondary process. Frequently, tertiary treatment employs various methods to remove contaminants in the particulate form. After tertiary treatment, the wastewater passes through a disinfection stage. Once disinfection is complete, effluent is released through output into the receiving water (Hammer and Hammer, 2001).

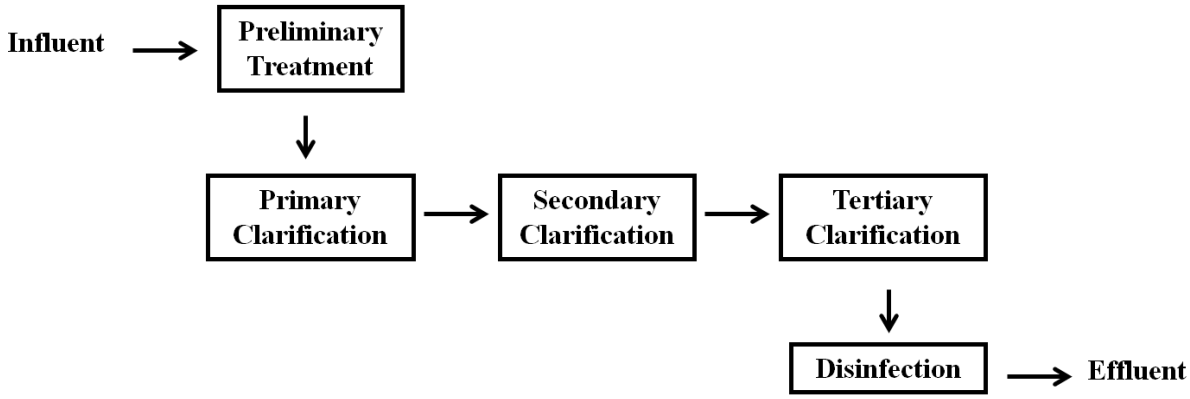

Figure 1.3: **Generalized flow chart of the wastewater treatment process.**

One of the goals of all wastewater treatment plants is to utilize various technologies to remove nutrients from wastewater. Wastewater treatment plants must implement technologies which effectively remove nutrients from effluent to meet the regulated daily limits unique to each wastewater treatment plant. Phosphorus removal is influenced by the chemical characteristics of water. Treatment technologies used to date have a combination of physical, biological and/or chemical removal to achieve low levels of phosphorus in wastewater effluent. However, phosphorus removal has mostly targeted the reactive phosphorus fraction (i.e. orthophosphate) of wastewater, and modern technologies have reached low level total phosphorus goals of 0.1-0.3mg P/L (Neethling et al., 2005; Gu et al., 2008; Drury et al., 2005). The following sub-sections describe the three removal processes in detail.

1.3.1 Physical Phosphorus Removal

As mentioned previously, physical removal leads to the removal of contaminants due to physical size. Processes such as sedimentation or filtration are used individually or in combination with other physical processes. Sedimentation is the process of particulate

contaminants settling out of solution based on the effects of gravity while filtration is the process of liquid passing through a membrane while solids which cannot pass the membrane are retained. In filtration, the amount of solids that is retained depends of the pore size of the filter.

A relatively new wastewater treatment technology is the use of nano filtration. Nano filtration removes contaminants from wastewater at molecular level (Neethling et al., 2010). An example of a nano process is reverse osmosis. Reverse osmosis (RO) uses pressure to force water through a membrane filter with a pore size of approximately 10^{-4} microns, just slightly larger than a water molecule (Abdel-Jawad et al., 2002). The permeate, water that passes through the filter, has very low levels of phosphorus. The contaminants that do not pass the membrane are concentrated into a separate waste stream, called the concentrate or brine. The RO concentrate is high in nutrients and often needs to be treated; this is discussed further in Chapter 4. Nano treatments are very costly; however, they have recently come into the spotlight due to their ability to remove nutrients to levels much lower than conventional nutrient removal technologies (Neethling et al., 2010).

1.3.2 Chemical Phosphorus Removal

Chemically mediated phosphorus removal is necessary in the wastewater treatment process to achieve the lowest levels of phosphorus in treatment effluent. Chemical removal targets the reactive phosphorus (i.e. orthophosphate) in wastewater through the addition of metal salts which precipitate phosphorus. Typical metal salts used in the removal process are lime ($Ca(OH)_2$), alum ($Al_2(SO_4)_3 \cdot 18H_2O$) or ferric chloride ($FeCl_3$) (Sedlak, 1991). Addition of Fe^{3+} to wastewater leads to the formation of hydrous

ferric oxide (HFO) precipitates which result from the neutralization of acidic ferric iron solution and alkaline wastewater (Smith et al., 2008). Once the process is complete, these precipitates are removed by sedimentation or filtration and taken to landfill.

The mechanism of phosphorus removal can occur though several pathways. Phosphorus can be removed through precipitation of ferric or mixed cation phosphates. Phosphorus can also be removed through adsorption of phosphates to the HFO surface or through co-precipitation of phosphate into the HFO structure. In this case, the term co-precipitate refers to when a component that is normally soluble precipitates with a macromolecule out of solution because of the formation of mixed crystals, adsorption, occlusion or mechanical entrapment. This definition of co-precipitation is from the International Union of Pure and Applied Chemistry (IUPAC) (McNaught and Wilkinson, 1997).

Surface complexation is the term used to describe adsorption of anions to hydroxylated surfaces (Altundoğan and Tümen, 2001). When the surface is positively charged, anions can adsorb creating inner and outer sphere surface complexes. This occurs in chemical wastewater removal when the phosphate ion absorbs to HFO precipitate surfaces. Outer sphere complexes form from the interaction between ion pairs, while inner sphere complexes form through chemical bonding. Inner sphere complexes can form in a monodentate or bidentate complexes (Figure 1.4).

In monodentate bonding, a single bond forms between the phosphate and surface, while bidentate bonding forms two covalent bonds between the phosphate and the surface. These two bonds make the bidentate complex stronger than the monodentate

complex. Binding of phosphate to the HFO surface is through the arrangement Fe-O-P. This arrangement is the result of the surface hydroxyl oxygen being replaced with the phosphate oxygen (Li and Stanforth, 2000). With filtration, total phosphorus concentrations of less than 0.1 mg P/L can be achieved consistently using chemical phosphorus removal (Neethling et al., 2010).

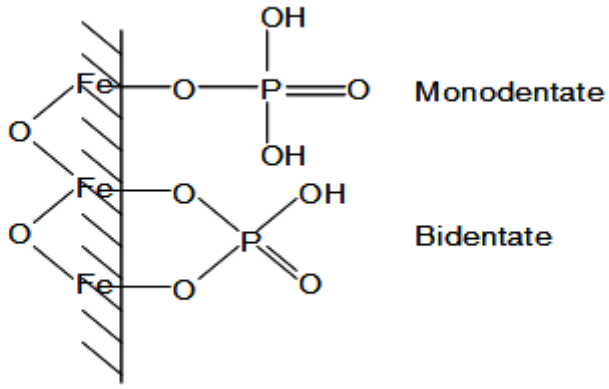

Figure 1.4: Monodentate and bidentate inner sphere complexes formed between phosphate and the HFO surface (adapted from Blaney et al., 2007).

1.3.3 Biological Phosphorus Removal

Biological removal of polyphosphates uses the phosphorus storing capabilities of certain microorganisms called polyphosphate accumulating organisms (PAOs). Under aerobic conditions, PAOs microorganisms store phosphorus in their cells. The biomass, under aerobic conditions contains phosphorus and called activated sludge (Neethling et al., 2010). An example of a PAO is *Accumulibacter phosphatis* (Sedlak, 1991). Once biological removal is complete, the activated sludge is removed. On average, the biomass has a percent phosphorus composition of 1.5 to 2% dry weight after phosphorus removal. Enhanced biological phosphorus removal (EBPR) increases phosphorus uptake by

cycling PAOs between an anaerobic carbon-rich and an aerobic environments (Neethling et al., 2010).

In a carbon-rich environment, PAOs store carbon (in different forms including volatile fatty acids) internally under anaerobic conditions. These carbon stores are required for cell growth, the more carbon stored, the larger the cell will grow. Phosphorus uptake occurs as PAOs grow. The larger the growth cycle, the more phosphorus is taken into the PAOs (Neethling et al., 2010). Under anaerobic conditions, phosphorus release from the PAOs is paired with the carbon uptake. This increases the soluble phosphorus present in the wastewater. However, by cycling between the anaerobic and aerobic conditions, phosphorus uptake by the biomass is drastically increased. The percent phosphorus composition of the activated sludge after EBPR is in the range of 20 to 30% dry weight (Metcalf and Eddy, 2003).

1.4 Quaternary Treatment: Implementing Advanced Oxidative Processes?

Due to an increasing demand on wastewater treatment plants to reach targets of less than 5-10 µg P/L effluent total phosphorus, a need has arisen to remove the most refractory portions of total phosphorus in wastewater. Chemical removal reaches the lowest levels of total phosphorus due to its focus on the removal of reactive phosphorus species. However to achieve extremely low total phosphorus levels, the refractory phosphorus fraction needs to be removed as well (Lancaster et al., 2008). A study by Lancaster et al. (2008) showed that condensed and organic phosphorus had a major impact on the effluent total phosphate. As mentioned above, reverse osmosis has become a popular choice for quaternary treatment. However, due to high phosphorus concentration, the RO brine needs to be treated. An advanced oxidative process (AOP)

uses oxidative degradation to break down dissolved organic compounds in aqueous environments (Legrini et al., 1993). These methods are attractive in hopes that they target the organic phosphorus fraction in wastewater. Several examples are ultraviolet (UV) light, ozone (O_3), hydrogen peroxide (H_2O_2) and ferrate (FeO_4^{2-}).

UV photolysis and H_2O_2 are AOPs in which radicals are generated by either photolysis or reaction with hydroxyl radicals (Legrini et al., 1993). Ozone, another AOP, is a highly reactive species that can react to oxidize bonds on contact. Ozone reacts with most species which contain pi bonds. These bonds can include the carbon to carbon double bond, or the carbon to nitrogen double bond (Gogate and Pandit, 2004). Ferrate has become an attractive AOP for wastewater treatment (Sharma, 2004). Once reduced, ferrate generates Fe (III) ions which act as a coagulant, removing contaminants through adsorption onto aggregates which are filtered using sedimentation and filtration technologies (Jiang et al., 2006). Also, addition of Fe (III) results in the precipitation of hydrous ferric oxide (HFO) which removes reactive phosphorus through surface complexation of the phosphorus to the HFO surface (Smith et al., 2008).

Combined AOPs have also been proposed as effective wastewater treatments due to the idea that two AOPs will work better together than the individual AOPs. Combining UV photolysis with H_2O_2 leads to the increased the rate of the generation of free radicals from H_2O_2 (Gogate and Pandit, 2004). Combination AOPs are popular in wastewater treatment and are used to remove several types of organic contaminants.

1.5 pH Simulation Modeling in Wastewater Treatment

Creating a model, or simulation, of the various processes in nutrient removal has become a very important step in the design and optimization of a wastewater treatment plant. Simulation of a wastewater treatment process, for example chemically mediated phosphorus removal, can help to determine ideal ferric dosage, the best level of mixing or the pH of the system. Simulation of pH is very important for almost all wastewater treatment processes. In biological removal, pH affects the biological activity of the microorganisms which have an optimal pH range. Outside of this pH range, biological activities are severely limited and may lead to microbe death (Takács et al., 2010). In chemical removal, pH affects the rates of chemical precipitation reactions; optimal pH values for phosphorus removal is in the range from 3 - 5 (Fairlamb et al., 2003; Neethling et al., 2010).

In the past, changes in alkalinity, the difference between the concentrations of strong anions and strong cations, were used as a gauge of potential problems with pH stability. This was because of the difficulty of simulating pH directly because of the complexity of the underlying reactions and constituents (Fairlamb et al., 2003). Using alkalinity to predict pH has several disadvantages. One disadvantage is that this method makes the assumption that pH in a range where it does not affect biological activity and that pH stays relatively constant. The second disadvantage is that precipitation and chemical reactions cannot be modeled using alkalinity (Takács et al., 2010). Due to these limitations, pH simulation has been the focus of several studies. One of the most applicable models was developed by Fairlamb et al. (2003) for use in the wastewater treatment processes. The model takes into account equilibrium modeling of the major

wastewater species, activity coefficients corrected for ionic strength, gas-liquid transfer and it includes compounds which effect biological activity.

1.6 Research Goals and Objectives

The objectives of this research are summarized in the following list.

1. To develop a "fingerprinting" technique to characterize dissolved organic matter in wastewater across wastewater treatment plants and their different treatment technologies.

2. To relate dissolved organic matter to phosphorus removal and phosphorus speciation.

3. To test advanced wastewater treatment methods for conversion from non-reactive to reactive phosphorus and/or decreased total phosphorus.

4. To test a pH prediction model based on electroneutrality for a simple synthetic wastewater.

5. To test the impacts of solids on pH prediction of the pH model based on electroneutrality.

6. If necessary, develop revised pH prediction model that will take the solids surface reactive sites into account.

The first two objectives of this thesis will be addressed in Chapter 3: Molecular variability in wastewater organic matter and implications for phosphorus removal across a range of treatment technologies. In this chapter fluorescence spectroscopy will be used

to characterize dissolved organic matter in wastewater. The fluorescent DOM will then be monitored throughout the various wastewater treatment plants to investigate any changes throughout the treatment train. Finally, correlations between fluorophore concentrations (concentrations determined for the different classifications of fluorescent DOM) and non-reactive phosphorus will be examined in hopes to discover implications for phosphorus removal.

Objective three is the main goal of Chapter 4: Screening of bench top wastewater treatment technologies for phosphorus removal. Chapter 4 looks into preexisting wastewater treatments for a cost effective and efficient method to breakdown refractory (organic) phosphorus. The chapter examines adsorption chemistry through the use of activated carbon and explores five different AOPs; hydrogen peroxide, ultraviolet photolysis, the combination of H_2O_2 and photolysis, ozone and ferrate.

The final three objectives are the focus of Chapter 5: Characterization of surface reactive sites in high solids synthetic wastewater and implications for pH simulation. Chapter 5 uses acid-base titrations to characterize both particulate (surface) and dissolved ionizable sites. The derived pKa spectra will allow for further molecular level discrimination between potential phosphorus reactivity at treatment plants as well as between processes within a given plant. Results obtained from synthetic wastewater surface characterization may lead to the improvement of phosphorus removal modeling and better pH prediction.

The findings of these three chapters and any thoughts of future exploration in these areas will be summarized in Chapter 6: Conclusions and Future Work.

Supplementary information can be found in the attached Appendices. Appendix A contains a table of the summarized statistical results for Chapter 1. Appendix B includes the MATLAB scripts used for pH simulations and calculation of reactive site concentrations for the data in Chapter 3. Fluorescence measurements were made on various samples and resulting PARAFAC data analysis contributed to the article. Appendix C describes the molecular weight cut off filter experiments that were completed to determine which molecular weight fraction contained nRP; these experiments were stopped due to phosphorus contamination of the centrifuge spin filters. Appendix D, uses a simple system to describe how to solve for total $[H^+]$; this appendix is supplementary information for Chapter 5. Appendix E contains the supplementary information and data which contributed to the journal in the final appendix, Appendix F, "Algal Uptake of Hydrophobic and Hydrophilic Dissolved Organic Nitrogen in Effluent from Biological Nutrient Removal Municipal Wastewater Treatment Systems" written by Haizhou Liu, Joonseon Jeong, Holly Gray, Scott Smith and David L. Sedlak and published in 2012, in Environmental Science and Technology.

1.7 REFERENCES

Abdel-Jawad, M., Al-Shammari, S. and Al-Sulaimi, J. (2002) Non-conventional treatment of treated municipal wastewater for reverse osmosis. *Desalination* **142**, 11-18.

Altundoğan, S.H., and Tümen, F. (2001). Removal of phosphates from aqueous solutions by using bauxite. 1: Effect of pH on the adsorption of various phosphates. *Journal of Chemical Technology and Biotechnology*, **77**, 77-85.

Blaney, L.M., Cinar, S., and SenGupta, A.K. (2007). Hybrind anion exchanger for trace phosphate removal from water and wastewater. *Water Research*, **41**, 1603-1613.

Drury, D.D., Shepherd, W. and B. Narayanan (2005). Phosphorus – How Low Can You Go?, *Proceedings Water Environment Federation 78th Annual Conference and Exposition*, Washington, DC, November 2005, 3454 – 3465.

Dupuis, T. and Jamesson, G. (2010). Regulation of Nutrients in the Effluents of Wastewater Treatment Plants. In *Nutrient Removal: WEF Manual of Practice No. 34.*; Water Environment Federation® (2010). WEF Press. Alexandria, VA.

Fairlamb, M., Jones, R., Takács, I. and Bye, C. (2003). Formulation of a general model for simulation of pH in wastewater treatment processes. In Conference proceedings, *76th annual water environmental federation technical exhibit and conference*, Los Angeles, CA, USA. Water Environment Federation: Alexandria, VA.

Gogate, P. R. and Pandit, A. B. (2004) A review of imperative technologies for wastewater treatement II: hybrid methods. *Advances in Environmental Research* **8**, 553-597.

Gu, A., J. Neethling, M. Benisch, D. Clark, D. Fisher, and H. S. Fredrickson (2007, October). Advanced phosphorus removal from membrane filtrate and filter filtrate using packed columns with different adsorptive media. In Conference proceedings, *80th annual water environmental federation technical exhibit and conference*, Baltimore, MD, USA, pp. 7899–7914. Water Environment Federation: Alexandra, VA.

Hammer, M. J. L., Hammer, M. J. J., 2001. Water and wastewater technology, 4th Edition. Prentice Hall, Upper Saddle River, New Jersey, USA.

Jiang, J., Wang, S., and Panagoulopoulos, A. (2006) The exploration of potassium ferrate(VI) as a disinfectant/coagulant in water and wastewater treatment. *Chemosphere* **63**, 212-219.

Katsoyiannis, A. and Samara, C. (2007) The fate of dissolved organic carbon (DOC) in the wastewater treatment process and its importance in the removal of wastewater contaminants. *Env. Sci. Pollut. Res*. **14** 284-292.

Lancaster, C. D. and J. E. Madden (2008, October). Not so fast! The impact of recalcitrant phosphorus on the ability to meet low phosphorus limits. In Conference proceedings, 81st annual water environmental federation technical exhibit and conference, Chicago, Chicago, IL, USA, pp. 3531–3544. Water Environment Federation: WEF.

Li, L., and Stanforth, R. (2000). Distinguishing adsorption and surface precipitation on phosphate and goethite (α-FeOOH). *Journal of Colloid and Interface Science*, **230**, 12-21.

Legrini, O., Oliveros, E. and Braun, A. M. (1993) Photochemical Processes for Water Treatment. *Chem. Rev.* **93**, 671-698.

Love, N., Bronk, D. A. and Mulholland, M. R. (2010). Nutrients and Their Effects on the Environment. In *Nutrient Removal: WEF Manual of Practice No. 34.*; Water Environment Federation® (2010). WEF Press. Alexandria, VA.

Maher, W., and Woo, L. (1998). Procedures for the storage and digestion of natural waters for the determination of filterable reactive phosphorus, total filterable phosphorus and total
phosphorus. *Analytica Chimica Acta*, **375**, 5-47.

McNaught, A. D. and Wilkinson, A. (1997) IUPAC Compendium of Chemical Technology; Blackwell Science: Oxford, United Kingdom.

Metcalf and Eddy, Inc. (2003) Wastewater Engineering: Treatment and Reuse, 4th ed.; Tchobanoglous, G.; Burton, H. L.; Stensel, H. D., Eds.; McGraw Hill: New York.

Neethling, J. B., M. Benisch, D. Clark, D. Fisher, and A. Z. Gu (2007, October). Phosphorus speciation provides direction to produce 10 μg/l. In Conference proceedings, 80th annual water environmental federation technical exhibit and conference, San Diego, California, USA, pp. 1607–1624. Water Environment Federation: WEF.

Ontario Ministry of the Environment (1994) Water management: policies, guidelines, provincial water quality objectives of the Ministry of the Environment: Appendix A.

Sharma, V. K. (2004) Use of iron(VI) and iron(V) in water and wastewater treatment. *Water Science and Technology* **49**, 69-74.

Sedlak, R. I., (1991) Phosphorus and Nitrogen Removal from Municipal Wastewater: Principles and Practice, 2nd Edition, Lewis Publishers, New York. 229 pages.

Smith, D. S., I. Takács, S. Murthy, G. Diagger, and A. Szabó (2008). Phosphate complexation model and its implications for chemical phosphorus removal. *Water Environment Research* **80**, 428–438.

Spivakov, B., Maryutina, T., & Muntau, H. (1999). Phosphorus Speciation In Water And Sediments. *Pure Applied Chem* , **71**, 2161-2176.

Takács, I., Belia, E., Boltz, J. P., Comeau, Y., Dold, P., Jones, R., Morgenroth, E., Schraa, O., Shaw, A. and Wett, B. (2010) Structured Process Models for Nutrient Removal. In *Nutrient Removal: WEF Manual of Practice No. 34.*; Water Environment Federation® (2010). WEF Press. Alexandria, VA.

vanLoon, G. W. and Duffy, S. J. (2000). *Environmental chemistry a global perspective*. New York, NY: Oxford University Press.

Chapter 2: Colorimetric Determination of Phosphorus

2.1 Standard Methods

The Standard Methods for the Examination of Water and Wastewater (1998) includes many analytical techniques used in the assessment of water quality. Standard Methods divides phosphorus into various fractions through different analytical techniques; these different fractions are divided in a way so they can be interpreted for practical use. The analytically defined phosphorus speciation is described further in Section 2.2. The method used in this thesis, specifically in Chapter 3 and Chapter 4, is the ascorbic acid method for the colorimetric determination of phosphorus. The ascorbic acid method, acid hydrolysis and the persulfate digestion for total phosphorus are described below.

2.2 Phosphorus Speciation

Through use of different digestion methods, total phosphorus can be divided further into analytically defined fractions. These fractions, and the methods used to isolate them, are presented in Figure 2.1. Through an ammonium persulfate digestion method of the filtered and unfiltered fractions, total phosphorus (TP) and total dissolved phosphorus (sTP) can be measured. For soluble and particulate phosphorus, fractions also include acid hydrolysable phosphorus (i.e. condensed phosphorus), reactive phosphorus (i.e. orthophosphate) and nonreactive phosphorus (nRP); fractions shown in Figure 1.1. Nonreactive phosphorus, the difference between total phosphorus and reactive phosphorus, is made up of several phosphorus species (including organic phosphorus) (Gu et al., 2007). In this study, colorimetric phosphorus determination and phosphorus

speciation methods from Standard Methods (4500P-E.) are used on the various fractions to measure soluble reactive phosphorus (sRP), soluble total phosphorus (sTP) and soluble nonreactive phosphorus (snRP) can be determined.

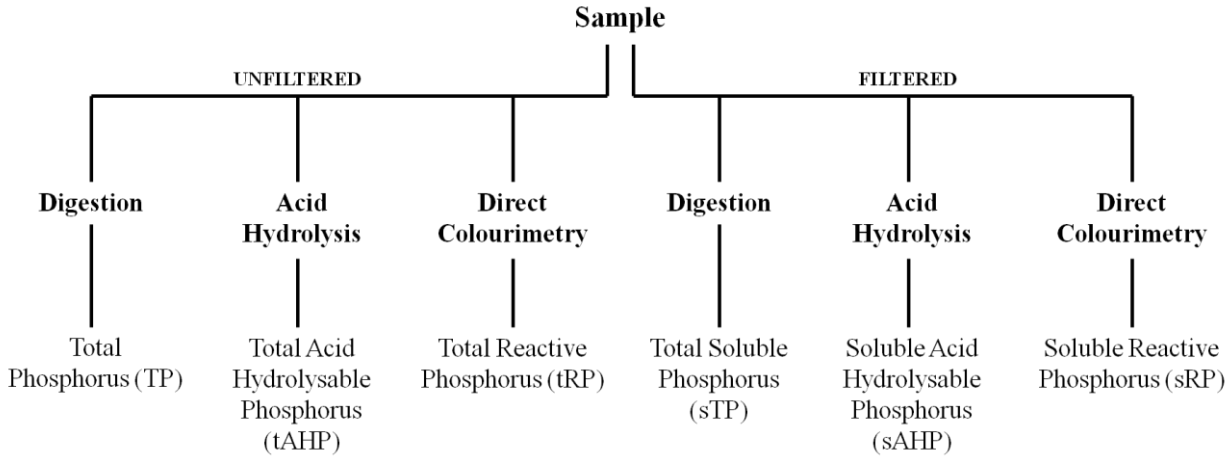

Figure 2.1: **Various phosphorus fractions determined by different analytical methods.**

2.2.1 Persulfate Digestion for Total Phosphorus

Ammonium persulfate ($(NH_4)_2S_2O_8$) is used along with sulfuric acid to oxidize organic and condensed phosphorus compounds in a sample and liberate reactive phosphorus. As described by the Standard Methods, a total phosphorus digestion of a 5mL sample is completed by adding 40mg of ammonium persulfate and 200µL of 11N H_2SO_4. The sample is then heated using a HACH DRB200 digital reactor block digestor (Loveland, Colorado) for 60 minutes at 105°C. After digestion, the sample is cooled to room temperature and 10µL of phenolphthalein indicator is added. The solution is then neutralized to a very faint pink by adding 1N NaOH dropwise into the sample. After

neutralization, the sample is diluted to 10mL and is ready for the addition of mixed reagent and colorimetric determination of phosphorus (see below).

2.2.2 Strong Acid Digestion for Acid Hydrolysable Phosphorus

Acid and heat are combined to break bonds between condensed phosphorus compounds there by liberating reactive phosphorus. The strong acid digestion used in this study followed the Standard Methods for the Examination of Water and Wastewater (1998). An addition of 200µL of a strong acid solution is added to a 5mL sample and followed by heating the sample at 105°C for 90 minutes using a HACH reactor block digestor. The strong acid solution is a 1L solution consisting of 300mL 98% sulfuric acid and 4mL concentrated HNO_3. After digestion, the sample is cooled to room temperature and 10µL of phenolphthalein indicator is added. The sample is then neutralized to a faint pink by the drop wise addition of 1N NaOH. The sample is then diluted to 10mL and is ready for the addition of mixed reagent.

2.3 Colorimetric Determination of Phosphorus Speciation

Colorimetric determination of phosphorus is a method which measures orthophosphate concentration using UV/Vis spectroscopy according to the Beer-Lambert law. Shown in Equation (2.1) the Beer-Lambert's law states that the concentration (c) of orthophosphate is proportional to the measured absorbance (A) of a coloured complex.

$$A = \varepsilon bc \tag{2.1}$$

In the equation, ε is the molar absorptivity ($M^{-1}cm^{-1}$) and b is the path length (cm) (Harris, 2007). In the ascorbic acid method, phosphoric acid reacts with ammonium molybdate and the resulting complex is reduced using ascorbic acid to produce a

coloured species whose absorbance we can measure, molybdenum blue. The absorbance of molybdenum blue can be measured at 650 to 880nm (Gilmore et al, 2008).

Absorbance was measured using an Ocean Optics (Sarasota, FL, USA) fiber optic spectrometer equipped with a Tungsten Halogen light source (Ocean Optics LS-1) and an Ocean Optics USB2000 detector unit. Samples were measured in a 10 cm path length quartz cuvette at 649.93 nm. Light intensity was recorded for each replicate and absorbance was calculated using equation 2.2.

$$A = -\log\left(\frac{I}{I_o}\right) \tag{2.2}$$

In the above equation A is absorbance, I is the light intensity measured from the sample and I_o is the light intensity measured from the blank standard. A calibration curve was plotted using the absorbance measured for each calibration standard. Concentrations of each sample were calculated using the equation of the line fit to the calibration standards.

Calibration standards were made daily from a secondary standard of 25 mg P/L which was prepared from a 1000 mg P/L standard solution made using $Na_3PO_4 \bullet 12H_2O$ (Fisher Scientific, New Jersey, USA). Three or four calibration standards were prepared in triplicate for the 10 cm path length. Standard concentrations included 0.010 mg P/L, 0.025 mg P/L, 0.050 mg P/L and 0.100 mg P/L. Blank standards, with a phosphorus concentration of 0.000 mg P/L, were prepared using ultrapure water (18.2MΩ, MilliQ). Samples and calibration standards were measured in triplicate.

2.4 Mixed Reagent

Mixed reagent recipe and the colour development method were taken from Standard Methods for Examination of Water and Wastewater (1998). The ascorbic acid method for phosphorus determination was used (4500P-E, 1998). The mixed reagent was a combination of sulfuric acid (H_2SO_4) (95-98% pure, Sigma Aldrich, St. Louis, MO, USA), ascorbic acid (99% pure, Sigma Aldrich, St. Louis, MO, USA), ammonium molybdate ($(NH_4)_6Mo_7O_{24}•4H_2O$, Fluka, Germany) and potassium antimonyl tartrate ($K(SbO)C_4H_4O_6•1/2H_2O$, 99% pure, Sigma Aldrich, St. Louis, MO, USA) . To prepare a 50 mL volume of mixed reagent, 25 mL 5N H_2SO_4 would be added to 2.5 mL of potassium antimonyl tartrate and 7.5 mL ammonium molybdate. The solution was then diluted to 50 mL with 0.1M ascorbic acid.

Upon addition of the mixed reagent, phosphomolybdic acid is formed by the presence of potassium antimonyl tartrate and ammonium molybdate with phosphoric acid. Phopshomolybdic acid is then reduced by ascorbic acid leading to the molybdenum blue complex. The sample is allowed to rest for 30 minutes for colour development and absorbance is measured at 650 or 830nm.

2.3 REFERENCES

Gilmore, R. L., Goertzen, S., Murphy, S., Takacs, I, and Smith, D.S. (2008) Chemically mediated phosphorus removal: Optimization of analytical methods. In Conference proceedings, the 81st annual water environmental federation technical exhibit and conference, Chicago, IL, USA, pp. 3756 – 3774. Water Environment Federation: Alexandria, VA.

Gu, A., J. Neethling, M. Benisch, D. Clark, D. Fisher, and H. S. Fredrickson (2007, October). Advanced phosphorus removal from membrane filtrate and filter filtrate using packed columns with different adsorptive media. In Conference proceedings, 80th annual water environmental federation technical exhibit and conference, Baltimore, MD, USA, pp. 7899–7914. Water Environment Federation: Alexandria, VA.

Standard Methods for the Examination of Water and Wastewater. (1998). (20th ed.). American Public Health Association (APHA) and American Water Works Association (AWWA) and Water Environment Federation (WEF); Washington D.C., USA.

Chapter 3: Molecular variability in wastewater organic matter and implications for phosphorus removal across a range of treatment technologies

3.1 ABSTRACT

To achieve the low levels of total phosphorus required in wastewater treatment plant effluent all chemical forms of phosphorus should be removed. The most refractory phosphorus in terms of removal is so-called "organic phosphorus". This study represents an effort to probe the relationship between organic phosphorus removal and the molecular nature of dissolved organic matter in wastewater. The results obtained by fluorescence characterization of dissolved organic matter (DOM) in 44 wastewater samples are presented. The samples were collected from 12 wastewater treatment plants and several different technologies, across the United States. Samples within treatment plants at various steps in the treatment process allow the observation of the effects of treatment processes on DOM and phosphorus. PARAllel FACtor analysis (PARAFAC) was used to resolve the fluorescence spectra into three components. Overall, wastewater DOM is highly variable, with variations due to source, as well as within each treatment plant. It was found that proteinaceous fluorophores, tyrosine (Tyr) and tryptophan (Trp), correlate well with nonreactive phosphorus (nRP) removal. The correlation between Trp, or Tyr, and nRP improved with use of biological treatment. The steepest correlation was determined to be between Trp and nRP for a plant using tertiary biological treatment (R^2=.810, r =.900, p<0.01). Secondary biological treatment plants have a more moderate slope and a correlation coefficient R^2=0.642, p<0.01 for nRP and Trp. Humic substances (HS) fluorescence was found to have no correlation with nRP removal. It was found that

as nRP decreased, HS fluorescence stays relatively the same. It is known that natural HS contain phosphorus; the inability to remove HS may represent a limit of technology on total phosphorus removal.

KEYWORDS

Wastewater Treatment, Fluorescence Spectroscopy, Dissolved Organic Matter

3.2 INTRODUCTION

Phosphorus removal is influenced by the chemical characteristics of waste water. Many different treatment technologies have been put into place to achieve low levels of phosphorus in wastewater effluent. To date, phosphorus removal has mostly targeted the reactive phosphorus fraction (i.e. orthophosphate) of wastewater, and modern technologies have reached low level total phosphorus goals of 0.1-0.3mg P/L (Neethling et al., 2007). Due to an increasing demand on wastewater treatment plants to reach targets of less than 5-10 µg P/L effluent total phosphorus, questions have formed surrounding the composition of wastewater effluents and tertiary treatment. In particular, the effect of wastewater composition on phosphorus removal has come into focus. In order to understand the relationship between organic matter and phosphorus removal, the composition of effluent total phosphorus must be better understood. The molecular nature of organic material in the wastewater stream may influence removal efficiencies. Phosphorus removal could be organic matter dependent in biological treatment because organic matter of different molecular structure would have different degrees of utility to microorganisms. In chemically mediated treatment, phosphates are removed after binding to hydrous metal (iron or alum) oxide particles but organic matter can potentially

occupy surface reactive sites where phosphates would also interact (Smith et al., 2008). The degree of particle - organic matter interactions depend on the molecular structure of the organic matter. Thus, variations in organic matter molecular structure can influence P removal efficiencies across a range of biological and chemical treatment technologies.

Total phosphorus in wastewater effluents is made up of dissolved and particulate phosphorus. The total phosphorus fraction which passes through a 0.45µm membrane filter is defined as dissolved phosphorus, while the remaining fraction is bound to particulate matter and thus called particulate phosphorus (Spivakov, 1999). The dissolved phosphorus fraction consists of a variety of phosphorus species including orthophosphate (PO_4^{3-}), inorganic condensed phosphates and phosphorus which is bound covalently to organic matter (organic condensed and organic phosphorus) (Maher and Woo, 1998). Not to be confused with phosphorus that has been adsorbed non-covalently to organic matter, organic phosphorus species include species in which phosphate is bound to an organic molecule through an ester bond (Maher and Woo, 1998). Other organic phosphorus forms contain phosphonates. Much like dissolved phosphorus, organic matter which passes through a 0.45µm pore size membrane filter is defined as dissolved organic matter (DOM) and is usually measured in mg C/L (Katsoyannis and Samara, 2007). When trying to achieve low phosphorus levels in wastewater effluent, focus need to be turned to the removal of dissolved organic phosphorus which remains in effluent after chemical addition.

While wastewater treatment plants utilize various technologies in the treatment process, most plants have the same series of steps. In brief, a wastewater treatment plant combines preliminary treatment with primary, secondary and tertiary clarification, and

then finishes the process with disinfection. To prevent damage to equipment down the line, preliminary treatment removes large grit and solids prior to the water entering the primaries. During primary treatment the larger particles settle and move to sludge digesters. Scum is also removed from the surface. In the secondary stages, an activated sludge is formed through aeration. The biologically activated sludge makes use of the natural behavior of microorganisms to disinfect the water (Hammer and Hammer, 2001). The remaining sludge from primary and secondary treatment processes is removed to landfill. Tertiary treatment, also referred to as advanced treatment, is a broad term used for any treatment process following the primary and secondary process. The wastewater treatment process is complete once effluent is released from the disinfection stage.

The process of chemical removal of orthophosphates as well as biological removal of polyphosphates is used for phosphorus removal in the wastewater treatment process. In orthophosphate removal, co-precipitates are formed between the soluble phosphorus and a metal salt, such as aluminum of iron salts (Smith et al. 2008). Solids are removed in with the sludge and taken to landfill (Neethling et al., 2007). Biological removal of polyphosphates uses the phosphorus storing capabilities of bacteria, for example *Accumulibacter* (Sedlak, 1991). Both methods may be combined in one wastewater treatment plant.

Studies focused on advanced multistep tertiary treatment processes showed very efficient phosphorus removal (Neethling et al., 2007; Gu et al., 2007). These tertiary treatments combine filtration, coagulation and adsorption in removal of phosphorus; total phosphorus was shown to have been reduced to a level of approximately 20µg P/L. These studies were able to conclude that the organic fraction of phosphorus was the most

refractory in effluents, and point out the need to study and define the actual chemical composition of refractory dissolved organic phosphorus. Results from a study conducted by Lancaster et al. (2008) showed that condensed and organic phosphorus had a major impact on the effluent total phosphate. The study also concluded that the removal efficiency for these two fractions were the lowest when compared to the insoluble and soluble reactive phosphorus fractions (Lancaster et al., 2008).

Fluorescence is a highly sensitive and selective technique to characterize DOM. In varied samples, fluorescence spectroscopy can determine molecular nature of DOM based on different fluorescent properties (DePalma et al., 2011). As a product of simultaneous scanning of the excitation and emission wavelengths of a sample, the fluorescence data can be complied into a fluorescence excitation-emission matrix (FEEM). These FEEMs can be analyzed using parallel factor analysis (PARAFAC) to provide information of a sample based on the peak position and intensity of the different fluorophores (DePalma et al., 2011). PARAFAC is a multivariate data analysis technique that separates the fluorescence signal into various fluorescent components which can quantify and characterize changes in dissolved organic matter (Fellman et al., 2009).

In previous research, fluorescence spectroscopy has been used as a technique to determine water quality in rivers and catchments. A study by Baker and Inverarity (2004) focused on protein-like fluorescence intensity and correlations with a number of water quality parameters, such as ammonia, nitrate and phosphate concentrations. A strong correlation between tryptophan and nitrate, phosphate and biological oxygen demand was observed from the measurements (tryptophan and phosphate correlate with an r value of 0.80, for 64 river samples). Baker and Inverarity (2004) were able to conclude that where

sewage sources of DOM are important, tryptophan-like fluorescence can be used as a surrogate.

The effect of wastewater treatment on the fluorescence of effluent waters has also been the focus of several studies. The fluorescence character of wastewater treated through preliminary treatment and primary, secondary and tertiary clarification was the focus of a series of studies (Reynold and Ahmad, 1997; Ahmad and Reynolds, 1999; Reynolds, 2002). These studies found that as wastewaters moved through the process, there was an overall decrease in the intensity of tryptophan-like fluorescence. This decrease was found to be in accordance to the correlating decrease in biological oxygen demand that was also observed. Tryptophan is a dynamic component of DOM in waste water.

Henderson et al. (2009) point out in their review on fluorescence as a tool for monitoring recycled water systems, that there has been very little research conducted on fluorescence and the effects tertiary treatments (or advanced treatment methods). The study completed in this chapter was implanted in hopes to achieve a new level of understanding on the effects of tertiary treatments on dissolved organic matter as well as the implications on phosphorus removal. Also, this study was completed in hopes of finding evidence pointing to which wastewater treatment process leads to removal of refractory (organic) phosphorus.

3.3 METHODOLOGY

Wastewater samples were collected from 12 wastewater treatment plants in the United States between November 2009 and June 2010. Wastewater treatment plants are kept anonymous for the purposes of this thesis. Each WWTP is coded alphabetically. Twenty-four hour composite samples were collected by rinsing high density polyethylene bottles three times with sample waters before filling and sealing with laboratory film (Parafilm®"M", Chicago, IL) to avoid leakage during transport.

Samples were transported in coolers to Wilfrid Laurier University at approximately 4°C. Upon arrival, 1L aliquots of each sample were filtered into a clean high density polyethylene bottle using a 0.45um pore size cellulose nitrate membrane filter (Whatman, Germany). Filtered and unfiltered samples were stored in a refrigerator at 4°C. Initial experiments showed that filtration is essential to stabilize phosphorus speciation in the samples. Without filtration phosphorus will continue to slowly bind to particles in suspension (Smith et al., 2008)

Stock solutions of reagent grade L-tryptophan ($1.0x10^{-2}$M) (>98% pure, Sigma-Aldrich, St. Louis, MO) and L-tyrosine ($1.0\ x10^{-3}$M) (>98% pure, Sigma-Aldrich, St. Louis, MO) were prepared using ultrapure water (18.2MΩ, MilliQ). These stock solutions, along with a terrestrial reverse osmosis organic matter isolate, Luther Marsh (LM) organic matter, were used to prepare daily fluorescence standards. Details on LM organic matter sample location as well as chemical characteristics are found in Gheorghiu et al. 2010. Daily standards were prepared from these stock solutions with a composition of 0.500µM tryptophan, 0.250µM tyrosine and 5mg C/L. This daily standard was used to

determine component concentration using a one point calibration and PARAFAC (see below).

An aliquot of each sample, as well as the daily standard, were measured in a 1cm quartz cuvette using a Varian Cary Eclipse Fluorescence Spectrometer (Varian, Mississauga, ON). Fluorescence emission wavelengths were measured from 250nm to 600nm in 1 nm increments for every 10nm excitation wavelengths between 200nm and 450nm. For each scan, the excitation and emission monochromator slit widths were set to 5nm and the photomultiplier tube was set to high sensitivity (800 V).

Using MATLAB^{TM} (MathWorks, Natick, MA), 3-dimesional FEEMs were created from the fluorescence data. Scattered light, an artifact of the fluorescence instrumentation, was removed from the spectra during preprocessing to prevent mathematical interferences in later spectral analysis. As in DePalma et al. (2011), all fluorescence spectra were used un-corrected and intensities were expressed in arbitrary fluorescence units (counts) to avoid propagation of errors and additional assumptions in data analysis. The same instrument and settings were used for all fluorescence measurements on the wastewater samples. Inner-filter corrections were not necessary in any case due to low absorbance, less than 0.3 units, at 254nm (Ohno, 2002).

In processing of data, the system was constrained to have three fluorescent components. Also, two of the three components are assumed to be amino acid-like; thus, pure tyrosine and tryptophan were used as spectral-shape calibration standards. These assumptions were made because it is important to focus on as simple a model as possible to represent the molecular structure (DePalma et al. 2011). If fluorescence spectroscopy

is determined to be a useful method in characterizing organic matter in wastewater samples, too many components may lead to overcomplicated data analysis. Here we are focusing on broad trends between treatment plants and samples within treatment plants. A simple model for dissolved organic matter fluorescence facilitates these comparisons.

Component concentrations were determined using PARAlell FACtor analysis

Figure 3.1: (a) Daily standard fluorescence excitation-emission contour plot. Contour lines are labeled to indicate the intensity of fluorescence at that excitation/emission wavelength. Fluorescence spectra of the three main components used to describe the dissolved fluorescent organic matter within the wastewater samples. The spectra correspond to (b) humic-like, (c) tryptophan-like and (d) tyrosine-like substances

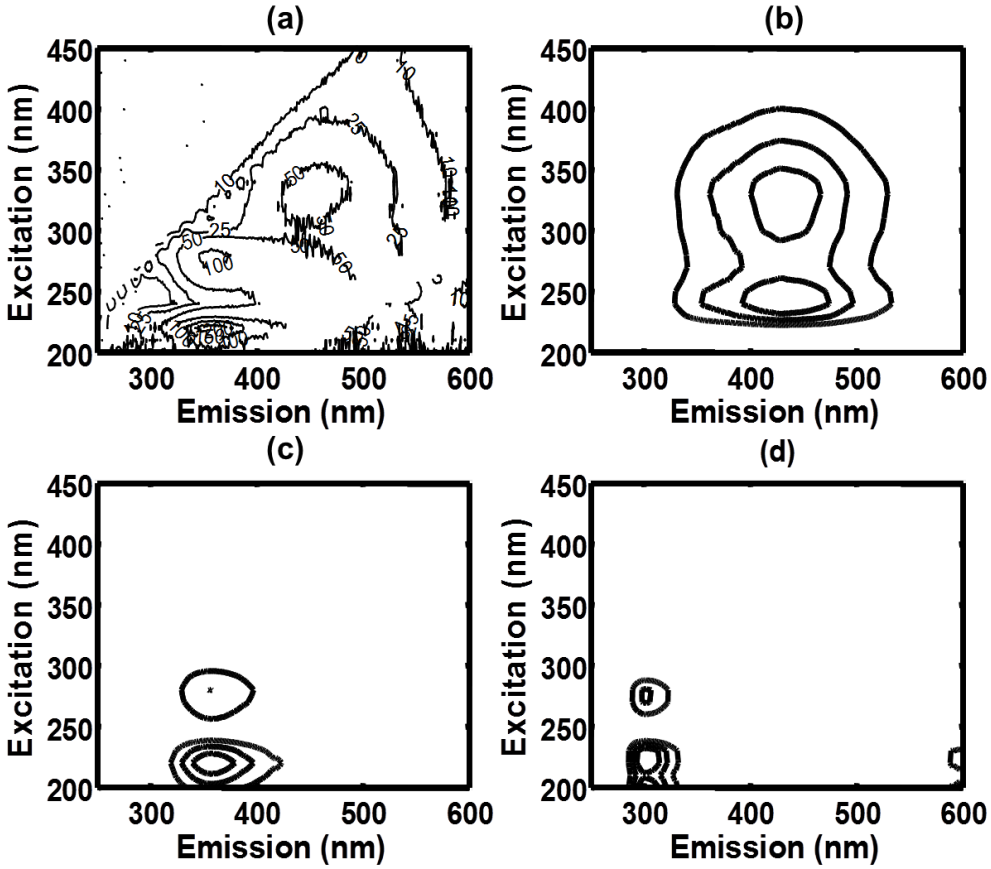

(PARAFAC) (Stedman and Bro, 2008). As previously mentioned, the system was constrained to have 3 components and pure tyrosine and tryptophan spectra were used as spectral-shape calibration standards to satisfy the *a priori* assumption that tyrosine and tryptophan-like fluorophores were present in the samples. The mathematics of this are discussed in DePalma et al. (2011). At the end of processing tyrosine, tryptophan, humic components are defined. In previous natural water sample analysis (DePalma et al., 2011) four components were selected, including tyrosine, tryptophan, humic and fulvic acid. For the wastewater samples collected in this study humic and fulvic components were integrated into one component "humic substances". There was no significant statistical advantage to four components and three components simplifies comparisons between

Figure 3.2: Example fluorescence excitation-emission contour plots. Contour lines are labeled to indicate the intensity of fluorescence at that excitation/emission wavelength. Sample spectra include (a) WWTP-H influent, (b) WWTP-G MBR influent, (c) WWTP-D granulated activated carbon effluent and (d) WWTP-A nitrification influent.

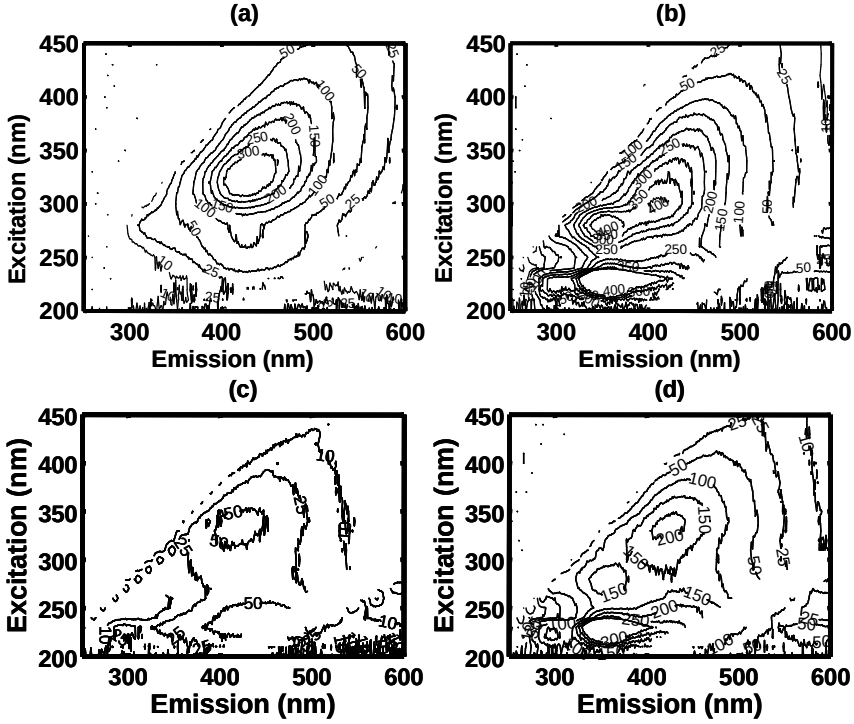

sampling sites and treatment plants. The concentration (μM or mg C/L) of these components are determined using a linear calibration curve and the resolved component concentrations from the daily standards. Luther Marsh isolate is predominately humic acid (Nadella et al. 2009). The Luther Marsh "concentrations" determined for wastewater samples assume that wastewater organic matter is the same as marsh derived organic matter. The two classes of molecules would definitely have differences so the quantitative values should be interpreted by relative comparisons between treatment plants and not necessarily as absolute values.

3.4 RESULTS

Fluorescence spectra were collected for 44 wastewater samples from 12 separate wastewater treatment plants. Each day as measurements were made, a fluorescence spectrum was also collected from the scan of the daily standard. An example of the daily standard contour plot is shown in Figure 3.1a. The three components of the prepared standard include tyrosine (excitation/emission at 300-350 nm/300 nm), tryptophan (excitation/emission at 250-300 nm/350 nm) and humic acid from Luther Marsh (excitation/emission at 250-390 nm/460-520 nm) (DePalma et al., 2011). The emission of each fluorophore is diagnostic; according to spectroscopic selection rules, there can be multiple excitations leading to this same emission. These components can be mathematically resolved using PARAFAC (see above). Results of spectral resolution on the entire dataset (44 samples as well as daily standards) are shown in Figure 3.1b-d. The three different components include; tyrosine-like (Figure 3.1d), tryptophan-like (Figure 3.1c) and humic substances (Figure 3.1b). In addition to resolving spectral profiles,

PARAFAC allows for component concentrations to be determined. This allows for quantitative tracking of fluorescent component concentration variations within and between treatment plants.

Figure 3.2 displays a representative collection of fluorescence contour plots. In the contour plots, emission wavelengths are on the x-axis while excitation wavelengths are on the y-axis. The selection of samples in Figure 3.2 represents the types of samples with the most variability in fluorophore concentration from the 44 measured. The same types of fluorophores exist in these samples as are seen in the daily standard (Figure 3.1a) and resolved as components (Figure 3.1b-d). Tyrosine emits at 300 nm and distinct peaks are visible in Figure 3.2b, c and d). Tryptophan is clearly resolved at 350 nm emission in Figure 3.2b and 3.2d. Humic-like fluorophores are present in all fluorescence maps shown in Figure 3.2. Visually it is possible to determine relative amounts of each component based on the fluorescence emission intensity (contour labels in Figure 3.2) but due to spectral overlap it is not possible to obtain more than qualitative information from the fluorescence surfaces directly. PARAFAC allows concentrations to be assigned to each of our three defined fluorophores. Table 3.1 summarizes the concentration for each of the fluorescent components for the 44 wastewater samples.

Table 3.1 divides the wastewater samples into wastewater treatment plant and sample location. The concentrations of soluble total phosphorus (sTP), soluble reactive phosphorus (sRP), dissolved organic phosphorus (DOP) and soluble non-reactive phosphorus (snRP) are displayed in the first four columns. Humic substances (HS), tyrosine (Tyr) and tryptophan (Trp) concentrations obtained from fluorescence measurements are shown in the last three columns. The treatment plant locations are kept

Table 3.1a: Phosphorus speciation and fluorescence data for various wastewater treatment plants. Phosphorus concentrations in mg P/L. HS corresponds to humic substance fluorophores (mg C/L). Tyr and Trp correspond to tyrosine and tryptophan-like fluorophores respectively (µmol/L).

Sample Location/Process	sTP	sRP	DOP	sNRP	HS	Tyr	Trp
WWTP-A							
Nitrification Influent	0.469	0.380	0.039	0.089	4.32	0.83	0.732
Nitrification Effluent	0.611	0.570	0.000	0.041	3.60	0.12	0.036
BNR Influent	1.44	1.21	0.146	0.234	3.46	0.80	1.080
BNR Effluent	0.123	0.078	0.000	0.045	3.48	0.23	0.130
Combined Nitrification and BNR	N/A	N/A	N/A	N/A	3.36	0.15	0.075
Filtration Influent	0.380	0.360	0.000	0.02	3.48	0.14	0.057
Filtration Effluent	0.136	0.120	0.000	0.016	2.22	0.12	0.013
WWTP-B							
Influent	0.250	0.054	0.113	0.196	2.85	0.14	0.051
Sedimentation 1 Effluent	0.01	0.007	0.008	0.003	2.55	0.15	0.058
Sedimentation 2 Effluent	0.008	0.0063	0.008	0.0017	2.60	0.16	0.057
C 1 Effluent	0.013	nd	0.013	nd	2.52	0.13	0.073
Sand Filtration 1 Effluent	0.010	0.0053	0.010	0.0047	2.45	0.15	0.075
Sand Filtration 2 Effluent	0.007	0.0063	0.007	0.0007	2.60	0.13	0.052
Membrane Filtration 1 Effluent	0.015	0.0071	0.015	0.0079	2.58	0.16	0.097
Membrane Filtration 2 Effluent	0.015	0.074	0.001	0.0076	2.56	0.16	0.067
F1E	0.008	0.0046	0.007	0.0034	2.5	0.12	0.077
F2E	0.008	0.0047	0.008	0.0033	2.44	0.17	0.064
WWTP-C							
BNR Influent	5.245	4.851	0.340	0.394	4.29	1.16	1.44
BNR Effluent	0.114	0.064	0.026	0.050	4.11	0.33	0.322
Final Effluent	0.013	0.000	0.011	0.013	4.39	0.36	0.310
WWTP-D							
Influent	4.861	4.910	0.493	0.671	4.037	2.38	1.74
MBR	0.035	0.026	0.002	0.009	3.23	0.54	0.627
GAC	0.023	0.022	0.000	0.001	0.86	0.26	0.069
WWTP-E							
Primary Effluent	1.616	1.569	0.015	0.047	2.37	1.43	1.09
Secondary Effluent	0.098	0.079	0.001	0.019	2.49	0.34	0.311
Tertiary Effluent	0.014	0.003	0.003	0.011	2.49	0.32	0.263
Combined Filtration Effluent	0.008	0.003	0.001	0.005	2.19	0.29	0.233
WWTP-F							
BAF	1.613	1.523	0.058	0.090	3.07	0.22	0.148
Filter	0.016	0.000	0.004	0.016	2.37	0.16	0.120

anonymous and simply labeled using a sequential alphabetic code. Results for representative WWTPs are specified below.

3.4.1 WWTP-A

WWTP-A is comprised of trickling filters upstream from a nitrification stage in which phosphorus removal is accomplished through dosing of ferric immediately upstream of the trickling filters. In parallel, an enhanced biological phosphorus removal plant is operating with optional ferric dose. The secondary effluent from both plants are

Table 3.1b: Phosphorus speciation and fluorescence data for various wastewater treatment plants. Phosphorus concentrations in mg P/L. HS corresponds to humic substance fluorophores (mg C/L). Tyr and Trp correspond to tyrosine and tryptophan-like fluorophores respectively (µmol/L).

Sample Location	sTP	sRP	DOP	sNRP	HS	Tyr	Trp
WWTP-G							
MBR Influent	3.057	2.703	0.354	0.354	5.07	2.34	1.764
MBR Effluent	0.249	0.199	0.025	0.050	3.88	0.15	0.148
Secondary Effluent	0.435	0.413	0.022	0.022	3.68	0.30	0.317
BW Effluent	0.012	0.000	0.009	0.012	3.31	0.28	0.163
Z Effluent	0.024	0.008	0.013	0.016	3.50	0.41	0.133
WWTP-H							
Influent	0.10	0.025	0.075	0.077	3.56	0.00	0.00
Final Effluent	0.014	0.001	0.004	0.013	5.34	1.57	0.573
WWTP-I							
Influent	0.112	0.080	0.005	0.032	2.24	0.20	0.087
Final Effluent	0.010	0.005	0.004	0.005	2.28	0.22	0.126
WWTP-J							
Influent	0.025	0.008	0.016	0.017	2.24	0.28	0.283
Final Effluent	0.017	0.005	0.012	0.012	1.88	0.25	0.208
WWTP-K							
Influent	0.004	0.002	0.001	0.002	1.16	0.17	0.113
Final Effluent	0.002	0.000	0.001	0.002	0.69	0.092	0.047
WWTP-L							
Influent	3.47	3.178	0.028	0.292	3.40	0.16	0.067
Final Effluent	0.000	0.000	0.000	0.000	2.37	0.18	0.141

combined and dosed with alum prior to a filtration step. Component concentrations determined from the fluorescence spectra of WWTP-A nitrification influent and effluent are represented in Figure 3.3. Through the process of nitrification there is a distinct decrease in the amino acid fluorophores (compare NitIN and NitEFF in Figure 3.3). Tyrosine drops from 0.8 to 0.1µM, while tryptophan decreases from 0.73 to 0.04 µM and humic substances decreases slightly from 4.3 to 3.6 mg C/L. Similar changes in the organic matter can also be seen in the wastewater samples when comparing the influent and effluent of the biological nutrient removal (BNR) process WWTP-A (Figure 3.3

Figure 3.3: Fluorescence component concentrations for the nitrification influent (NitIN) and effluent (NitEFF) for WWTP-A. Also, BNR influent and effluent (BNRIN, BNREFF) and combined secondary effluent (Comb), and filtration influent and effluent (FilIN and FilEFF). Humic substances (HS) concentration is expressed in mg C/L, while tyrosine (Tyr) and tryptophan (Trp) concentrations are expressed in µmol/L.

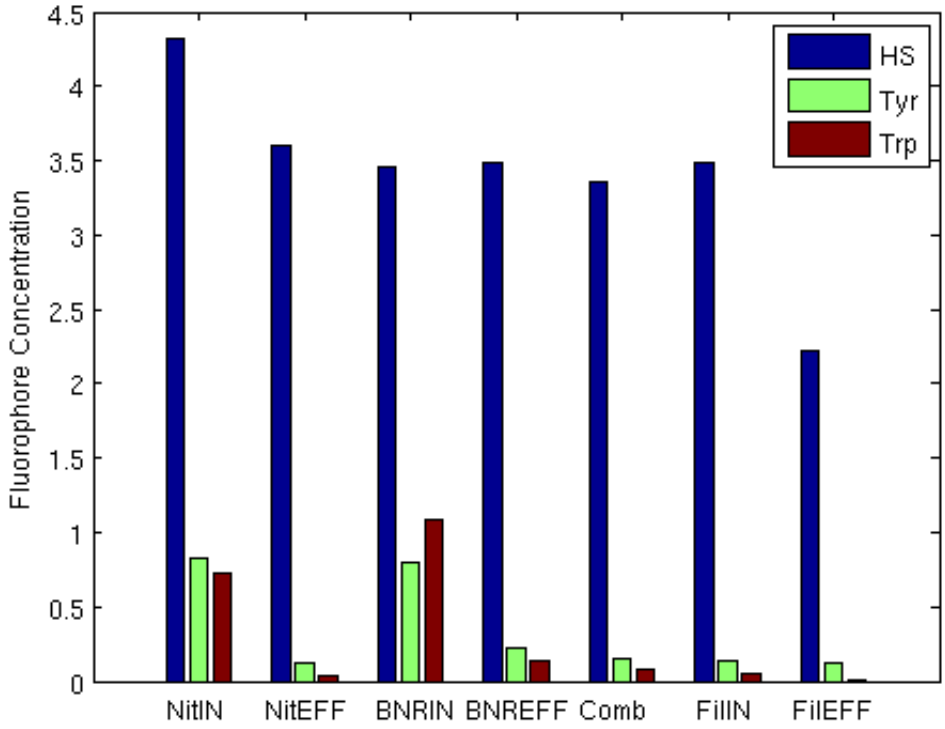

BNRIN compared to BNREFF). While the concentration of humic substances stays relatively the same at around 3.5 mg C/L, tyrosine decreases from 0.8 to 0.2µM and tryptophan decreases almost an order of magnitude, from 1.08 to 0.13 µM.

At WWTP-A, additional samples were taken from the nitrification and BNR combined effluents before alum addition (Comb), after alum addition (FilIN) and after filtration (FilEFF). Component concentrations from these three steps are shown as the last three samples in Figure 3.3. Although there is very little change in concentration, some decrease is observed in the three fluorophores, the most obvious being the change in humic substances over the process from 3.48 to 2.22 mg C/L. Tryptophan also decreases from 0.06 to 0.01 µmol/L through the process of alum addition and filtration.

3.4.2 WWTP-B

The influent, which is actually secondary effluent, into the WWTP-B can take one of six treatment pathways. The plant operates five different types of tertiary treatment: (1) conventional sedimentation with coagulant and polymer addition, (2) magnetic powder ballasted sedimentation process with coagulant and polymer addition, (3) multi-media granular filtration with coagulant and polymer addition, (4) dual-stage continuous backwash moving bed sand filtration with coagulant addition and (5) membrane separation. A schematic showing the different pathways is shown in Figure 3.4. Red points in the figure correspond to the different sample sites which are labeled according to the treatment they are sampled from. Sample sites include sedimentation (S1E, S2E), magnetic powder ballasted (MPB) sedimentation (C1E), dual-stage continuous backwash

moving bed (BWMB) sand filtration with coagulant addition (B1E, B2E), multi-media granular (MBS) filtration with coagulant and polymer addition (F1E, F2E), membrane filtration (Z1E, Z2E). The fluorophore concentrations through different possible pathways are presented below.

The fluorescence component concentrations of the first pathway in WWTP-B are presented in Figure 3.5a. In this pathway, the influent (INF) flows through traditional sedimentation tube settler 1 (S1E) and is followed by granular media filtration (F1E). Through this process there is very little change in the concentrations of the fluorophores. There is a small decrease in humic substances, from 2.8mg C/L in influent to 2.5mg C/L in final effluent, and a small increase in tryptophan, 0.05µM in influent to 0.08µM in final effluent. This is very similar to the changes in fluorophore concentrations seen in the second pathway (Figure 3.5b). In the second pathway, influent (INF) flows through traditional sedimentation tube settler 1 (S1E) but follows with upflow sand filtration

Figure 3.4: A schematic of the treatment pathways in WWTP-B. Red dots correspond to the various sample sites at the WWTP.

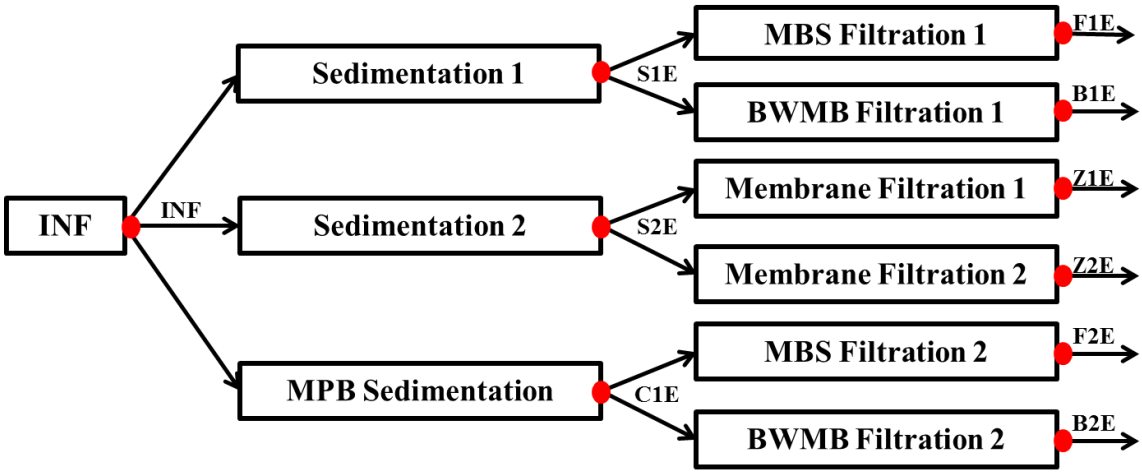

(B1E). In both pathways, tyrosine concentrations remain relatively unchanged. With respect to the fluorescent species concentrations, granular media filtration and sand filtration methods do not differ within experimental error.

In the third and fourth pathways, influent (INF) goes through traditional sedimentation tube settler 2 (S2E) but follows with two separate membrane filtration units. The sample in the third pathway goes through membrane filtration 1 (Z1E) and the sample in the fourth pathway follows through to membrane filtration 2 (Z2E). Results for the fluorescence component concentrations for the third and fourth pathways are presented in Figure 3.5c and Figure 3.5d, respectively. The trend from the first two pathways was also observed in these pathways; through the third and fourth pathways, humic substances decreases slightly while tryptophan increases. The change in tryptophan is much greater in membrane filtration 1 (Z1E), an increase of 0.06 to 0.09 µM, than membrane filtration 2 (Z2E), which increases from 0.06 to 0.07 µM. Again, like the first two pathways, tyrosine concentrations remain relatively unchanged. Although these small changes are noticeable, the two types of membrane filtration do not differ within experimental error.

The final two pathways follow the influent (INF) through a magnetic based sedimentation unit (C1E) and ends in filtration, either as granular media filtration (F2E, pathway 5) or upflow sand filtration (B2E, pathway 6). Results for the fluorophore concentrations for pathway five are presented in Figure 3.5e. As seen in the other pathways, there is a decrease in humic substances and a small increase in tryptophan through the magnetic based sedimentation process. Again, as with the other pathways, tyrosine remains relatively constant within sample variability.

Figure 3.5: Fluorescence component concentrations WWTP-B for treatment pathways 1 (a), 2 (b), 3(c), 4(d), 5(e) and 6(f). Sample sites include sedimentation (S1E, S2E), magnetic powder ballasted sedimentation (C1E), dual-stage continuous backwash moving bed sand filtration with coagulant addition (B1E, B2E), multi-media granular filtration with coagulant and polymer addition (F1E, F2E), membrane filtration (Z1E, Z2E). Humic substances (HS) concentration is expressed in mg C/L, while tyrosine (Tyr) and tryptophan (Trp) concentrations are expressed in µmol/L.

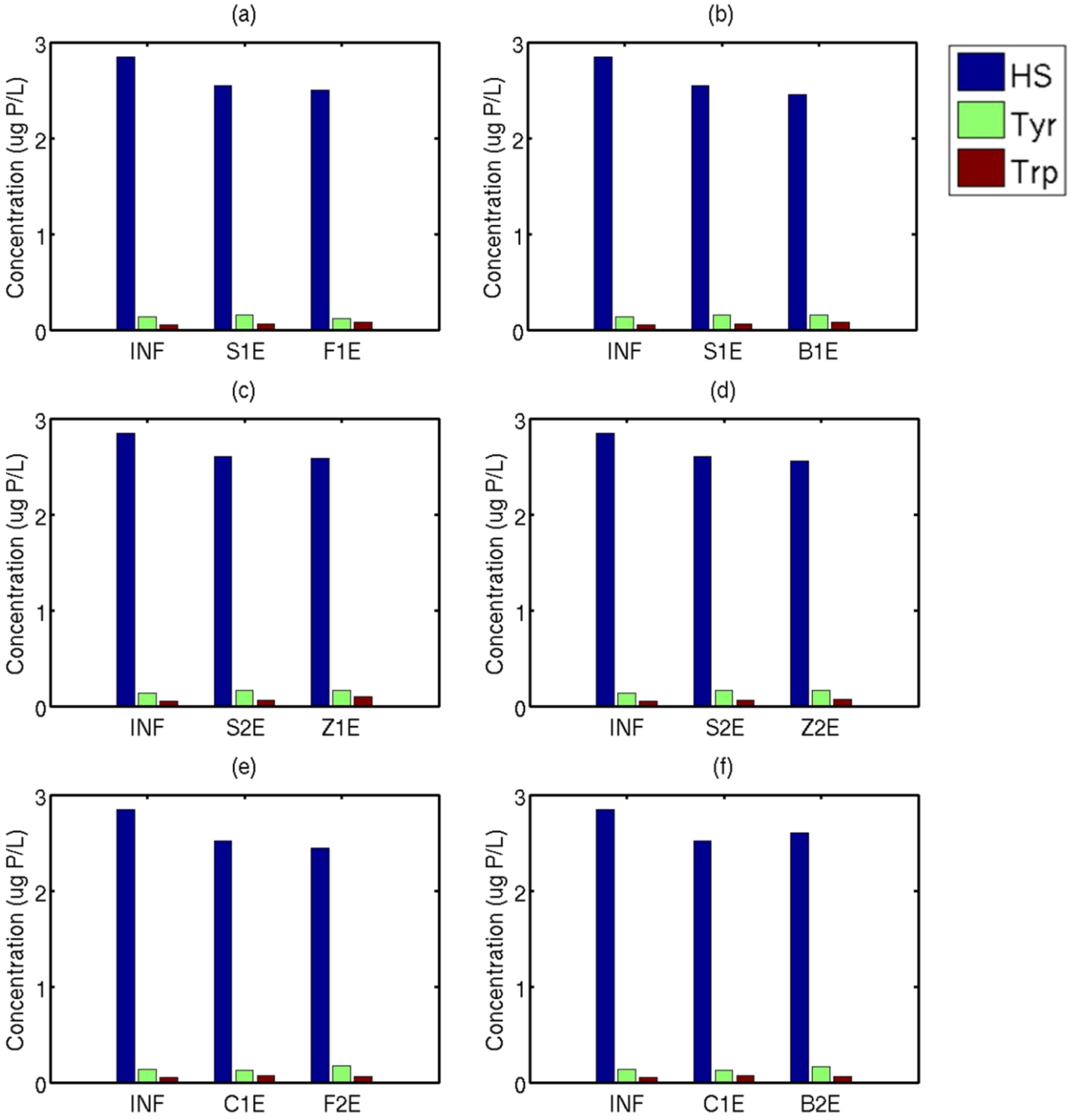

Figure 3.6: Fluorescence component concentrations for WWTP-G. Samples correspond to influent and effluent from MBR (MBRIN, MBREFF), influent to dual-stage continuous backwash moving bed sand filtration with coagulant addition (SECIN) and effluent (BWEFF) and membrane filtration effluent (ZEFF). Humic substances (HS, blue) concentration is expressed in mg C/L, while tyrosine (Tyr, green) and tryptophan (Trp, red) concentrations are expressed in µmol/L.

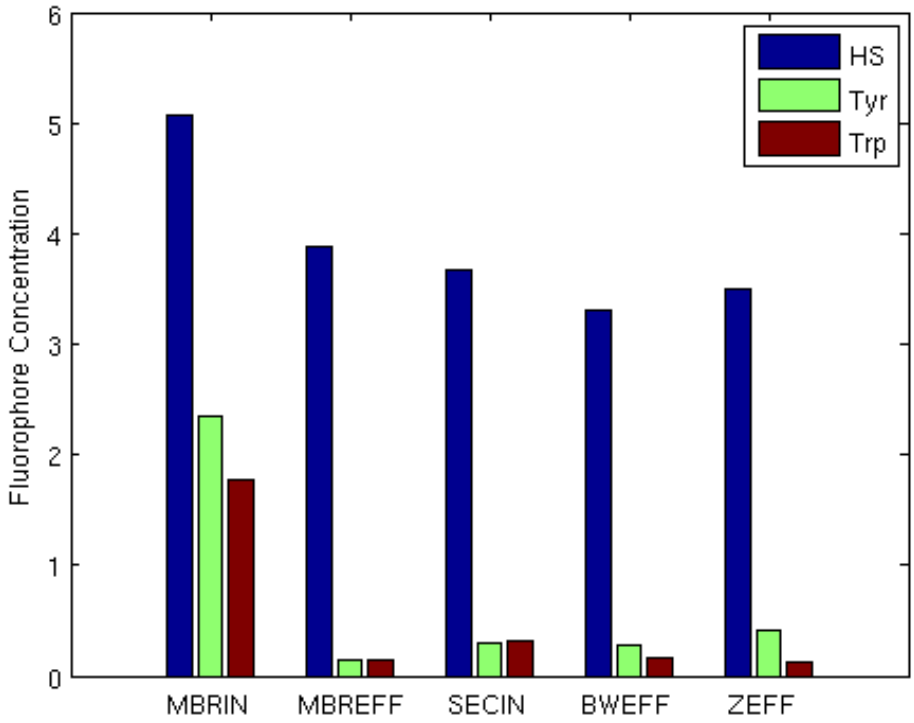

3.4.3 WWTP-G

WWTP-G includes a membrane bioreactor (MBR) as well as downstream dual media filtration and membrane filtration. Results for the fluorophore concentrations of different sample sites at the WWTP-G are shown in Figure 3.6. Through the (MBR) treatment process, humic substances decrease from 5.07 to 3.88 mg C/L. There is also a decline in tyrosine and tryptophan concentrations from 2.34 to 0.15 µmol/L and 1.76 to 0.15 µmol/L, respectively. There was also a small decrease observed in tryptophan concentration in the treatment process; a change from the concentration detected in the

secondary effluent to the concentrations detected in the filtration effluents. The dual media filtration (BWEFF), as well as the membrane filtration (ZEFF) process showed a tryptophan concentration decrease. There was very little change in the concentration of humic substances and tyrosine fluorophores through these filtration processes.

Figure 3.7: Fluorescence component concentrations for WWTP-H. Humic substances (HS, blue) concentration is expressed in mg C/L, while tyrosine (Tyr, green) and tryptophan (Trp, red) concentrations are expressed in µmol/L.

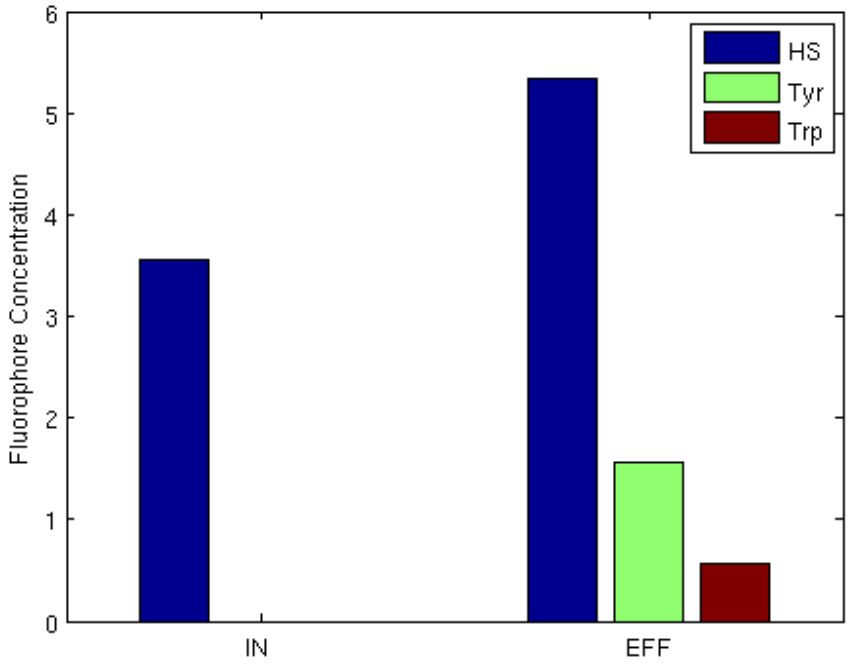

3.4.4 WWTP-H

Samples of the secondary treatment effluent (IN) and final tertiary effluent from WWTP-H (EFF) were collected and measured (see Figure 3.7). WWTP-H is not a municipal wastewater treatment facility but is in fact a pulp and paper waste processing facility. Results from the fluorescence component analysis for these samples are shown in Figure 3.7. The input to tertiary treatment process (secondary treatment effluent) consists

entirely of humic substances at a concentration of 3.56 mg P/L. Through the treatment process, there is an observed increase in each of the fluorophore concentrations. Humic substances increase to 5.43 mg C/L while tyrosine and tryptophan increase to 1.57 and 0.57 μmol/L, respectively.

3.5 DISCUSSION

Excitation-emission matrices can be determined using fluorescence spectroscopy. The aromatic character of organic matter causes fluorescence; moieties such as humic and fulvic acid as well as amino acid residues produce characteristic fluorescence signals. Contour plots showing fluorescence intensity (Figures 3.1 and 3.2) can be used to visualize qualitative differences between samples. Since fluorescence spectroscopy responds to molecular electronic transitions, these contour plots can be seen as the "molecular fingerprints" of the wastewater samples. If the spectra of the wastewater samples look different, the underlying molecular natures of the organic matter of the samples are different. Figure 3.1a shows the spectra of the daily standard and Figure 3.1b-d shows the three main components used to describe the fluorescence quality of the organic matter in the wastewater samples.

Fluorescence data from the various samples were resolved using PARAFAC into three different components; tyrosine-like, tryptophan-like and humic substances (Figure 3.1b-d). Fluorescence contour plots have emission wavelengths on the x-axis and excitation wavelengths on the y-axis. Using the contour plot, you can see a three-dimensional peak on a two-dimensional surface. A continuous contour line is shows an elevation of one intensity and as you move into the center of the plot, the intensity

increases until the most intense point. Using Figure 1a, the locations of the different fluorophores can be observed. Humic substances (Figure 3.1b) fluoresce at an emission wavelength of around 420nm, while tryptophan (Figure 3.1d) and tyrosine (Figure 3.1c) fluoresce at emission wavelengths around 350 nm and 300 nm, respectively. Emission wavelengths are more indicative of fluorophores than excitation wavelengths because a single fluorophore can have multiple electronic excitation transmissions, while only one emission transition.

Due to the large number of contour plots obtained from the measurements of the samples, a collection of the most diverse samples are shown in Figure 3.2. Figure 3.2a depicts the influent sample from a pulp and paper treatment plant (WWTP-H). This sample is unique in the way that it is the only sample with a significantly high concentration of humic substances (emission around 420 nm) compared to the other components; in fact the fluorescence character of the sample is described entirely by humic substances. There is no indication of either amino acid fluorophores, unlike the MBR influent sample from the WWTP-G plant (Figure 3.2b). In this sample, emissions are observed at 300 nm, 350 nm and 420 nm indicating that all three fluorophores are present. This can also be said for the final two samples; an effluent sample from the granular activated carbon process at WWTP-D (Figure 3.2c) and an influent sample prior to nitrification process at WWTP-A (Figure 3.2d).

It is important to note here that, with respect to fluorescence, there is high diversity in the molecular nature of the DOM in these wastewater samples. While the MBR influent sample from WWTP-G, the effluent sample from WWTP-D and the nitrification influent sample from WWTP-A all have all three fluorophores, they all

fluoresce at different intensities making each sample very different at a molecular level. The samples differ in their relative amounts of proteinacious and humic substances. For example, WWTP-G input to the MBR process has a higher tryptophan component concentration (1.764 µmol/L) than the concentration for WWTP-A nitrification input (0.732 µmol/L). The sample from the output of the granular activated carbon from WWTP-D has a very low tryptophan concentration of 0.069 µmol/L. This is explained by studies which have shown that the composition of wastewater influent and effluent is dependent on wastewater treatment technologies as well as input source (Baker and Inverarity, 2004).

3.5.1 Relationship between Fluorescence and Phosphorus Removal

One of the main objectives of this study was to develop an understanding of the implications of phosphorus removal on organic matter in wastewater. In other words, to look at non-reactive phosphorus and dissolved organic matter with respect to the fluorescent qualities measured in the samples. In some samples DOP was below detection; thus, non-reactive phosphorus was used as a surrogate; nRP consists of DOP and AHP, as mentioned previously in Chapter 2. The same trends are revealed for DOP as for nRP but the below detection DOP samples reduce the number of data points and weaken the statistical interpretation (graphical results below are shown for snRP data but DOP correlation statistics are given for comparison). For each sample, using a Pearson Correlation Matrix, the fluorophores were tested for correlations with non-reactive phosphorus; the strongest correlation was found between tryptophan concentration and non-reactive phosphorus. A summary of these results are given in Table A.1 which can be found in Appendix A.

Figure 3.8 (a, b) illustrates that in some of the wastewater samples, when non-reactive phosphorus increases there is also an increase in tryptophan. Observing this correlation, we cannot assume that tryptophan concentrations are directly associated with non-reactive or organic phosphorus. However, it can lead to the reasoning that whichever process in wastewater treatment that is removing tryptophan, may also be removing non-reactive phosphorus. Still, not all treatment processes show this correlation. Figure 3.8a shows Trp concentration (in µmol/L) on the y-axis while snRP concentration (in mg P/L) is on the x-axis. Due to the clustering of data points, Figure 3.8b shows the same data, however snRP concentration is shown on a log scale. Data points for the different wastewater treatment processes are colour coded. Wastewater treatment processes include secondary treatment processes (red), tertiary treatment with biological removal (blue), and tertiary treatment with physical removal (green).

Overall, there was a significant relationship between non-reactive phosphorus and tryptophan concentration ($r = 0.795$, $p < 0.01$). After organizing the samples into the three different types of wastewater treatment, the relationship between non-reactive phosphorus and tryptophan concentration strengthened for the treatment processes which utilize biological removal. Significant relationships between snRP and Trp concentrations were found for samples obtained from secondary processes ($r = 0.801$, $p < 0.01$) and for samples from tertiary biological treatment ($r = 0.900$, $p < 0.01$). DOP and Trp correlation coefficients were $r=0.790$, $p = 0.011$ for secondary processes, $r=0.950$, $p=0.01$ for tertiary treatment with biological removal and $r = -0.139$, $p = 0.516$ for tertiary treatment which utilizes physical removal. Observing this correlation, we cannot assume that tryptophan concentrations are directly associated with non-reactive or organic phosphorus. However,

it can lead to the reasoning that whichever process in wastewater treatment that is removing tryptophan, may also be removing non-reactive phosphorus.

A significant relationship was also found between non-reactive phosphorus and tyrosine concentration for all data points (r = 0.734, p< 0.01). As with the relationship with tryptophan, the relationship between non-reactive phosphorus and tyrosine strengthens once the data is organized into the different types of wastewater treatment. Figure 3.9 (a, b) depicts the correlation between soluble non-reactive phosphorus (snRP) and tyrosine (Tyr) fluorophore concentrations. The same colour code that was used in Figure 3.8(a, b) is also used in Figure 3.9a; secondary treatment processes are shown in red, samples from tertiary treatment with biological removal are shown in blue, and data from tertiary treatment with physical removal are shown in green. Figure 3.9a shows Tyr concentration on the y-axis (measured in µmol/L) while snRP concentration is on the x-axis (measured in mg P/L). Again, since the data points are clustered in the bottom left hand corner, Figure 3.9b shows the same data but with snRP concentration is shown on a log scale. A significant relationship was found between snRP and Tyr concentrations for samples obtained from samples from tertiary biological treatment (r = 0.926, p< 0.01). Secondary treatment processes with biological removal and physical removal was found to have no correlation between non-reactive phosphorus and tyrosine concentration (r = 0.539, p = 0.134 and r = -0.084, p = 0.697, respectively). DOP and Tyr correlation coefficients were r =0.535, p = 0.138 for secondary processes, r=0.949, p=0.01 for tertiary treatment with biological removal and r = 0.026, p=0.451 for tertiary treatment which utilizes physical removal. This relationship shows that in wastewater samples from tertiary biological treatment, when non-reactive phosphorus increases there is also an

Figure 3.8: (a) A plot for the correlation between soluble non-reactive phosphorus (snRP) and tryptophan concentration. (b) The same correlation with soluble non-reactive phosphorus on a logarithmic scale. The red points correspond to secondary treatment, blue points correspond to MBR treatment and the green points correspond to physical removal. Solid lines represent data of statistical significance, while the dashed lines represent data of little statistical significance. The red line has an R^2 of 0.642, an r of 0.801 and a p<0.01, while the blue and green line values are R^2=0.810, r=0.900, p <0.01 and R^2=0.019, r=-0.139, p=0.516 respectively. Statistics for the overall data are as follows; R^2=0.539, r=0.795 and p <0.01.

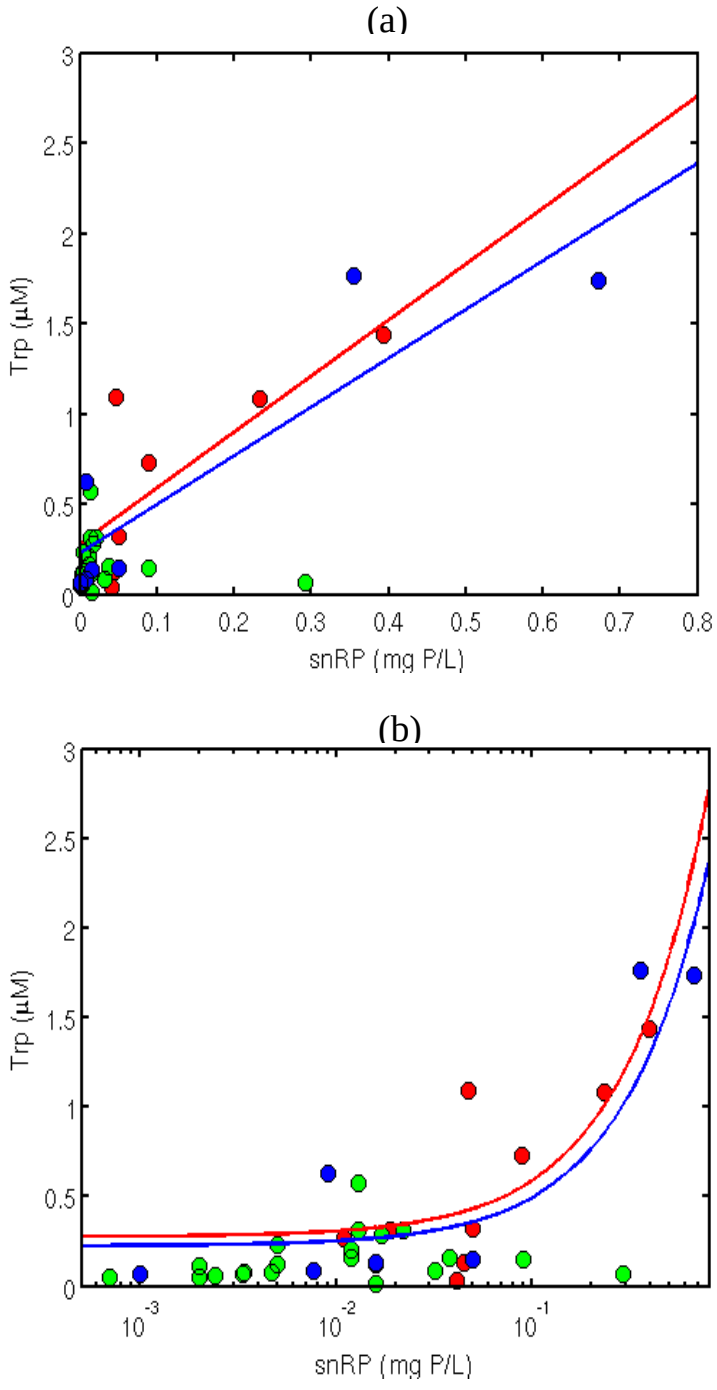

increase in tyrosine. Like the correlations between Trp and snRP, we cannot assume that tyrosine concentrations are directly associated with non-reactive or organic phosphorus.

Overall, a correlation was found between non-reactive phosphorus and tryptophan and non-reactive phosphorus and tyrosine concentrations. This association, between non-reactive phosphorus and proteinatious fluorophores, was expected due to the above mentioned research completed by Baker and Inverarity (2004). After dividing the samples into the wastewater treatment process type, some relationships were more significant while some treatments had no relationship at all. For secondary wastewater treatment and tertiary biological removal the correlation between the Trp fluorophore and non-reactive phosphorus is fairly robust. Also, the association between tertiary biological removal and the Tyr fluorophore is also significant. There was no significant relationship between snRP and Tyr or Trp concentrations for the tertiary treatment without biological removal (physical removal process).

From a mechanistic perspective this can mean two things about the association between nRP and Trp or Tyr. First, Trp and Tyr can be associated with the same type of molecules. When comparing the correlations between snRP and Trp concentrations and snRP and Tyr concentrations for tertiary biological removal, there was no significant difference between the two relationships. This could help support the idea that the two fluorophores could be associated with the same type of molecules because both of the fluorophores are proteinatious (Ahmad and Reynolds, 1999). Trp and Tyr are essential amino acids which occur in peptides and protein biomolecules. Similarly, phosphorus can occur in biological molecules such as phospholipids, organic phosphates, ATP, as well as proteins and peptides. Phosphorus associated with peptides and proteins would likely

Figure 3.9: (a) A plot for the correlation between soluble non-reactive phosphorus (snRP) and tyrosine concentration. (b) The same correlation with soluble non-reactive phosphorus on a logarithmic scale. The red points correspond to secondary treatment, blue points correspond to MBR treatment and the green points correspond to physical removal. Solid lines represent data of statistical significance, while the dashed lines represent data of little statistical significance. The red line has an R^2 of 0.291, an r of 0.539 and a p of 0.134, while the blue and green line values are R^2=0.857, r=0.926, p <0.01 and R^2=0.007, r=-0.084, p=0.697 respectively. Statistics for the overall data are as follows; R^2=0.633, r=0.734 and p <0.01.

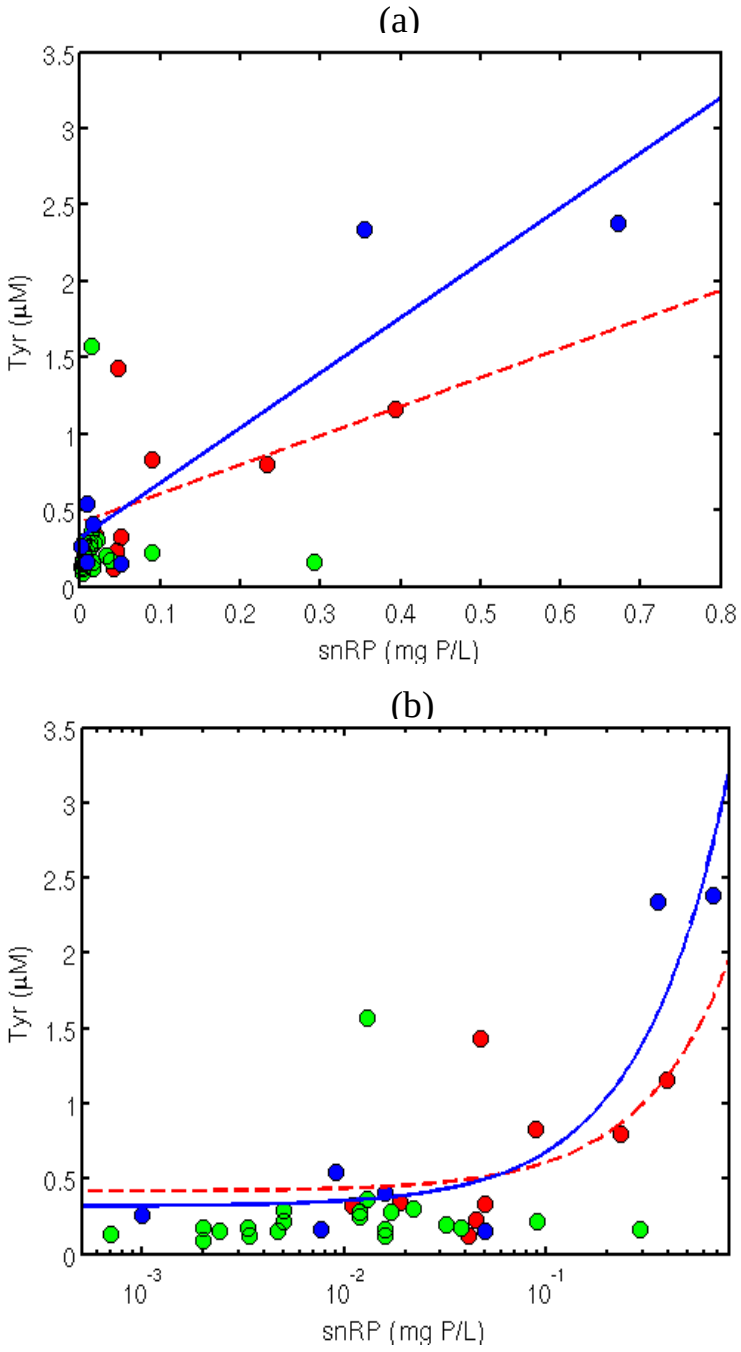

correlate with Trp and Tyr because they are common amino acids. If phosphorus occurs predominately in phospholipids or organic phosphates the concentrations of the components (nRP and Trp, or nRP and Tyr) would be less likely to be related – unless the same processes influence both quantities. This leads to second point that could be made for the associations between snRP and Trp or Tyr; snRP, Trp and Tyr could be removed in similar processes.

Using statistical methods to test for correlations between two independent correlations, no difference was found between the correlations for non-reactive phosphorus and Trp concentrations for secondary treatment and tertiary treatment with biological removal. This makes sense due to the fact that both processes have steps in the process that use the natural behavior of microorganisms to break down contaminants. For example, in biological nutrient removal (found in secondary treatment) the bacteria are stimulated to promote polyphosphate uptake and removal of phosphorus from solution, into solid bacteria. These same bacteria can utilize organic matter and the biomolecules containing Trp (or Tyr) seem to be bioavailable. In fact, a study by Ahmad and Reynolds (1995) classified proteinatious fluorescence peaks as biodegradable aromatic hydrocarbon. Thus, Trp and nRP both decrease even if the nRP is not directly associated with Trp containing molecules. The same can be said for Tyr and nRP.

The correlation between non-reactive phosphorus and humic substances concentration is the last to be presented in Figure 3.10 (a, b). Unlike the other two fluorophores, humic substances concentration shows a very weak correlation with an overall R^2 of 0.216 (r = 0.464) and $p < 0.01$. As mentioned previously, similar treatment

Figure 3.10: (a) A plot for the correlation between soluble non-reactive phosphorus (snRP) and humic substances concentration. (b) the same correlation with soluble non-reactive phosphorus on a logarithmic scale. The red points correspond to secondary treatment, blue points correspond to MBR treatment and the green points correspond to physical removal. Dashed lines represent data of little statistical significance. The red line has an R^2 of 0.271, an r of 0.521 while the blue and green line values are R^2=0.065, r=0.256 and R^2=0.304, r=0.552, respectively. All ps > 0.15 Statistics for the overall data was found to be R^2=0.216, r=0.464 and p <0.01.

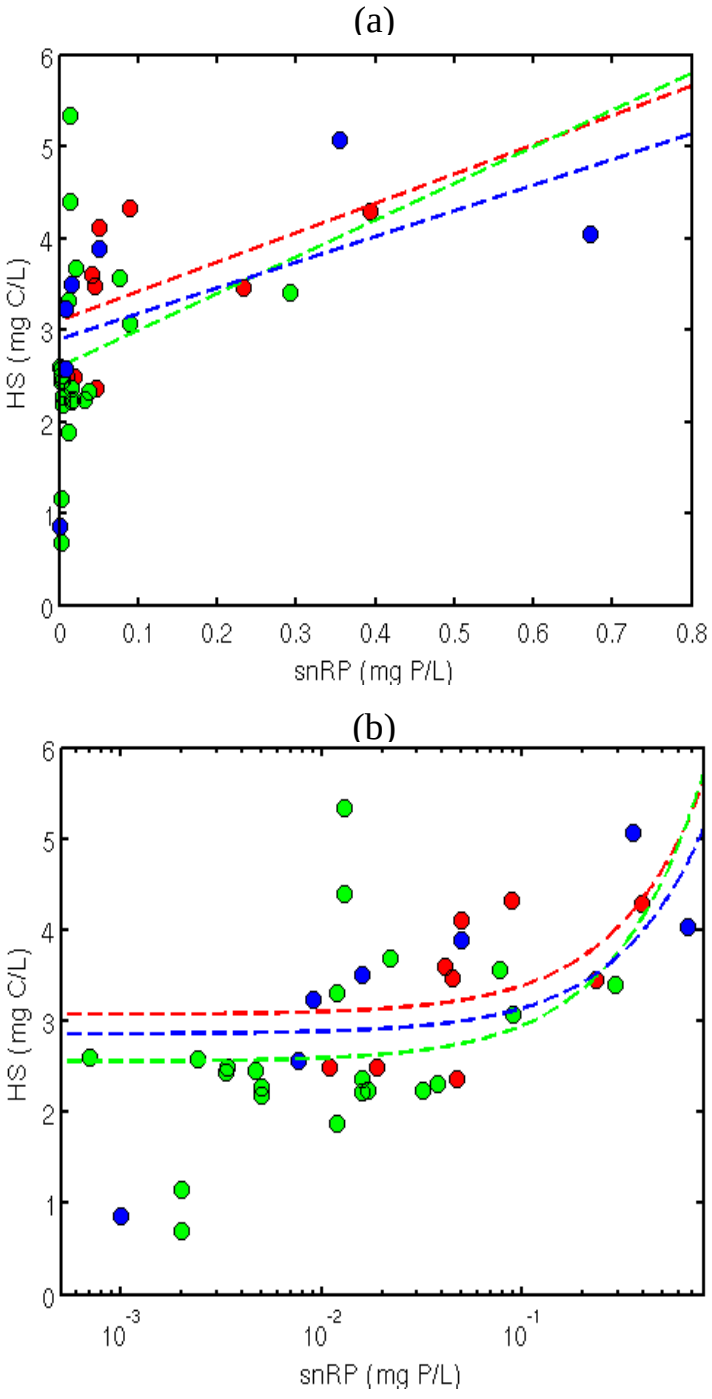

processes have been color coded. Samples from secondary treatment are shown in red, tertiary treatment with biological removal in blue and tertiary treatment using physical removal in green. There were no correlations found between snRP and HS for any of the wastewater treatment plant processes. The correlation coefficients for snRP and HS concentrations were found to be R^2 =0.271 with r =0.521, R^2 = 0.304 with r = 0.552 and R^2 = 0.065 with r = 0.256 for secondary treatment, tertiary treatment with biological removal and tertiary treatment with physical removal, respectively (all ps >0.15). The correlation coefficients for DOP and HS concentrations were found to be r =0.486 (p = 0.185), r = 0.607 (p=0.148) and r = 0.344 (p=0.100) for secondary treatment, tertiary treatment with biological removal and tertiary treatment with physical removal, respectively.

As stated above, no significant association between non-reactive phosphorus and humic substances concentrations was found for the three types of wastewater treatment separately. In this case as non-reactive phosphorus increases, humic substances concentration stays relatively constant. This was not surprising when one considers the study from Ahmad and Reynolds (1995). When measuring fluorescence of several waters, natural and wastewater sources, Ahmad and Reynolds found the presence of the humic peak to be persistent. Phosphorus is known to be found in the humic fractions of natural organic matter. However, the association between phosphorus and humic substances in waste water is not fully understood. In natural waters, humic substances may not have phosphorus incorporated into the molecular structure. Humic substances are known to have a high affinity for Al and Fe which can bind to phosphorus (He *et al*., 2006). This leads us to question if the same can be said for humic substances derived

from the wastewater treatment process. If so, the inability to remove humic substances from waste water may represent a limit of technology on total phosphorus removal. If treatment processes are able to remove humic substances, will lower levels of total phosphorus be observed in final effluents?

Humic substances can be large, bulky molecules in nature; the molecular weight of humic substances have been found to be quite variable and in the range of 0.01 to 700 kDa (Perminova et al., 2003). The previous knowledge that physical processes remove contaminants based on physical size, further investigation of the association between HS and snRP with respect to physical processes used in wastewater treatment was required. Physical removal processes can be further categorized into the type of physical removal implemented by the WWTP. These processes include single and double filtration, single sedimentation and sedimentation plus filtration. Correlations were explored for the four categories as well as combining the processes into filtration based and sedimentation based processes. The process of sedimentation plus filtration was only looked at separately because it could not be categorized as either sedimentation or filtration.

When looked at independently, the single filtration and double filtration processes did not have a significant relationship between HS and DOP. When grouped together however, snRP and HS were found to have a statistically significant correlation (R^2=0.701, r =0.837, p=0.019) for the filtration removal method, shown in Figure 3.11. DOP and HS were also found to have a statistically significant relationship however it was not as strong (R^2=0.587, r =0.766, p=0.027). For single sedimentation, the correlation was observed between HS and DOP (R^2=0.882, r=0.939, p=0.018) instead of HS and snRP concentrations. This correlation was depicted in Figure 3.12. Correlations

between HS and snRP were not statistically significant (R^2=0.842, r=0.917, p=0.83), most likely due to data points being removed due to being below detection. The fact that correlations were observed between HS and DOP was especially interesting because DOP is the hard to remove fraction of snRP, ergo the fraction is of great importance. That being said, the data point with a humic substances concentration of around 3.3 mg P/L could be considered an outlier. The correlation coefficients of the data set with the data point removed were not considered statistically significant with an r of 0.708 and a p of 0.180. Although not statistically significant, the relationship can be considered

Figure 3.11: Correlation dissolved organic phosphorus (sOP) and humic substances concentration for physical removal using filtration. The solid line represents data of statistical significance. The line has an R^2 of 0.701, r of 0.837 and a p of 0.019.

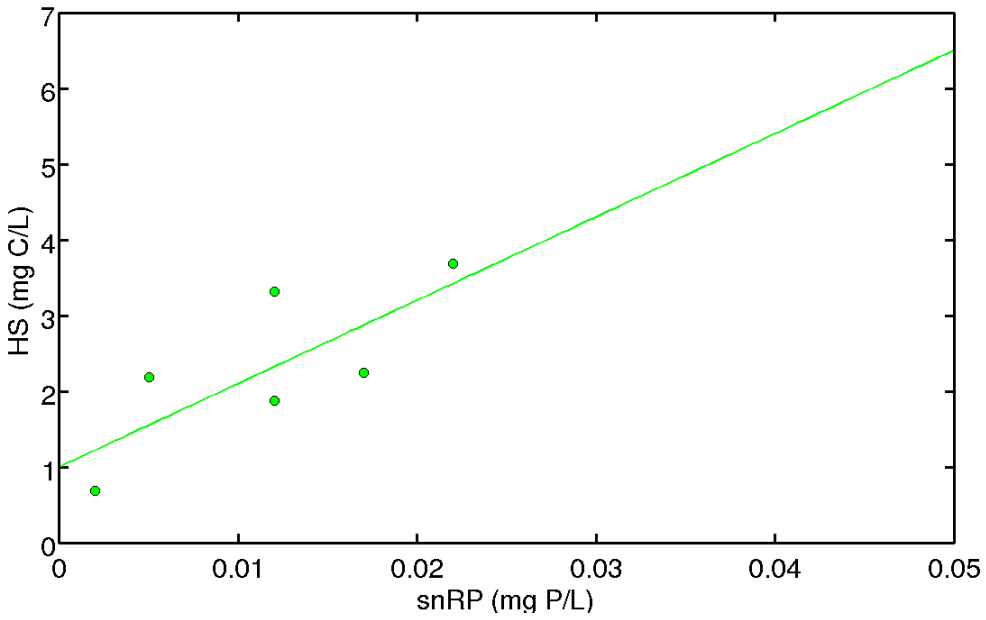

practically significant because it could give some indication about DOP in wastewater, knowledge that current wastewater industry is lacking. With further examination of wastewater samples from single sedimentation treatment, the relationship could be proven to be significant.

Figure 3.12: Correlation dissolved organic phosphorus (DOP) and humic substances concentration for physical removal using single sedimentation. The solid line represents data of statistical significance. The line has an R^2 of 0.882, r of 0.939 and a p of 0.018.

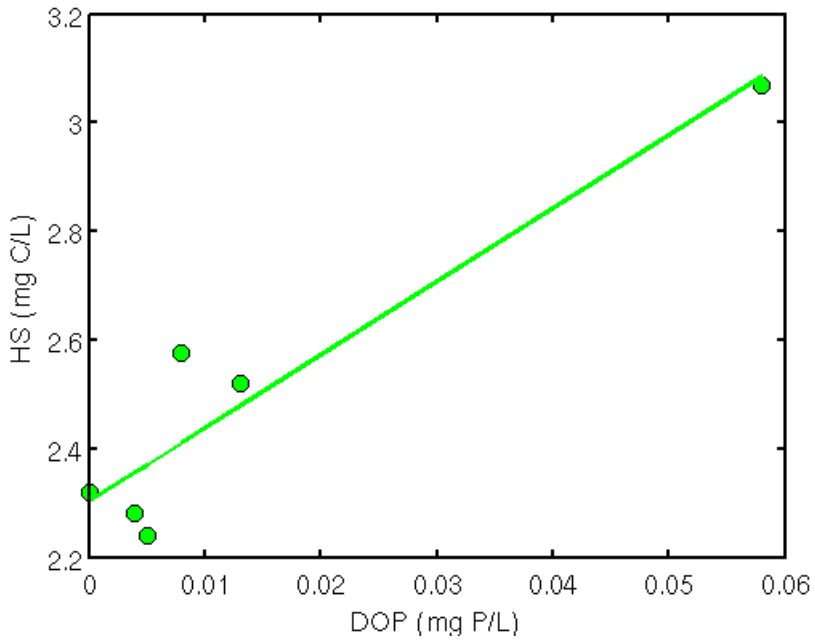

3.5.2 Wastewater Samples Representative of the Different Types of Removal

As noted above, wastewater treatment samples can be organized into categories based on the types of treatment used. These categories include secondary treatment, tertiary treatment with biological removal and tertiary treatment which use physical removal (no biological removal). Representative processes from wastewater treatment

plants will be discussed in more detail below. Secondary treatment processes are highlighted by samples from WWTP-A, physical removal processes are highlighted by WWTP-B and tertiary treatment with biological removal process is highlighted by WWTP-G. Finally, WWTP-H will be discussed because it is different from the rest of the plants.

Secondary Treatment Processes

Secondary treatment processes were found to have a strong correlation between tryptophan and non-reactive or organic phosphorus. These processes utilize biological nutrient removal (BNR). BNR uses biochemical reactions to convert what is normally found in wastewater to a form that is more easily removed, for example non-reactive or organic phosphorus can be converted to orthophosphate (Neethling et al., 2010). BNR is made up of different processes, for example nitrification is used in WWTP-A.

As observed in Figure 3.3, through the process of nitrification (NitIN and NitEF) there is a distinct decrease in the amino acid fluorophores; tryptophan and tyrosine both decrease by 0.7 µmol/L. Similar changes in the organic matter can also be seen in the wastewater samples when comparing the influent and effluent of the BNR processes of WWTP-A. The tryptophan fluorophore decreases by 0.95 µmol/L while the tyrosine fluorophore decreases by 0.6 µmol/L. Throughout the BNR process, the humic substances component concentration stays relatively the same. This seems to suggest that while the amino acid residues are likely used as nutrients by bacteria in the nitrification and BNR processes, the humic substances are not as bioavailable.

Tertiary Treatment with Biological Removal Processes

Membrane bioreactor processes are tertiary treatments which use BNR technologies in addition to chemical removal. Membranes aid in liquid/solid separation and these systems have the advantage that the solids will be retained on the membrane, ergo not contributing to nutrient concentrations in effluents (Neethling et al., 2010). Component concentrations obtained from the fluorescence spectra from WWTP-G can be seen in Figure 3.6. WWTP-G uses membrane bioreactor technology as well as parallel membrane filtration and moving bed dual media filtration units. Influent and effluent samples from each of the processes were collected. The two parallel filtration units have the same input source.

Through the MBR process, there is a significant decrease in the proteinatious fluorophores; tryptophan and tyrosine decrease by 1.66 and 2.19 µmol/L, respectively. As mentioned earlier, MBR processes have a stronger correlation between non-reactive phosphorus and Tyr than non-reactive phosphorus and Trp. While this differs from BNR processes, the two processes have some similarity. Like BNR processes, the humic substances component concentration shows little change (a decrease of 1.19 mg C/L) throughout the MBR process. Once again suggesting that while the amino acid residues are likely used as nutrients by bacteria in the nitrification and BNR processes, the humic substances are not used (i.e. bioavailable).

Tertiary Treatment with Physical Removal

Filtration and sedimentation remove pollutants based on physical size. Some processes use chemical addition to form precipitates which take up certain pollutants

during the precipitation process. These precipitates, also known as flocs, are large and easy to remove. WWTP-B operates three parallel sedimentation units, two traditional sedimentation tubes and one magnetic based sedimentation unit. The main influent into WWTP-B flows into the three separate units of the intermediate process. The effluent from each these units then flows into two parallel filters, resulting in six pathways the influent may take through the plant. To test the removal efficiency of the various pathways, the main influent was sampled as well as effluents from the three intermediate units and final effluents from each of the six filtration units.

In the final two pathways, magnetic based sedimentation process uses finely divided magnetic ballast to bind small particulates, including precipitated phosphorus. Results for the fluorophore concentrations for pathway five and six are presented in Figure 3.5. As seen in each of the six pathways, there is a decrease in humic substances and a small increase in tryptophan. Again, as with the other pathways, tyrosine remains relatively constant within sample variability. Overall, and there is very little change to the three components throughout the entire treatment process at WWTP-B. Any loss in humic substances may be due to the large molecular nature and easy filtration of humic substances. Also, as stated above, granular media filtration and sand filtration methods do not differ within experimental error in the fluorophore concentrations.

WWTP-H

An exception to both of the trends found in the correlation between tryptophan and non-reactive phosphorus is found when looking at the results from the one pulp and paper treatment facility sampled (WWTP-H). The trend seen in this treatment process shows that as non-reactive phosphorus decreases, the tryptophan fluorophore

concentration increases. This is exactly opposite to the treatment of municipal effluents. Influent into the tertiary treatment is made up entirely of humic substances and as the wastewaters move through the process all three fluorophores increase in concentration. It is likely that the high lignin content of the pulp waste results in very different behavior compared to municipal waste. This highlights the issue that nRP removal is not only treatment method specific but should also depend on influent characteristics.

The wastewater treatment process of interest at WWTP-H is the moving bed biofilm reactor technology. This technology uses a fixed film growth of biomass on a plastic carrier media. Secondary treatment effluent enters the tertiary process and flows through a process that includes high rate settling in a tube clarifier, contact clarification and mixed media filtration. Alum, or ferric, is added to the water just before it enters the tube clarifier. Secondary effluent, prior to the addition of alum, as well as final effluent of the process was sampled. In this instance instead of biological treatment decreasing organic matter, it in fact increased organic matter, while nRP decreased. In natural waters, the proteinatious fluorophores are directly associated with the growth stage of bacterial communities. The concentration of proteinatious fluorophores is a combination of what is used up and produced by the bacterial community within the biological treatment (Cammack et al., 2004; Elliot et al., 2006; Dignac et al., 2000). This could be true also in biological treatment depending on the bacterial communities involved.

3.5.3 Fluorescence Quenching

Several environmental factors can cause fluorescence quenching in wastewater samples. Fluorescence intensity of organic matter constituents can be affected by temperature, pH and the presence of metal ions. Temperature has been found to have an

inverse relationship to fluorescence; as temperature increases, fluorescence decreases (Hudson et al., 2007). At higher temperatures, there are larger amounts of collisional quenching due to faster diffusion (Lakowicz, 2006). To correct for temperature, each day the samples were allowed to come to room temperature, 22 ± 1°C, before measurement.

Changes in organic matter fluorophores due to pH were observed by several studies described in the review by Hudson et al. (2007). Humic substances were found to have an increase in fluorescence intensity as pH increased from 4 – 5.5 (Vodacek and Philpot, 1987). Above pH 5.5, Vodacek and Philpot (1987) found that there was still an increase in fluorescence intensity; however, it was much less dramatic. There was found to be little impact on fluorescence of tryptophan fluorophores in solutions with a pH between 5 and 8 (Hudson et al., 2007). This makes sense when the pK_as for tyrosine and tryptophan are taken into account. Tryptophan has two pKa values, 2.38 and 9.39, for the carboxylic and amine groups, respectively. Tyrosine has a pK_as of 2.2 and 9.11, for the protonation of the carboxylic and amine groups, respectively (Nelson and Cox, 2004). These two pKa values are outside of the range of typical pH for wastewater. Due to the fact that wastewater samples have a circumneutral pH, fluorescence variation caused by pH is of little concern.

Metal ions and their effect on fluorescence of organic matter have been well studied. Copper, iron and aluminum are known to quench fluorescence effectively at low concentrations. The review by Hudson et al. (2007) found that a most fluorescence quenching studies focused on low concentrations to avoid the formation of insoluble complexes. In wastewater treatment, low concentrations of iron and aluminum are not relevant. Aluminum and iron are added to wastewater in large amounts to remove

orthophosphate through co-precipitation (Smith et al., 2008). At these high concentrations, iron and aluminum would precipitate out of solution. Once filtered, the metal ions would be removed, therefore having little effect on DOM fluorescence. The effect copper has on fluorescence has also been the focus of several studies. Reynolds and Ahmad (1995) found that humic substances fluorescence can decrease by up to 40% when copper is present. Smith and Kramer (2000) found that as copper concentration increased (from 10^{-6} to 10^{-4} mol/L), fluorescence intensity decreased by approximately half. Copper concentration is variable in waste water; however, concentrations are usually low with effluent limits of $1.5x10^{-8}$ to $7.8x10^{-8}$ mol/L (Ontario Ministry of the Environment, 1994); thus, any effects copper has on fluorescence is less than the differences between samples.

3.6 CONCLUSIONS

Associations between non-reactive phosphorus and the different fluorophores of dissolved organic matter were explored. A correlation was found between snRP and Trp concentrations for secondary treatment (R^2 = .642, r =.801, p<.01) and for tertiary treatment with biological removal (R^2 = .810, r =.900, p<.01). A correlation was also found between snRP and Tyr concentrations for tertiary treatment with biological removal (R^2 = .857, r =.926, p<.01). Wastewater organic matter has variable fluorescent components; water varies in terms of input source as well as within treatment plants. This variability has implications for phosphorus removal. The so-called non-reactive phosphorus (nRP) is defined colorimetrically to include all non-orthophosphate phosphorus. This fraction of total phosphorus tends to be more difficult to remove than

orthophosphate. Biological treatment technologies tend to remove nRP to low levels correlated with a decrease in the fluorescent component tryptophan.

ACKNOWLEDGMENTS

This study was partly supported by the U.S. Water and Environment Research Foundation (WERF) as well as EnviroSim Associates Inc. and a NSERC Collaborative Research and Development grant. The authors would like to thank the anonymous plant staff and technicians for their assistance in sampling and process information collection. Special thanks are also given to the WERF Nutrient Challenges Program Team for their support.

3.7 REFERENCES

Ahmad, S. R., Reynolds, D.M. (1999). Monitoring of water quality using fluorescence technique: prospect of on-line process control. *Wat. Res*. **33** 2069-2074.

Baker, A. (2001). Fluorescence excitation-emission matrix characterization of some sewage-impacted rivers. *Environ. Sci. Technol.*, **35**, 948-953.

Baker, A. and Inverarity, R. (2004) Protein-like fluorescence intensity as a possible tool for determining river water quality. *Hydrol. Process.* **18**, 2927– 2945.

Cammack W. K. L., Kalf, J., Prarie, Y. T. and Smith, E. M. (2004) Fluorescent dissolved organic matter in lakes: relationship with heterotrophic metabolism. *Limnology and Oceanography*, **49** 2034 – 2045.

DePalma, S.G.S., Arnold, W.R., McGeer, J.C., Dixon, D.G., and Smith, D.S. (2011). Variability in dissolved organic matter fluorescence & reduced sulphur concentration in coastal marine & estuarine environments. *Appl. Geochem.* **26**, 394-404

Elliot, S., Lead, J. R. and Baker, A. (2006) Thermal quenching of fluorescence of freshwater, planktonic bacteria. *Analytica Chimica Acta*, **564**, 219 – 225.

Fellman, J.B., Miller, P.M., Cory, R.M. D'Amore, D.V., and White, D. (2009). Characterizing dissolved organic matter using PARAFAC modeling of fluorescence spectroscopy: A comparison of two models. *Environ. Sci. Technol.*, **43**, 6228-6234.

Gheorghiu, C., Smith, D. S., Al-Reasi, H.A., McGeer, J.C. and Wilkie, M.P. (2010) Influence of natural organic matter (NOM) quality on Cu–gill binding in the rainbow trout (*Oncorhynchus mykiss*). *Aquat. Tox*. **97**, 343-352.

Gu, A., J. Neethling, M. Benisch, D. Clark, D. Fisher, and H. S. Fredrickson (2007, October). Advanced phosphorus removal from membrane filtrate and filter filtrate using packed columns with different adsorptive media. In Conference proceedings, 80th annual water environmental federation technical exhibit and conference, Baltimore, MD, USA, pp. 7899–7914. Water Environment Federation: WEF.

Hammer, M. J. L., Hammer, M. J. J., 2001. Water and wastewater technology, 4th Edition. Prentice Hall, Upper Saddle River, New Jersey, USA.

He, Z., Ohno, T., Cade-Menun, B. J., Erich, M.S. and Honeycutt, C.W. 2006. Spectral and Chemical Characterization of Phosphates Associated with Humic Substances. *Soil Science Society of America Journal* **70**, 1741-1751.

Henderson, R.K., Baker, A., Murphy, K.R., Hambly, A., Stuez, R.M., Khan, S.J. (2009) Fluorescence as a potential monitoring tool for recycled water systems: A review. *Wat. Res*. **43,** 863-881.

Hudson, N., Baker, A. and Reynolds, D. (2007) Fluorescence analysis of dissolved organic matter in natural, waste and polluted waters – A review. *River. Res. Applic*. **23**, 631 – 649.

Katsoyiannis, A. and Samara, C. (2007) The fate of dissolved organic carbon (DOC) in the wastewater treatment process and its importance in the removal of wastewater contaminants. *Env. Sci. Pollut. Res*. **14** 284-292.

Lakowicz, J. R. (2006). Principles of Fluorescence Spectroscopy. 3rd Edition. Springer, New York, New York, USA.

Lancaster, C. D. and J. E. Madden (2008, October). Not so fast! The impact of recalcitrant phosphorus on the ability to meet low phosphorus limits. In Conference proceedings, 81st annual water environmental federation technical exhibit and conference, Chicago, Chicago, IL, USA, pp. 3531–3544. Water Environment Federation: WEF.

Maher, W., & Woo, L. (1998). Procedures for the storage and digestion of natural waters for the determination of filterable reactive phosphorus, total filterable phosphorus and total phosphorus. *Analytica Chimica Acta* , **375**, 5-47.

Nadella, S.R., Fitzpatrick, J.L., Franklin, N., Bucking, C., Smith, D.S., and Wood, C.M. (2009). Toxicity of Cu, Zn, Ni, and Cd to developing embryos of the blue mussel (*Mytilus trossolus*) and the protective effect of dissolved organic carbon. *Comparative Biochemistry & Physiology Part C*, **149**, 340-348.

Neethling, J. B., M. Benisch, D. Clark, D. Fisher, and A. Z. Gu (2007, October). Phosphorus speciation provides direction to produce 10 μg/l. In Conference proceedings, 80th annual water environmental federation technical exhibit and conference, San Diego, California, USA, pp. 1607–1624. Water Environment Federation: WEF.

Ohno, T. (2002). Fluorescence inner-filtering correction for determining the humification index of dissolved organic matter. *Environ. Sci. Technol.* **36**, 742-746.

Ontario Ministry of the Environment (1994) Water management: policies, guidelines, provincial water quality objectives of the Ministry of the Environment: Appendix A.

Perminova, I. V., Frimmel, F. H., Kudryavtsev, A. V., Kulikova, N. A., Abbt-Braun, G., Hesse, S. and Petrosyan, V. S. (2003) Molecular weight characteristics of humic substances from different environments as determined by size exclusion chromatography and their statistical evaluation. *Environ. Sci. Technol.* **37**, 2477-2485.

Reynolds, D. M. (2002). The differentiation of biodegradable and non-biodegradable dissolved organic matter in wastewaters using fluorescence spectroscopy. *J. Chem. Technol. Biotechnol.* **77**, 965-972.

Reynolds, D. M., Ahmad, R. (1997) Rapid and direct determination of wastewater BOD values using a fluorescence technique. *Wat. Res*. **31**, 2012-2018.

Reynolds, D. M., Ahmad, R. (1995) The effect of metal ions on the fluorescence of sewage wastewater. *Wat. Res*. **29**, 2214-2216.

Sedlak, R. I., (1991) Phosphorus and Nitrogen Removal from Municipal Wastewater: Principles and Practice, 2nd Edition, Lewis Publishers, New York. 229 pages.

Smith, D. S. and Kramer, J. R. (2000) Multisite metal binding to fulvic acid determined using multiresponse fluorescence. *Analytica Chimica Acta* **416**, 211-220.

Smith, D. S., I. Takács, S. Murthy, G. Diagger, and A. Szabó (2008). Phosphate complexation model and its implications for chemical phosphorus removal. *Water Environment Research* **80**, 428–438.

Spivakov, B., Maryutina, T., & Muntau, H. (1999). Phosphorus Speciation In Water And Sediments. *Pure Applied Chem* , **71**, 2161-2176.

Stedman, C.A. and Bro, R. (2008). Characterizing dissolved organic matter fluorescence with parallel factor analysis: a tutorial. *Limnol. Oceanogr. Methods*, **6**, 572-579.

Vodacek, A and Philpot, W. D. (1987). Environmental effects on laser-induced fluorescence spectra of natural waters. *Remote Sensing of Environment* **21**, 83 – 95.

Chapter 4: Screening of wastewater treatment technologies for phosphorus removal: activated carbon, hydrogen peroxide, ultraviolet light exposure, ozone and ferrate

4.1 ABSTRACT

Municipal wastewater treatment plants are a point source for nutrients and have impacted river systems leading to eutrophic conditions. To prevent eutrophication, wastewater effluent is highly monitored and new guidelines wish to cap total phosphorus concentrations in effluent to be less than 10µg P/L. In hopes of achieving low level phosphorus in effluents, wastewater treatment plants are now interested in implementing advanced oxidative processes (AOPs) to break down non-reactive (or organic) phosphorus. Non-reactive phosphorus is the residual phosphorus fraction in wastewater after treatment which needs to be broken down into reactive phosphorus which is easier to remove. This study explores six wastewater treatment processes in hopes to break down non-reactive phosphorus for ease of removal. These methods have been used in the past for wastewater disinfection but have never been tested for phosphorus removal. These treatments included AOPs hydrogen peroxide (H_2O_2), ultraviolet (UV) photolysis, ferrate (FeO_4^{2-}), ozone (O_3) and combined H_2O_2 and UV photolysis. Absorption chemistry was also investigated using activated carbon, which was discovered to be a source of phosphorus and thus not useful for nRP removal. Changes in non-reactive phosphorus were observed in all AOP treatments except ozone where no change occurred. When used separately, UV photolysis was found to decrease non-reactive phosphorus by approximately 26% percent. In the combined UV/H_2O_2 treatment, non-reactive phosphorus was decreased by 18%. Ferrate, the final AOP investigated in this

study, was found to decrease total phosphorus by approximately 35%. With the exception of activated carbon, the different treatments investigated show promise of conversion of non-reactive to reactive phosphorus. Ferrate treatment could be very useful due to it being a combination treatment, combining oxidation and chemical precipitation.

KEYWORDS

Wastewater Treatment, Reverse Osmosis, Advanced Oxidative Processes, Activated Carbon, Ferrate, Ozone, Hydrogen Peroxide

4.2 INTRODUCTION

Municipal wastewater treatment plants are a point source for nutrients and have impacted river systems leading to eutrophic conditions. Eutrophication occurs when wastewater effluents with high levels of phosphorus enters an aquatic environment; abnormally high concentrations of phosphorus increases algal growth dramatically. This process can pose as a threat to higher aquatic organisms (vanLoon and Duffy, 2000). To prevent eutrophic conditions from occurring, wastewater treatment plants have been aiming for effluent total phosphorus concentrations of less than 10µgP/L. Thus far, technologies have been able to achieve total phosphorus concentrations in effluent of 100 – 300 µg P/L (Neethling et al., 2007). These technologies mostly focus on reactive phosphorus (i.e. orthophosphate), which is easy to remove using chemical phosphorus removal (Smith et al, 2008). In order to reach even lower concentrations of total phosphorus, industry must eliminate the hard to remove non-reactive phosphorus (nRP). Non-reactive phosphorus consists of organic and condensed phosphorus (Maher and Woo, 1998). Organic phosphorus (and condensed phosphorus) will be able to be removed

more easily if they are converted to reactive phosphorus; the fractions would then be able to be removed via chemical removal.

Various treatments have been implemented to try to remove the non-reactive phosphorus from municipal wastewater. Wastewater treatment plants are beginning to expand past tertiary treatment and including even more advanced treatment. A relatively new wastewater treatment technology being implemented is reverse osmosis (RO). Reverse osmosis uses pressure to force water through a membrane filter with a pore size of approximately 10^{-4} microns, just slightly larger than a water molecule (Harris, 2007). The contaminants that do not pass the membrane are concentrated into a separate waste stream. The water that passes through the RO system has nutrients levels much lower than conventional nutrient removal technologies (Neethling et al., 2010). However, the water that is rejected from the RO system, the RO concentrate or brine, is high in hard to remove nRP which needs to be treated.

However, use of complicated systems has caused the cost of building, operating and maintaining wastewater treatment plants to increase drastically. This has led to the demand in industry for a quick and cost effective method of advanced treatment to achieve low levels of total phosphorus in wastewater. The purpose of the study in this chapter is to screen preexisting wastewater treatment technologies in order to determine whether or not they are an effective method for phosphorus removal, focusing on non-reactive phosphorus as the difficult to remove form of phosphorus. Treatments included activated carbon, hydrogen peroxide (H_2O_2), ultraviolet (UV) light, combined H_2O_2 and UV light, ozone, and ferrate as well as activated carbon for the adsorption of nRP species.

Due to its effectiveness of producing effluent low in dissolved organic compounds, adsorption systems, such as activated carbon, are increasing in popularity in wastewater treatment (Walker and Weatherley, 1997). Historically, activated carbon has been used to remove synthetic organic contaminants from drinking water (Kilduff and Wigton, 1999). Adsorbing contaminants onto it surface, activated carbon has also been proven to be one of the most cost effective methods of removing phenol and its derivatives from industrial wastewater (Lei et al., 2002). In a study by Gur-Reznik et al. (2008) activated carbon was used as a membrane bioreactor pretreatment to target dissolved organic matter (DOM). After the use of granular activated carbon, DOM removal was between 80 and 90%.

An advanced oxidative process (AOP) uses oxidative degradation to break down dissolved organic compounds in aqueous environments (Legrini et al., 1993). Ultraviolet (UV) light, H_2O_2 and combined technologies are AOPs in which radicals are generated by either photolysis, reaction with hydroxyl radicals, and in the case of the combined treatment, both (Legrini et al., 1993). Ksibi (2006) states that H_2O_2 has been used in wastewater treatment to reduce chemical oxygen demand (COD), biological oxygen demand (BOD), foaminess and offensive odor. Ksibi (2006) observed reduced coliform bacteria with increased dose of H_2O_2 which lead to the proposal that H_2O_2 is a cost efficient method to disinfect domestic wastewater prior to reuse in agriculture.

Ozone is a highly reactive species that can react to oxidize bonds on contact. Ozone reacts with most species which contain multiple bonds. These bonds can include the carbon to carbon double bond, or the carbon to nitrogen double bond (Gogate and Pandit, 2004). Upon contact, ozone can also form oxyanions with ionized species like S^{2-},

to form SO_3^{2-} and SO_4^{2-}. Several studies have used ozone to try to remove total and dissolved organic carbon species. Gogate and Pandit (2004) used ozonation to try to remove total organic carbon in industrial wastewater by breaking it into smaller, more biodegradable species. In the study, they discovered that after an hour of ozone exposure there was a distinct colour change in the effluent and TOC was decreased by 20%. Ozone was also used in a study conducted Ternes et al. (2003) to breakdown trace levels of pharmaceuticals in wastewater effluent. Ozone was successful in reducing the pharmaceuticals to below detection limit.

Combined AOPs have also been proposed as effective wastewater treatments due to the idea that two AOPs will work better together than the individual AOPs. A popular combination of AOPs is the combination of UV photolysis with H_2O_2. As seen in reaction Equation 4.1, the energy provided by exposure to UV light increases the rate of the generation of free radicals from H_2O_2 (Gogate and Pandit, 2004).

$$H_2O_2 + h\nu \rightarrow 2OH\bullet \quad (4.1)$$

Combination AOPs are popular in wastewater treatment and are used to remove several types of contaminants. Hou et al., (2001) used hydrogen peroxide coupled with a low pressure UV lamp to treat industrial wastewater. A low pressure UV lamp uses an electric arc coupled with mercury vapour at low pressure to produce UV light (Legrini et al., 1993). The group found that chemical oxygen demand was completely reduced after treatment and that treatment length depended on H_2O_2 concentration. A different study used the same combined AOP to treat olive mill wastewater to remove phenol and lignin, compounds known to resist biological degradation. It was discovered that the combined

UV/H_2O_2 treatment was able to remove 70% of lignin and 99.5% of phenol (Ugurlu and Kula, 2007).

The final treatment of focus in this study is oxidation by ferrate (FeO_4^{2-}, iron (VI) salts). Due to being a very strong oxidizing agent in aqueous environments and having the one of the highest redox potentials of commonly used oxidants under acidic conditions; ferrate has become an attractive method for wastewater treatment (Sharma, 2004). The redox reaction for ferrate is shown in reaction Equation 4.2.

$$FeO_4^{2-} + 8H^+ + 3e^- \leftrightarrow Fe^{3+} + 4H_2O \quad (4.2)$$

Once reduced, ferrate generates Fe(III) ions which acts as a coagulant, removing contaminants through adsorption onto aggregates which are filtered using sedimentation and filtration technologies (Jiang et al., 2006). Also, generation of Fe(III) results in the precipitation of hydrous ferric oxide (HFO) which removes reactive phosphorus through surface complexation of the phosphorus to the HFO surface (Smith et al., 2008). Unlike the other treatments mentions, ferrate has been developed for use in the wastewater industry as a method for phosphorus removal as well as to oxidize contaminants and disinfect waste water. Lee *et al*. (2009) used ferrate to simultaneously oxidize micropollutants, such as pharmaceuticals and organic model compounds, and remove phosphorus. The study was successful in reducing micropollutants up to 85%, while phosphorus removal was around 77%.

In this study we plan to achieve a new level of understanding on the effects of absorption and various AOP treatments on non-reactive phosphorus in a RO concentrate, or brine. This investigation of various bench top technologies will be completed in hopes

of finding an efficient and cost effective method for refractory (organic) phosphorus removal.

4.3 METHODOLOGY

4.3.1 Phosphorus Speciation

Phosphorus concentration of each sample was measured following Standard Methods 4500 P.E. using the ascorbic acid method (Standard Method, 1998). A complete description of the ascorbic acid method can be found in Chapter 2. Before measurement of each sample, a secondary standard of 25 mg P/L was prepared from a 1000 mg P/L standard solution made using $Na_3PO_4 \bullet 12H_2O$ (Fisher Scientific, New Jersey, USA). The secondary standard was then used to prepare three or four calibration standards for the 10 cm path length. Standard concentrations included 0.010 mg P/L, 0.025 mg P/L, 0.050 mg P/L and 0.100 mg P/L. A blank standard was prepared using millipore grade water (ultrapure water) (18.2MΩ, MilliQ). Samples and calibration standards were measured in triplicate.

Absorbance was measured using an Ocean Optics (Sarasota, FL, USA) fiber optic spectrometer equipped with a Tungsten Halogen light source (Ocean Optics LS-1) and an Ocean Optics USB2000 detector unit. Samples were measured in a 10 cm path length quartz cuvette at 649.93 nm. Light intensity was recorded for each replicate and absorbance was calculated using equation 4.3.

$$A = -\log\left(\frac{I}{I_o}\right) \tag{4.3}$$

In the above equation A is Absorbance, I is the light intensity measured from the sample and I_o is the light intensity measured from the blank standard. A calibration curve was plotted using the absorbance measured for each calibration standard. Concentrations of each sample were calculated using the equation of the line fit to the calibration standards.

4.3.2 Reverse Osmosis Concentrate

As mentioned above, reverse osmosis (RO) removes contaminants at a molecular level (Neethling et al., 2010). The RO filtrate has remarkably low levels of nutrients. However, the remaining RO brine contains non-reactive phosphorus which now needs to be removed. Reverse osmosis concentrate samples were collected from a wastewater treatment plant in Southwestern Ontario May 11th, 2011 and July 26th, 2011. Plant identity will remain anonymous for the purposes of this thesis. Samples were transported in coolers to Wilfrid Laurier University at approximately 4°C. Upon arrival, 1L aliquots of each sample were filtered into a clean high density polyethylene bottle using a 0.2µm pore size cellulose nitrate membrane filter (Whatman, Germany). Filtered and unfiltered samples were stored in a refrigerator at 4°C. A full phosphorus speciation was measured on the RO concentrate samples. Phosphorus species concentration obtained from direct measurement include total phosphorus (TP), soluble total phosphorus (sTP), total measured acid hydrolysable phosphorus (mtAHP), soluble measured acid hydrolysable phosphorus (smAHP), total reactive phosphorus (tRP) and soluble reactive phosphorus (sRP).

Absorbance was measured on the July 26th, 2011 RO Concentrate sample using a Varian Cary 50 Conc UV-Visible Spectrophotometer (Varian, Mississauga, ON). The

sample was measured in a quartz cuvette with a 1cm path length. Absorbance was measured over the range of 200 to 600nm, as well as measuring absorbance specifically at 254nm.

4.3.3 Activated Carbon

Two samples of activated carbon were obtained from Calgon Carbon Corporation (Pittsburgh, Pennsylvania); Calgon Activated Carbon (CAS#7440-44-0) DSR-A and FILTRASORB300. Activated carbon was tested with and without cleaning. The cleaning method involved rinsing the activated carbon thoroughly using ultrapure water. The activated carbon was then soaked in ultrapure water overnight and rinsed an additional three times with ultrapure water before weighing into scintillation vials or drying. The drying process involved drying the activated carbon in an oven (95°C) for 10 hours.

Three 15mL aliquots of RO concentrate was added to three scintillation vials containing approximately 1.0g, wet or dry weight, of each Calgon Activated Carbon type. The samples were allowed to sit overnight. After filtering the sample through a 0.1um polyvinyl difluoride membrane filter (Millex W Durapore®, Cork, Ireland), soluble total reactive phosphorus was measured.

4.3.4 Photolysis

A sub-sample of the July 26th, 2011 RO concentrate was sent to Trojan Technologies to be treated with ultraviolet light and shipped back to Wilfrid Laurier University for analysis. Using a xenon lamp of unspecified origin, the RO concentrate was exposed to UV light in the range of 200-300nm with a dosage of 1000 mJ/cm^2. An unfiltered sample of approximately 200mL was obtained and was stored in a refrigerator

at 4°C. Total phosphorus (TP), total acid hydrolysable phosphorus (mtAHP) and total reactive phosphorus (tRP) were measured.

4.3.5 Hydrogen Peroxide

Two 100mL samples of the May 11th, 2011 RO concentrate were treated with 20µL of 0.01% H_2O_2 (Sigma Aldrich, St. Louis, MO). After an hour, total reactive phosphorus (tRP) was measured. To remove excess H_2O_2, 10mL aliquots of each sample were heated for 20 minutes at 90°C with 800µL of 5N H_2SO_4. For these samples, the mixed reagent was made without the addition of H_2SO_4 and added to each. For more information about the mixed reagent, please refer to Chapter 2.

4.3.6 Photolysis with Hydrogen Peroxide

A sub-sample of the July 26th, 2011 RO concentrate was sent to Trojan Technologies to be treated with ultraviolet light and hydrogen peroxide and shipped back for analysis. RO concentrate was dosed with 200mg/L hydrogen peroxide and exposed to a UV dosage of 1000 mJ/cm^2. UV light exposure was a range of wavelengths between 200 and 300nm, using a xenon lamp. An unfiltered sample of approximately 200mL was obtained. Upon arrival, the sample was stored in a refrigerator at 4°C. Total phosphorus (TP), total acid hydrolysable phosphorus (mtAHP) and total reactive phosphorus (tRP) was measured on the sample.

4.3.7 Ozone

Using an Air-Zone Ozone Water Purifier XT-301 (Air-Zone Inc., Virginia), a sample of July 26th, 2011 RO Concentrate was dosed with ozone. After a ten minute warm up stage, the ozone generator produces 300 mg hour^{-1} of ozone. After rinsing, the

bubbling rock was placed into a 50 mL sample of RO Concentrate for 18 seconds, exposing the RO concentrate to an ozone dosage of 30 mg/L assuming ozone was fully dissolved in solution. Total reactive phosphorus (tRP) was measured on the ozone sample.

Absorbance of the sample was measured over different ozone exposure times using a Varian Cary 50 Conc UV-Visible Spectrophotometer (Varian, Mississauga, ON). The ozone exposure times were 0, 30, 60, 90 and 120 minutes. Ozone exposures were calculated to be 0, 150, 300, 450 and 600 mg O_3/L, respectively. Once again, ozone exposures assume complete dissolution of O_3. The sample was measured in a quartz cuvette with a 1cm path length. Absorbance was measured over the range of 200 to 600 nm, as well as at 254 nm.

4.3.8 Ferrate

A sub-sample of the July 26th, 2011 RO Concentrate was sent to Ferrate Treatment Technologies, Inc. to be treated with ferrate $(FeO_4)^{2-}$ and shipped back for analysis. RO concentrate was dosed with 1.5, 3.0, 4.0 and 6.0 mg Fe/L ferrate. Aliquots of each sample were filtered on site using a 0.2 µm cellulose nitrate membrane filter. Filtered and unfiltered samples of each ferrate dosage were shipped overnight to Wilfrid Laurier University. Upon arrival, samples were stored in a refrigerator at 4°C. Full speciation was measured on each sample.

4.3.9 Treatment of Data

Phosphorus measurements were completed in triplicate (unless stated otherwise) and tested for outliers. Any samples that were not completed in triplicate are noted.

Averaged results are presented in the results section. Results were tested for significant differences using a one way ANOVA (ANalysis Of VAriance). Data with statistically significant findings are stated as being statistically different. In the case of figures, statistically significant results are presented with asterisks over the error bars.

4.4 RESULTS

The results for the full phosphorus speciation for the July 26th, 2011 RO Concentrate sample is given in Table 4.1. Concentrations are given in µg P/L. Measured phosphorus species are described in Section 4.3.1; a more detailed description of phosphorus speciation can be found in Chapter 2. Concentrations from the measured phosphorus speciation are depicted in Figure 4.1.

Table 4.1: Concentrations (µg P/L) and standard deviation of the measured and calculated speciation fractions for the July 26th, 2011 reverse osmosis concentrate. N is the number of replicates used to calculate the concentration and standard deviation of each measurement.

	Concentration (µg P/L)	Standard Deviation	N
Total Phosphorus (TP)	61	±7	7
Soluble Total Phosphorus (sTP)	60	±2	8
Soluble Reactive Phosphorus (sRP)	11	±6	10
Total Reactive Phosphorus (tRP)	11	±4	10
Total Acid Hydrolysable Phosphorus (tAHP)	8	±3	5
Soluble Acid Hydrolysable Phosphorus (sAHP)	10	±4	5
Total Organic Phosphorus (tOP)	42	±5	5
Soluble Organic Phosphorus (sOP)	33	±5	5
Total non-Reactive Phosphorus (tnRP)	50	±3	7
Soluble non-Reactive Phosphorus (snRP)	42	±3	8

No statistical difference was found between the soluble and total analytical fractions for the July 26th, 2011 RO Concentrate, therefore data was pooled for the soluble and total fraction concentrations. These pooled concentrations are shown in Table 4.2. Average concentrations for TP, AHP and RP were measured to be 60, 9 and 11 µg/L, respectively. Organic phosphorus concentration, the difference between TP and the sum of AHP and RP, was calculated to be 40 µg/L while non-reactive phosphorus concentration, the difference between TP and RP, was calculated to be 49 µg/L. Non-reactive phosphorus is often used as a proxy for organic phosphorus. This is because concentrations of AHP and OP for the same sample are calculated from the measured fractions and the calculated concentrations can be quite different for similarly sized numbers. Figure 4.2 shows the breakdown of July 26th, 2011 RO Concentrate total phosphorus into the various phosphorus species. Total phosphorus (navy) is the sum of the reactive (red) and non-reactive species (blue), Non-reactive phosphorus can further be described as the sum of the AHP species (orange) and OP species (yellow).

Table 4.2: Averaged concentrations (µg P/L) for the measured and calculated phosphorus species for the July 26th, 2011 reverse osmosis concentrate.

	Concentration (µg P/L)
Total Phosphorus (TP)	61
Non-Reactive Phosphorus (NRP)	49
Reactive Phosphorus (RP)	11
Acid Hydrolysable Phosphorus (AHP)	9
Organic Phosphorus (OP)	40

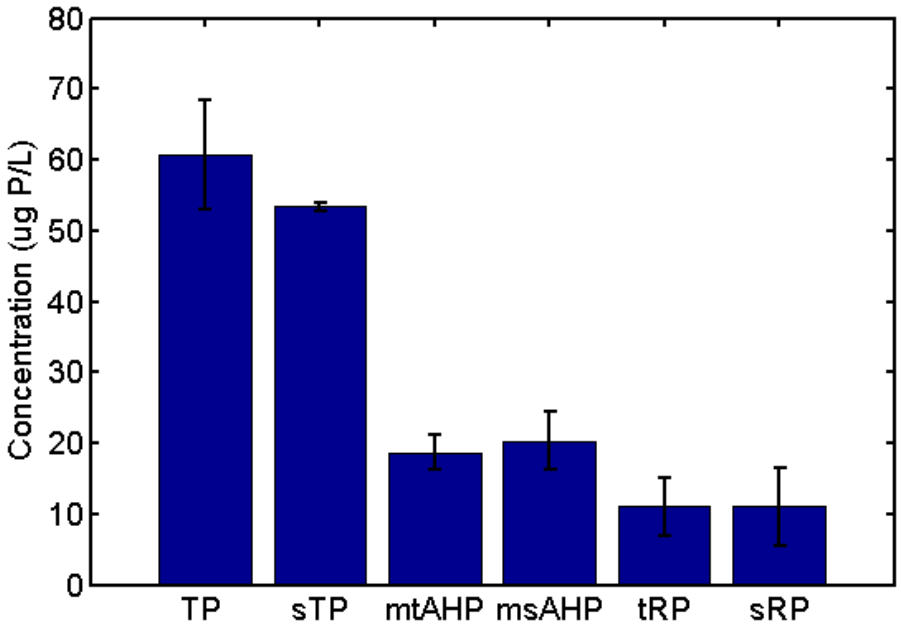

Figure 4.1: Total phosphorus (TP), soluble total phosphorus (sTP), measured total acid hydrolysable phosphorus (mtAHP), measured soluble acid hydrolysable phosphorus (msAHP), total reactive phosphorus (tRP) and soluble reactive phosphorus (sRP) measurements for the untreated RO concentrate sample from July 26th, 2012.

4.4.1 Activated Carbon

Reactive phosphorus concentrations for samples treated with either activated carbon are summarized in Table 4.3. RO Concentrate treated with rinsed activated carbon of type DSR-A had total phosphorus concentration of around 0.423 mg P/g C. After rinsing and drying the DSR-A activated carbon, the total phosphorus concentration was measured to be 0.409 mg P/g C.

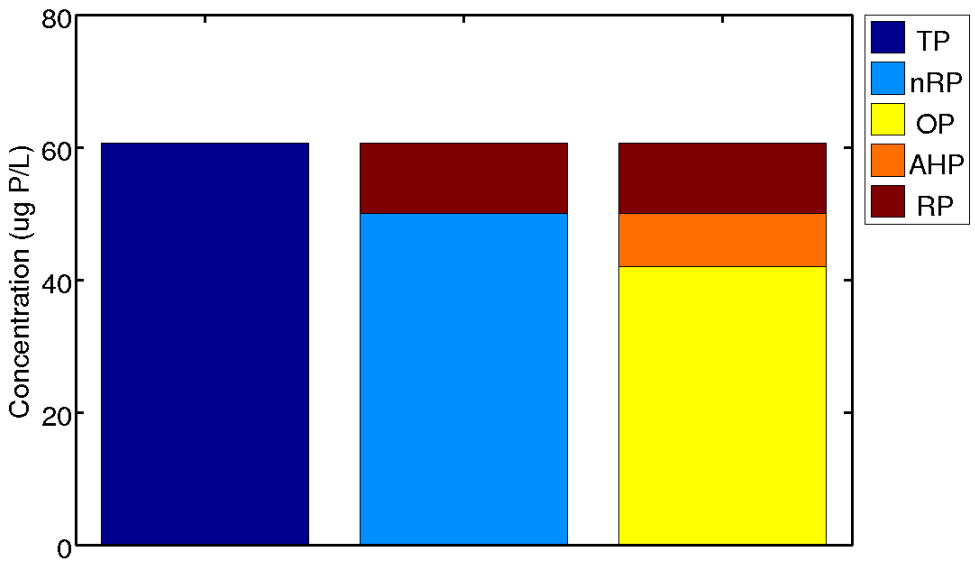

Figure 4.2: Concentration (in µg P/L) of the difference phosphorus species for the RO concentrate sample. Analytical fractions include TP (Navy), nRP (Blue), OP (Yellow), AHP (Orange), and RP (Red).

RO concentrate was also treated with rinsed low phosphorus granular activated carbon (FILTRASORB 300). Reactive phosphorus was measured to be 82µg P/L after treatment with the rinsed active carbon. Samples were then treated with low phosphorus activated carbon which had been rinsed and dried. After this treatment, reactive phosphorus was measured to be 83µg P/L. Finally, blank samples were also treated using the FILTRASORB 300 activated carbon to test for contamination. Orthophosphate was measured; sRP was measured to be 8µg P/L, or 0.008µg P/L per milligram activated carbon.

Table 4.3: Total phosphorus concentrations (mg P/g C) for the reverse osmosis concentrate treated with activated carbon.

	Concentration (mg P/g C)	% P increase
DSR-A		
Pre-rinsed	0.423	600
Pre-rinsed and Dried	0.409	570
FILTRASORB 300		
Pre-rinsed	0.082	34
Pre-rinsed and Dried	0.083	36

4.4.2 Photolysis

As previously mentioned, a sub-sample of RO Concentrate was treated with ultraviolet light. The RO concentrate was exposed to a UV dosage of 1000 mJ/cm^2. A sample of approximately 200mL was obtained. Total phosphorus (TP), acid hydrolysable phosphorus (mAHP) and total reactive phosphorus (RP) species were measured. A summary of the results for the RO brine treated with UV photolysis are presented in Table 4.4.

Average concentrations for TP, AHP and RP were measured to be 55, 4 and 24µg P/L, respectively. Organic phosphorus concentration, the difference between TP, AHP and RP, was determined to be 27µg P/L while non-reactive phosphorus concentration, the difference between TP and RP was 31µg P/L. Figure 3 shows the concentrations of phosphorus species determined through direct measurement, of the July 26th, 2011 RO Concentrate treated with UV radiation. Due to sample shortage, TP and tAHP concentrations are based on only a single measurement.

Table 4.4: Concentrations for total phosphorus (TP), acid hydrolysable phosphorus (AHP), organic phosphorus (OP), non-reactive phosphorus (nRP) and reactive phosphorus (RP) in µg P/L for the July 26th, 2011 RO Concentrate treated with UV photolysis. Standard deviation is ±1.5 for RP; TP and AHP concentrations resulting from one measurement.

	Concentration (µg P/L)
Total Phosphorus (TP)	55
Reactive Phosphorus (RP)	24
Acid Hydrolysable Phosphorus (AHP)	4
Organic Phosphorus (OP)	27
Non-Reactive Phosphorus (nRP)	31

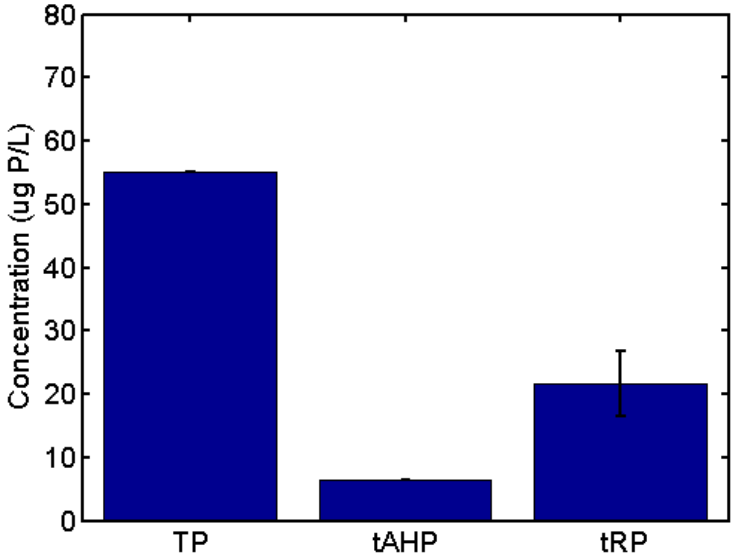

Figure 4.3: Concentration (in µg P/L) of total phosphorus (TP), total acid hydrolysable phosphorus (tAHP) and total reactive phosphorus (tRP) measured for the July 26th, 2011 RO Concentrate sample exposed to UV radiation.

4.4.3 Hydrogen Peroxide

Hydrogen peroxide treatment was used on the May 11th, 2011 RO concentrate sample. Table 4.5 and Figure 4.4 present the reactive phosphorus concentrations resulting from the H_2O_2 treatment. Untreated RO concentrate had a RP concentration of 90µg P/L.

Once treated with hydrogen peroxide, RP concentration was measured to be 149µg P/L. To remove excess H_2O_2, the samples were heated at 105°C for 30min with 800µL of 5N H_2SO_4. Reactive phosphorus was also measured for a control of RO concentrate heated with 800µL of 5N H_2SO_4 without H_2O_2. The measured concentration of reactive phosphorus for the control was 117µg P/L.

Table 4.5: Reactive phosphorus (RP) concentrations in mg P/L for the May 11th, 2011 RO Concentrate and RP of May 11th, 2011 RO Concentrate, heated with H_2SO_4 treated with and without H_2O_2. Measurements were made in triplicate.

	RP (mg P/L)	Standard Deviation
RO Concentrate (Untreated)	0.090	± 0.002
RO Concentrate without H_2O_2	0.117	± 0.003
RO Concentrate with H_2O_2	0.149	± 0.025

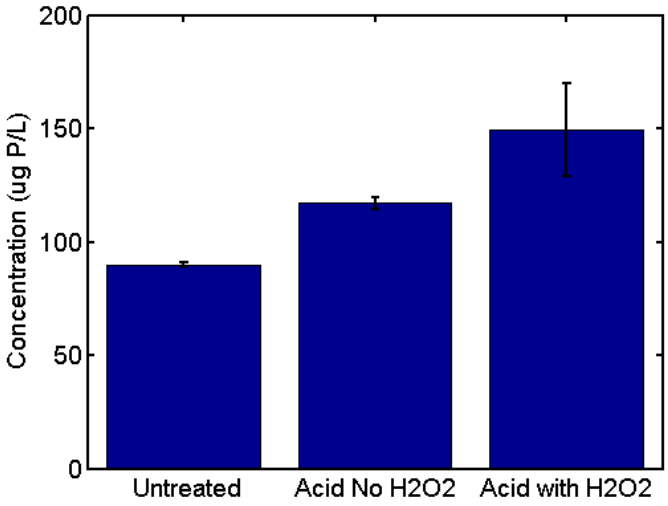

Figure 4.4: Total reactive phosphorus (tRP) concentrations in mg P/L for the May 11th, 2011 RO Concentrate and May 11th, 2011 RO Concentrate, heated with H_2SO_4 treated with and without H_2O_2.

4.4.4 Photolysis with Hydrogen Peroxide

A sub-sample of the July 26th, 2011 RO concentrate was treated with the combination of ultraviolet light and hydrogen peroxide. RO concentrate was dosed with 200 mg/L hydrogen peroxide and exposed to a UV dosage of 1000 mJ/cm^2. A sample of approximately 200 mL was obtained. Total phosphorus (TP), acid hydrolysable phosphorus (mAHP) and reactive phosphorus (RP) were measured; a summary of these results are presented in Table 4.6. A total phosphorus concentration of 64 µg P/L was measured for the treated sample while RP was measured to be 20 µg P/L. The remaining phosphorus species were determined to have concentrations of 16, 28 and 44 µg P/L for AHP, OP and nRP, respectively. The full speciation breakdown of TP into the various phosphorus species is shown in Figure 4.5.

Table 4.6: Total phosphorus (TP), total acid hydrolysable phosphorus (AHP), total organic phosphorus (OP), total non-reactive phosphorus (nRP) and total reactive phosphorus (RP) concentrations in µg P/L for the July 26th, 2011 RO Concentrate treated with UV photolysis and H_2O_2. Measurements were made in triplicate.

	Concentration (µg P/L)	Standard Deviation
Total Phosphorus (TP)	64	±6
Reactive Phosphorus (RP)	20	±3
Acid Hydrolysable Phosphorus (AHP)	16	±2
Organic Phosphorus (OP)	28	±2
Non-Reactive Phosphorus (nRP)	44	±2

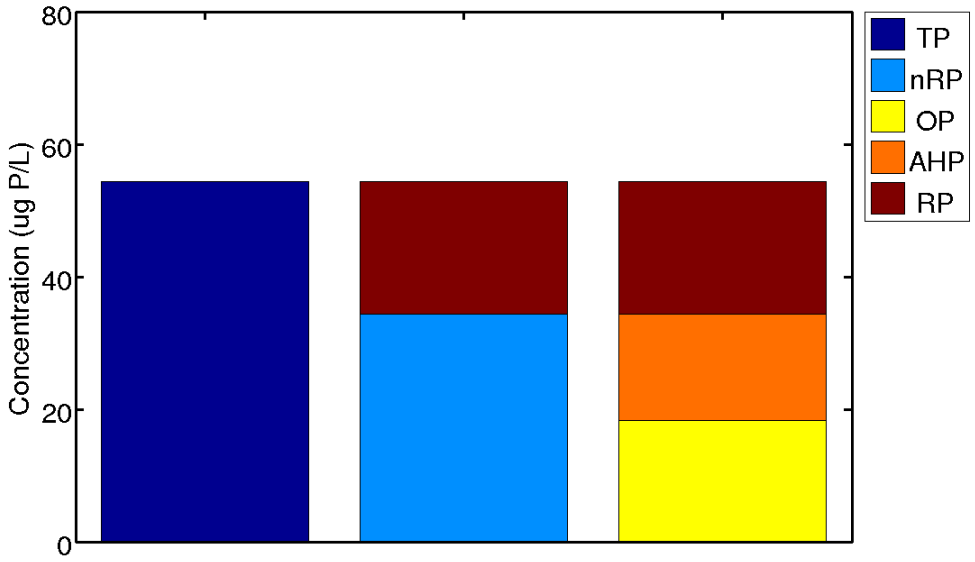

Figure 4.5: Concentration (in µg P/L) of each analytical fraction measured for the July 26th, 2011 RO Concentrate sample treated with the combined hydrogen peroxide and photolysis. Analytical fractions include TP (Navy), nRP (Blue), OP (Yellow), AHP (Orange), RP (Red).

4.4.5 Ozone

Figure 10 shows the measured reactive phosphorus (RP) concentrations for the July 26th, 2011 RO concentrate and the RO concentrate treated with ozone. RO concentrate was exposed to 30 and 2000 mg O_3/L. Concentrations of RP were determined to be 11 µg P/L for both exposure times.

Absorbance of RO concentrate was measured at different ozone exposure times. Absorbance was measured over the range from 250 to 500 nm. Absorbance, measured at 254 nm, decreases from 0.42 to 0.21 during the first 30 minutes of ozone exposure. After 60 minutes of exposure, absorbance at 254 nm was 0.21. Absorbance is measured to be 0.22 and 0.24 for ozone exposure times of 90minutes and 2 hours. After exposure to

ozone, absorbance increased at 300nm; absorbance was measured to be 0.12, 0.14, 0.20 and 0.27 for ozone exposure times of 30, 60, 90 and 120 minutes. These results are shown in Figure 4.6(a,b). Figure 4.6a shows the complete absorbance spectra from 800 to 225nm while Figure 4.6b is the change in absorbance observed at 254nm (blue) and 300nm (green).

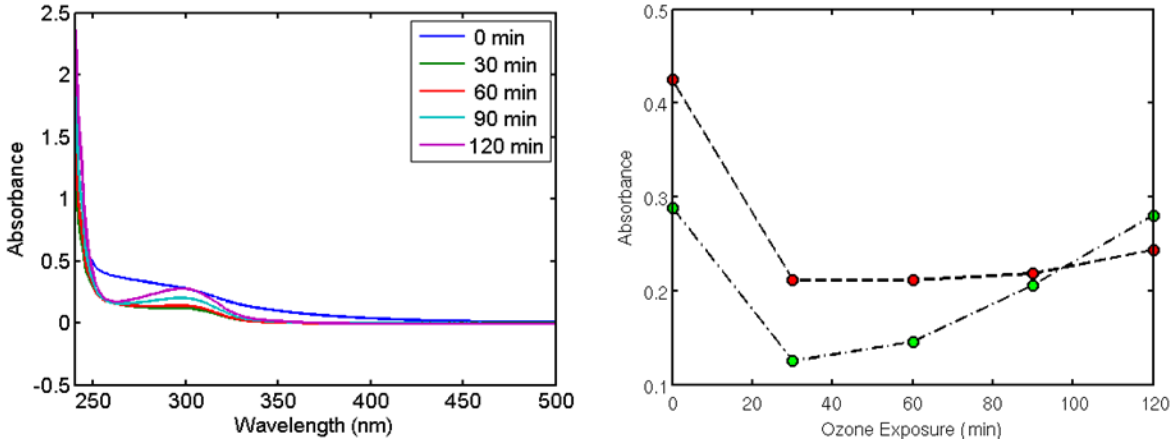

Figure 4.6: Absorbance spectra for RO Concentrate with different ozone exposure times(a), and (b) absorbance measured at 254 (red) and 300nm (green) over ozone exposure time (in minutes).

4.4.6 Ferrate

RO concentrate was treated with ferrate $[FeO_4]^{2-}$ at four different concentrations; dosages of 1.5, 3.0, 4.0 and 6.0 mg Fe/L ferrate. A subsample of each dose was filtered on site using a 0.2µm cellulose nitrate membrane filter. Filtered and unfiltered samples were shipped overnight. Upon arrival, full phosphorus speciation was measured for each ferrate dose. Phosphorus speciation results are summarized in Table 4.7. Measured species for each ferrate dosed sample are presented in Figure 4.7. Phosphorus concentrations are in units of µg P/L.

Phosphorus species concentrations determined for total analytical fractions were measured on unfiltered samples treated with 1.5, 3.0, 4.0 and 6.0mg Fe/L ferrate. Total phosphorus results for each ferrate concentration were plotted together in Figure 4.7a. Total acid hydrolysable phosphorus and total reactive phosphorus results for each ferrate concentration are shown in Figure 4.7c and 4.7e, respectively. RO concentrate treated with 3.0 mg Fe/L ferrate was determined to have a TP concentration of 61µg P/L while brine treated with 1.5 and 4.0 mg Fe/L ferrate both had concentrations of 62µg P/L. Brine treated with ferrate dosage of 6.0 mg Fe/L was determined to have a total phosphorus concentration of 63 µg P/L. For total acid hydrolysable fraction, concentrate dosed with 1.5 mg Fe/L ferrate had phosphorus concentrations of 15µg P/L and brine dosed with 4.0 mg Fe/L ferrate had concentrations of 13µg P/L. Ferrate doses of 3.0 and 6.0 mg Fe/L both had tAHP concentrations of 14µg P/L. The final fraction, tRP, was determined to be 7 µg P/L for 4.0 mg Fe/L ferrate and 6 µg P/L for 6.0 mg Fe/L ferrate. Total reactive phosphorus was measured to be 12 µg P/L for the 1.5 and 3.0 mg Fe/L ferrate treatment. There was no significant difference between phosphorus concentrations of the measured analytical fractions with respect to ferrate dose.

Table 4.7: Concentrations (µg P/L) for measured and calculated speciation fractions for ferrate dosed July 26th, 2011 RO Concentrate sample.

Ferrate Dose (mg Fe/L)	TP	tRP	tAHP	tOP	tnRP	sTP	sRP	sAHP	sOP	snRP
1.5	62	15	12	35	47	40	5	8	27	34
3.0	61	13	12	36	48	35	5	18	12	31
4.0	62	14	7	41	49	44	6	8	31	39
6.0	63	13	6	44	50	39	8	11	21	31

Ferrate treated RO concentrate had a total organic phosphorus concentration (tOP), the difference between TP and the sum of tAHP and tRP, of 36 µg P/L and a total non-reactive phosphorus concentration (tnRP), the difference between TP and tRP of 48 µg P/L. Figure 4.8 shows a breakdown of TP into the different unfiltered (total) analytical fractions of the July 26th, 2011 RO Concentrate treated with ferrate. Total phosphorus is shown in navy, the total organic phosphorus fraction is blue, total acid hydrolysable phosphorus is shown in cyan, non-reactive phosphorus is orange and total reactive phosphorus is shown in yellow and red.

Filtered ferrate samples were used to measure each analytical fraction of the soluble phosphorus species for each ferrate dosage. Soluble total phosphorus concentrations for samples dosed with 1.5, 3.0, 4.0 and 6.0 mg Fe/L ferrate are shown in Figure 4.7b, while soluble acid hydrolysable phosphorus and soluble reactive phosphorus results for each ferrate concentration are shown in Figure 4.7d and 4.7f, respectively. RO concentrate dosed with 1.5 mg Fe/L ferrate had an sTP concentration of 40 µg P/L, an sAHP concentration of 8 µg P/L and an sRP concentration of 5 µg P/L. Brine treated with a ferrate dose of 3.0 mg Fe/L also had an sRP of 5 µg P/L, but had an sAHP concentration of 18 µg P/L and an sTP concentration of 35 µg P/L. RO concentrate dosed with 4.0 mg Fe/L of ferrate had sTP concentrations of 44 µg P/L, sAHP concentrations of 8 µg P/L and sRP concentrations of 6 µg P/L. Sample dosed with the final ferrate concentration, 6.0 mg Fe/L, had sTP concentrations of 39 µg P/L, sAHP concentrations of 11 µg P/L and an sRP concentration of 8 µg P/L. There was no significant difference in phosphorus species concentration between the four ferrate concentrations.

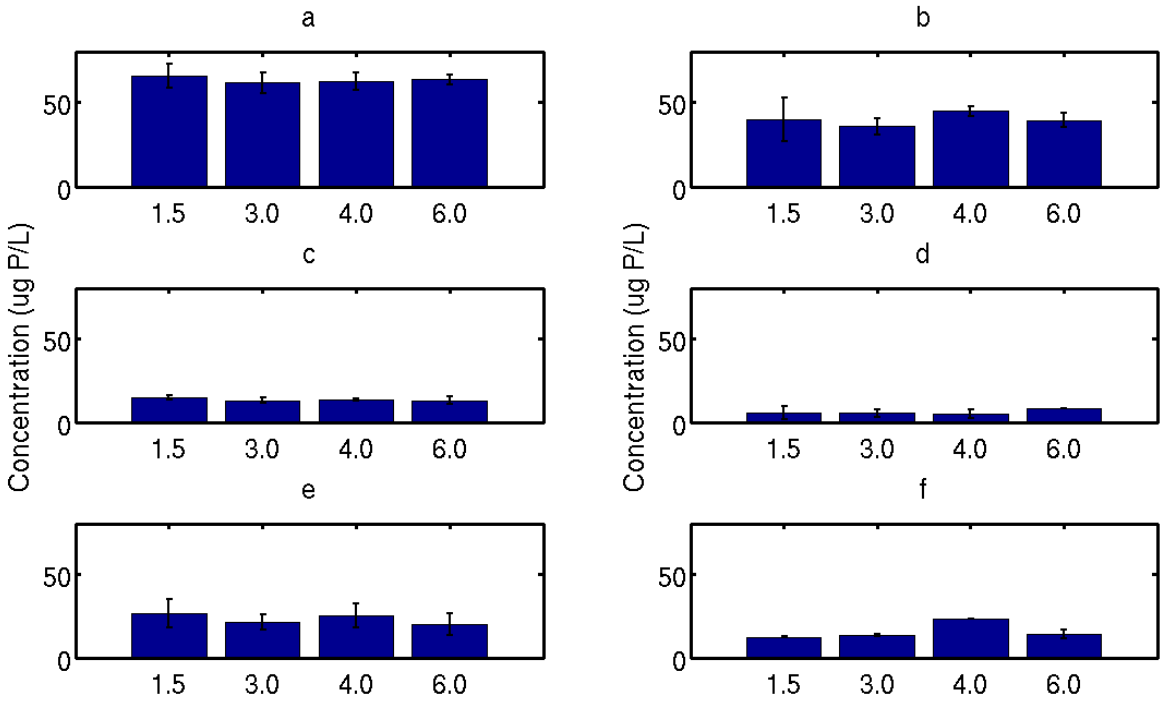

Figure 4.7: Total and soluble measured analytical phosphorus species for RO concentrate dosed with 1.5, 3.0, 4.0 and 6.0 mg Fe/L ferrate. Phosphorus species include total phosphorus (a), soluble total phosphorus (b), total reactive phosphorus (c), soluble reactive phosphorus (d), measured total acid hydrolysable phosphorus (e) and measured soluble acid hydrolysable phosphorus (f).

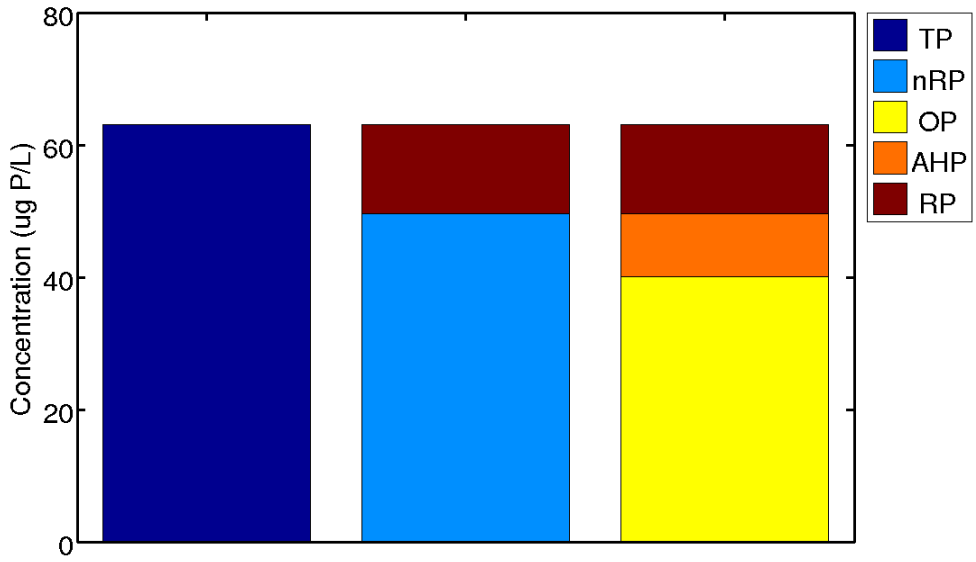

Figure 4.8: Concentration (in µg P/L) of each total phosphorus species measured for the July 26th, 2011 RO Concentrate sample treated ferrate. Analytical fractions include TP (Navy), OP (Blue), AHP (Cyan), RP (Yellow), nRP (Orange) and RP (Red).

Figure 4.9 is a breakdown of sTP into the different filtered (soluble) phosphorus species. Soluble total phosphorus for all four ferrate concentrations is shown in navy. Soluble total phosphorus can be described as being the sum of total organic phosphorus (blue), total acid hydrolysable phosphorus (cyan) and total reactive phosphorus (yellow and red). Non-reactive phosphorus is the sum of the acid hydrolysable and organic phosphorus fractions (cyan + yellow). Overall, RO concentrate treated with ferrate contains 23 µg P/L sOP and an sAHP concentration of 11µg P/L. After being treated with ferrate, RO concentrate had sRP and snRP in turn had concentrations of 6 and 34 µg P/L, giving an sTP concentrations of 40 µg P/L.

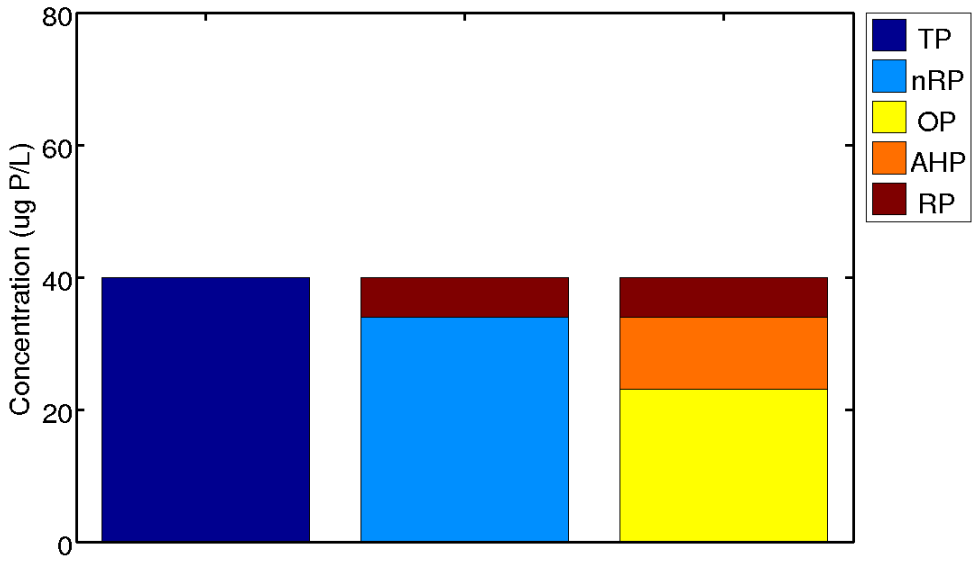

Figure 4.9: Concentration (in µg P/L) of each soluble phosphorus species measured for the July 26th, 2011 RO Concentrate sample treated ferrate. Analytical fractions include TP (Navy), OP (Blue), AHP (Cyan), RP (Yellow), nRP (Orange) and RP (Red).

4.5 DISCUSSION

With the exception of the H_2O_2 treatment, the screening of various phosphorus removal methods was completed on a reverse osmosis (RO) concentrate sample. The concentrate was sampled, shipped and filtered on the same day, July 26th, 2011. The H_2O_2 treatment was tested on a RO concentrate sampled May 11th, 2011 from the same wastewater treatment plant.

As noted in Section 4.4, differences between total and soluble analytical fractions were not found to be statistically significant. This is most likely due to the reverse osmosis process. During reverse osmosis wastewater is pushed through membrane filters at high pressure. These membrane filters have pore sizes in the nanoscale, much smaller

than the operationally defined 0.2 µm filtered fraction of this study. Ergo, due to filtration by the RO membrane system, soluble and total phosphorus species in the untreated RO concentrate were expected to be the same.

4.5.1 Activated Carbon

Activated carbon has been used in the past to remove organic contaminants from industrial run off (Lei et al., 2002). Because of its historical use, activated carbon was chosen in this study in hopes to target organic phosphorus. Originally, RO concentrate was dosed with either one of two forms of activated carbon and soluble total phosphorus (sTP) was measured. This analytical fraction was focused on because of the nature of absorption chemistry. It was expected that activated carbon would remove phosphorus by absorption to its surface. RO concentrate was treated with activated carbon and filtered through a 0.1µm filter to remove as much activated carbon as possible. After digestion, sTP was measured. Once the mixed reagent was added to each sample, the sample was so highly coloured the concentration was above the detection range of the spectrophotometer. This lead to the development of the rinsing procedure described in Section 4.3.3.

After rinsing, in both forms of activate carbon, an increase in sTP was observed when activated carbon was mixed with brine. Figure 4.10 shows the percent increase in phosphorus for activated carbon DSR-A and FILTRASORB 300 (FILTRA) for both pre-washing methods. RO concentrate treated with activated carbon of type DSR-A had an increase in total phosphorus of 362µg P/L, an increase of 600%. To try to reduce the phosphorus concentration, the activated carbon was rinsed excessively after the overnight soak and dried in the oven overnight. Total phosphorus in the RO concentrate treated

with the rinsed and dried DSR-A once again increased from 61µg P/L (untreated) to 409µg P/L, an increase of around 570%. The additional washing had no effect on the contamination from the activated carbon. Activated carbon of type DSR-A was determined to be a source of phosphorus.

Both washing procedures, pre rinsing with and without drying, were completed on the low phosphorus activated carbon (FILTRASORB 300). RO concentrate treated with rinsed wet low phosphorus activated carbon had an increase in total phosphorus of 21µg P/L, an increase of 34% from 61 to 82µg P/L. After further rinsing of the activated carbon and drying in the oven, total phosphorus once again increased from 61µg P/L (untreated) to 83µg P/L, an increase of 36%. Once again, the additional rinse procedure did not have a significant effect on the phosphorus contamination.

To determine the extent of phosphorus contamination, the low phosphorus activated carbon was rinsed several times with ultrapure water before weighing out 1.0

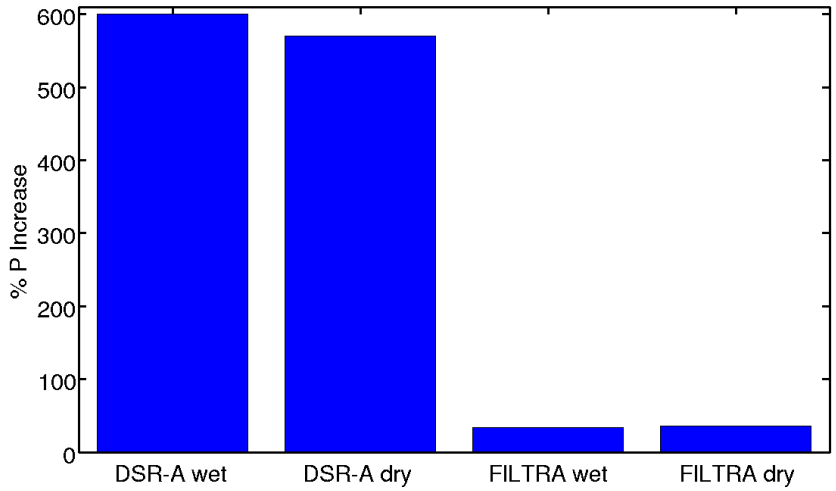

Figure 4.10: Percent increase in total phosphorus for activated carbon type DSR-A and FILTRASORB 300 for the wet and dried activated carbon.

gram of wet activated carbon into 15 mL of ultrapure water. Soluble reactive phosphorus was measured immediately. Orthophosphate was present in the blank samples; tRP was measured to be 8 µg P/L, or 0.008 µg P/L per milligram activated carbon. Upon further investigation, it was found that phosphoric acid is used as a chemical treatment to develop the internal pore structure of the carbon material (Lei et al, 2002). Unfortunately, because the forms of activated carbon used in this study were sources of phosphorus, it cannot be used for phosphorus removal.

4.5.2 Photolysis

RO concentrate was treated with UV radiation in hopes to break up non-reactive phosphorus and liberate orthophosphate. For this reasoning, soluble reactive phosphorus was the analytical fraction of focus. After UV exposure, sRP increased from 11 to 24µg P/L. A comparison between the sRP, sAHP and sOP analytical fractions for the treated and untreated RO concentrate is shown in Figure 4.11. The increase in sRP is due to

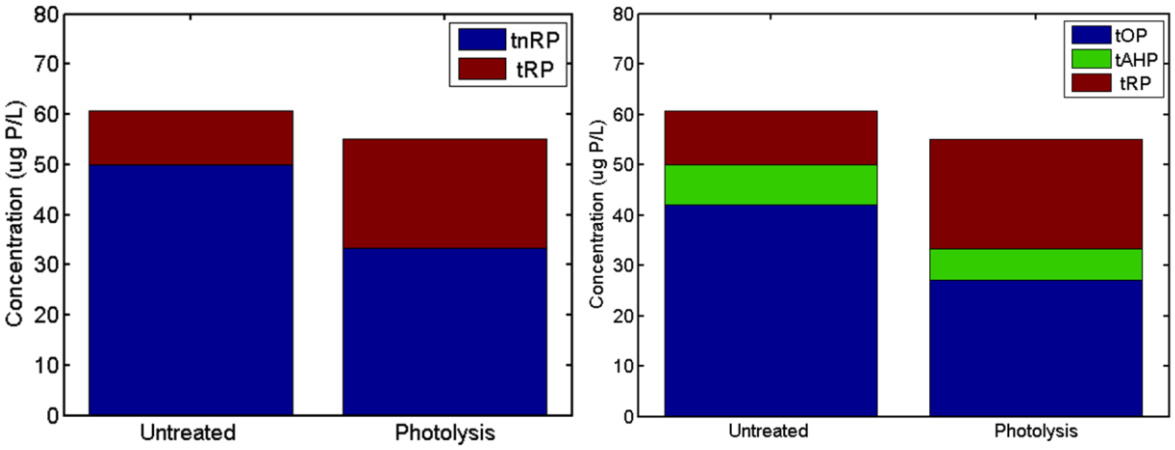

Figure 4.11: Comparison of the phosphorus species between untreated and photolysis treated RO concentrate. Total organic phosphorus, total acid hydrolysable phosphorus and total reactive phosphorus are compared on the left, while total reactive phosphorus and total non-reactive phosphorus is shown on the right.

conversion of OP to orthophosphate. After treatment with UV photolysis, OP decreased from 40 to 27µg P/L, a conversion of nRP to RP of approximately 13µg P/L (a conversion of 26%).

The goal of UV photolysis treatment was to decrease nRP. The treatment was successful in reducing non-reactive phosphorus by 18µg P/L, a difference of almost 38%; however it did not liberate as much orthophosphate as hoped. Although photolysis has potential, to breakup more non-reactive phosphorus the UV dosage would have to be increased. This increase would lead to an increase in overall treatment cost which, in addition to the cost already associated with running a wastewater treatment plant, would not be practical in the wastewater industry.

4.5.3 Hydrogen Peroxide

Hydrogen peroxide is known for its ability to oxidize bonds in organic compounds (Gogate and Pandit, 2004). RO concentrate was treated with hydrogen peroxide in hopes to cleave bonds within AHP and OP to liberate orthophosphate. Reactive phosphorus was the analytical fraction of focus to determine if orthophosphate is being released. Problems occurred with colour development during the first round of treatment. Instead of the blue colour change typical of phosphorus determination, the solution turned bright yellow. This is due to the presence of H_2O_2 in the sample. Normally, when mixed reagent is added to the sample, phosphomolybdic acid is reduced by ascorbic acid. This causes a colour change from yellow (oxidized) to blue (reduced). All H_2O_2 was not used up during treatment of the sample, causing further oxidation of the molybdate complex and thereby retaining the complexes yellow colour. Upon this discovery, the method of measurement was altered. In lieu of adding 5N H_2SO_4 to the

mixed reagent, the same proportion of acid was added directly to each sample and the sample was heated to remove excess H_2O_2.

A comparison between the untreated RO concentrate, a RO concentrate control heated with acid and the H_2O_2 treated RO concentrate is shown in Figure 4.4. While reactive phosphorus concentrations increased in both the H_2O_2 treated and untreated the RO concentrate heated with acid, there is was a larger increase for the H_2O_2 treated RO Concentrate. Heating the control with 5N H_2SO_4 led to an increase in reactive phosphorus of 27µg P/L. Liberating another 5µg P/L, the H_2O_2 treated RO Concentrate heated with 5N H_2SO_4 had an increase in tRP concentration of 32µg P/L. Unfortunately, the conditions which were needed to remove the excess H_2O_2 were not desirable due to the fact that the effectiveness of H_2O_2 could not be measured alone; a hot digestion of H_2O_2 with H_2SO_4 was liberating reactive phosphorus.

4.5.4 Photolysis with Hydrogen Peroxide

Separately, photolysis and hydrogen peroxide were both able to oxidize non-reactive phosphorus, however not to the extent expected. UV photolysis was used in combination with H_2O_2 in hope to enhance oxidation of non-reactive phosphorus. Exposure of H_2O_2 to UV light increases the liberation of hydroxyl radicals as seen in reaction Equation 4.1. Figure 4.12 compares several unfiltered phosphorus speciation fractions of the UV/H_2O_2 treated RO Concentrate sample to the untreated RO Concentrate. In the UV/H_2O_2 treated RO Concentrate sample, a decrease was observed in tnRP from 49 to 44 µg P/L. This was mostly seen in a reduction of tOP which decreased from 40 to 28 µg P/L, a decrease of almost 30%. An increase was observed for the tAHP (8 to 16 µg P/L). This could indicate that use of UV/H_2O_2 oxidation process converts the

larger molecules tOP and tnRP to the smaller tAHP and tRP molecules. Overall, the percent conversion of nRP to RP was 18%.

Combined UV and H_2O_2 treatment proved to be more efficient at breaking down non-reactive phosphorus than the two treatments did separately. UV photolysis broke down 38% of nRP, while the effect of H_2O_2 alone was not quantified because an additional hot acid digestion was required to remove excess H_2O_2. As with straight UV photolysis, changing the UV dose could give a higher conversion. However, as mentioned previously, increasing UV dosage may not be economically feasible. Increased concentrations of hydrogen peroxide while maintaining the same UV dosage of 1000 mJ/cm^2 could lead to promising results, but more investigation is needed.

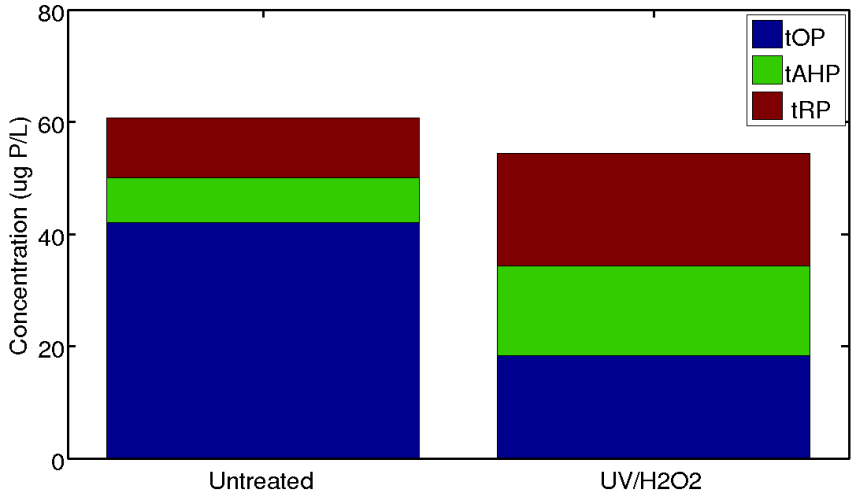

Figure 4.12: Organic phosphorus (tOP), non-reactive phosphorus (tAHP) and reactive phosphorus (tRP) concentrations in mg P/L for the July 26th, 2011 RO Concentrate and RO Concentrate treated with H_2O_2/UV photolysis mixed technologies.

4.5.5 Ozone

Introduction of ozone into solution will lead to the oxidation of bonds by direct contact of ozone with the contaminant. Since ozone is highly reactive towards multiple bond (for example double bonds), it was hoped that non-reactive phosphorus would be targeted and reactive phosphorus would be released. Reactive phosphorus was measured to determine if this was indeed the case. After exposure to a short contact time to ozone, RP was measured and no change was observed. This showed no oxidation of phosphorus containing molecules. An increased ozone exposure time was also tried, in which the ozone was in contact with a total nominal ozone dosage of approximately 2000 mg/L. Once again there was no change in reactive phosphorus concentrations. Gogate and Pandit (2004) also found that the use of ozone alone resulted in low reaction rates for the degradation of several contaminants.

Although it was unfortunate that there was no evidence of non-reactive phosphorus oxidation, there was a small colour change in the solution. This decrease in colour was also observed in a study conducted by Ruppert and Bauer (1994) when they subjected dye industry wastewater to ozone. The change in colour gave evidence that ozone was oxidizing some organic matter, although the organic matter did not contain phosphorus. To examine the change in DOM in the RO concentrate with respect to ozone exposure, absorbance spectra were collected over ozone exposure time, shown in Figure 4.7. With increased ozone exposure there was a decrease in absorbance at 254nm indicating a decrease in dissolved organic carbon (USEPA, 2005). Another interesting result of exposure to ozone was the increase in absorbance at approximately 300nm. This

may be due to the accumulation of ozone in the brine, although further investigation is necessary.

4.5.6 Ferrate

Ferrate treatment had the largest effect on the soluble fractions of phosphorus. This is due to ferrate oxidizing the non-reactive and organic phosphorus molecules to release orthophosphate which is then removed from solution through co-precipitation of the orthophosphate into the hydrous ferric oxide via the surface complexation mechanism proposed by Smith et al. (2008). Figure 4.14 compares untreated brine with brine (filtered and unfiltered) treated with ferrate. Soluble total phosphorus (sTP) fraction of the ferrate samples, on average, showed a removal of 20 µg P/L. Soluble organic phosphorus (sOP), soluble non-reactive phosphorus (snRP) and soluble reactive phosphorus (sRP) all decreased due to the ferrate treatment. With the highest amount of removal, sOP decreased from 33 to 23 µg P/L, while sRP decreased from 11 to 6 µg P/L, respectively.

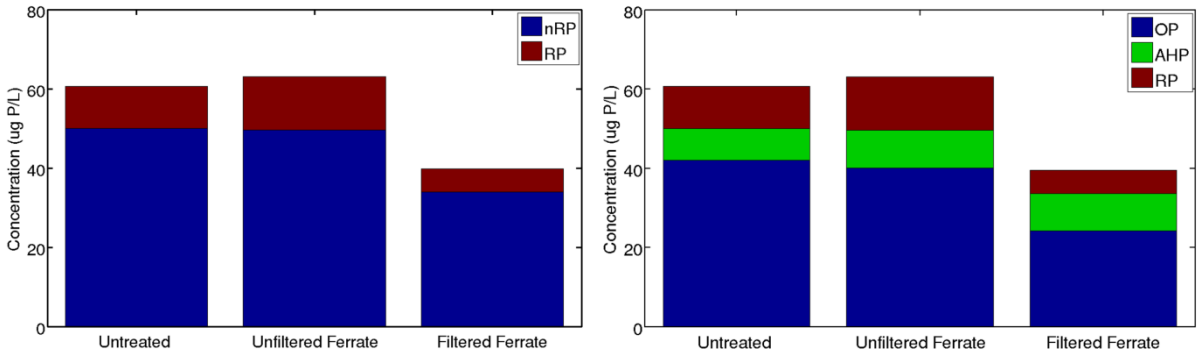

Figure 4.13: **Comparison between the untreated RO concentrate and RO concentrate treated with ferrate. Analytical fractions include organic phosphorus (sOP), acid hydrolysable phosphorus (AHP) and reactive phosphorus (RP), total phosphorus (TP), total organic phosphorus (tOP), total acid hydrolysable phosphorus (tAHP) total non-reactive phosphorus (tnRP) and total reactive phosphorus (tRP) concentrations in µg P/L.**

Soluble acid hydrolysable phosphorus (sAHP) slightly increased from 10 to 11 µg P/L. This may be explained by larger organic and nonreactive phosphorus molecules being broken down into smaller condensed phosphorus molecules; however, further investigation is required to rule out experimental error. Chemical precipitation is a part of ferrate treatment; therefore conversion from nRP to RP is not an appropriate comparison.

Figure 4.14 shows the speciation fractions for the unfiltered ferrate samples. Total reactive phosphorus (tRP) increased from 11 to 14 µg P/L during the ferrate treatment. This could also be due to the release of orthophosphate from the oxidized total organic phosphorus fraction. As mentioned previously, once ferrate is reduced to Fe(III), the liberated orthophosphate is removed from solution through co-precipitation. Therefore, as a quality assurance method, TP was measured on the well mixed, unfiltered ferrate samples. Total phosphorus of the unfiltered sample was 62 µg P/L which is not significantly different from the original TP concentration; therefore total phosphorus was recovered.

Ferrate treatment includes filtration of the final effluent as part of the treatment process. Therefore, it is important to compare total phosphorus and soluble total phosphorus after treatment to see if ferrate treatment is effective. In this case, soluble total phosphorus is 20µg P/L less than total phosphorus, a TP removal of 35%, indicating that ferrate may be a promising phosphorus removal treatment.

4.6 CONCLUSION

Several bench top AOP technologies and activated carbon were investigated in hope of discovering a cost effective and efficient method to oxidize non-reactive phosphorus for ease of removal. Due to the method used to prepare the surface of activated carbon, activated carbon was deemed to be a source of phosphorus contamination and not an appropriate method for phosphorus removal. Ozone had no effect on non-reactive phosphorus, but was found to be oxidizing some labile form of organic matter that did not contain phosphorus. Complications with colour formation arose with use of hydrogen peroxide leading to reactive phosphorus liberation with the use of H_2O_2 hot acid digestion. When used separately, UV photolysis was found to decrease non-reactive phosphorus by approximately 26% percent. In the combined UV/H_2O_2 treatment, non-reactive phosphorus was decreased by 18%. Ferrate, the final AOP investigated in this study, was found to decrease total phosphorus by approximately 35%. With the exception of activated carbon, the different treatments investigated show promise of conversion of non-reactive to reactive phosphorus. Ferrate treatment could be very useful due to it being a combination treatment, combining oxidation and chemical precipitation.

4.7 REFERENCES

Gogate, P. R. and Pandit, A. B. (2004) A review of imperative technologies for wastewater treatement II: hybrid methods. *Advances in Environmental Research* **8**, 553-597.

Gur-Reznik, S., Katz, I. and Dosoretz, C. G. (2008) Removal of dissolved organic matter by granular-activated carbon adsorption as a pretreatment to reverse osmosis of membrane bioreactor effluents. *Wat. Res.* **42**, 1595-1605.

Hou, W., Tsuneda, S. and Hirata, A. (2001) Efficient TOC removal of wastewater containing 1,2-naphthoquinone-2-diazido-5-sulfonic acid sodium salt with H_2O_2/UV in a batch reactor. *J. of Chemical Engineering of Japan* **34**, 1084-1090.

Jiang, J., Wang, S., and Panagoulopoulos, A. (2006) The exploration of potassium ferrate(VI) as a disinfectant/coagulant in water and wastewater treatment. *Chemosphere* **63**, 212-219.

Kilduff, J. E. and Wigton, A (1999) Sorption of TCE by Humic-Preloaded Activated Carbon: Incorporating Size-Exclusion and Pore Blockage Phenomena in a Competitive Adsorption Model. *Environ. Sci. Technol.* **33**, 250-256.

Ksibi, M. (2006). Chemical oxidation with hydrogen peroxide for domestic wastewater treatment. *Chemical Engineering Journal* **119**, 161 -165.

Lee, Y., Zimmerman, S. G., Kieu, A. T. and von Gunten, U. (2009) Ferrate (Fe(VI)) Application for Municipal Wastewater Treatment: A Novel Process for Simultaneous Micropollutant Oxidation and Phosphate Removal. *Environ. Sci. Technol.* **43**, 3831-3838.

Legrini, O., Oliveros, E. and Braun, A. M. (1993) Photochemical Processes for Water Treatment. *Chem. Rev.* **93**, 671-698.

Lei, L., Quinlwan, P. A. and Knappe, D. R. U. (2002) Effects of activated carbon surface chemistry and pore structure on the adsorption of organic contaminants from aqueous solution. *Carbon* **40**, 2085-2100.

Maher, W., & Woo, L. (1998). Procedures for the storage and digestion of natural waters for the determination of filterable reactive phosphorus, total filterable phosphorus and totalphosphorus. *Analytica Chimica Acta* , **375**, 5-47.

Monser, L and Adhoum, N. (2002) Modified activated carbon for the removal of copper, zinc, chromium and cyanide from wastewater. *Separation and Purification Technology* **26**, 137-146.

Neethling, J. B., M. Benisch, D. Clark, D. Fisher, and A. Z. Gu (2007, October). Phosphorus speciation provides direction to produce 10 μg/l. In Conference proceedings, 80th annual water environmental federation technical exhibit and conference, San Diego, California, USA, pp. 1607–1624. Water Environment Federation: WEF.

Neethling, J. B., Gu, A. Z. and Pattarkine, V. M. (2010) Overview of Nutrient Removal Processes. In *Nutrient Removal: WEF Manual of Practice No. 34*; Water Environment Federation® (2010). WEF Press. Alexandria, VA.

Ruppert, G. and Bauer, R. (1994) UV-O_3, UV-H_2O_2, UV-TiO_2 and the photo-Fenton reaction – Comparison of advanced oxidation processes for wastewater treatment. *Chemosphere* **28**, 1447-1454.

Sharma, V. K. (2004) Use of iron(VI) and iron(V) in water and wastewater treatment. *Water Science and Technology* **49**, 69-74.

Smith, D. S., I. Takács, S. Murthy, G. Diagger, and A. Szabó (2008). Phosphate complexation model and its implications for chemical phosphorus removal. *Water Environment Research* **80**, 428–438.

Standard Methods for Examination of Water and Wastewater. (1998). (20th ed.). American Public Health Association (APHA) and American Water Works Association (AWWA) and Water Environment Federation (WEF); Washington D.C., USA.

Ternes, T. A., Stüber, J., Hermann, N., McDowell, D., Reid, A., Kampmann, M. and Teiser, B. (2003) Ozonation: A tool for removal of pharmaceuticals, contrast media and musk fragrances from wastewater? *Wat. Res.* **37**, 1976-1982.

Urgurlu, M. and Kula, İ. (2007) Decolourization and Removal of Some Organic Compounds from Olive Mill Wastewater by Advanced Oxidation Processes and Lime Treatment. *Env. Sci. Pollut. Res.* **14**, 319-325.

USEPA (2005). Method 415.3 Determination of Total Organic Carbon and Specific UV Absorbance at 254 nm in Source and Drinking Water. February 2005, 1 – 56.

vanLoon, G. W. and Duffy, S. J. (2000). *Environmental chemistry a global perspective*. New York, NY: Oxford University Press.

Walker, G. M. and Weatherley, L. R. (1997). Adsorption of acid dyes on to granular activated carbon in fixed beds. *Wat. Res.* **31**, 2093 – 2101.

Chapter 5: Characterization of surface reactive sites in high solids synthetic wastewater and implications for pH simulation

5.1 ABSTRACT

Simulation of pH is very important for almost all wastewater treatment processes. Current modeling determines pH based on the concentrations of strong base cations, strong acid anions, weak acids and ammonia. This causes an underestimation of pH because the modeling does not take into account positively charged surface reactive sites in wastewater solids. The effect on proton concentration can be seen in the following rearranged electroneutrality equation: $[H^+] = \sum$[Strong acid anions] - $\sum$[Strong base cations] + $\sum$[Weak acid anions] - $\sum$**[positive surface sites]**. Characterization of the bolded terms could lead to the improvement of phosphorus removal modeling. Acid-base titrations are an excellent method to probe surface reactivity in terms of proton binding affinities (pK_a) and capacities. For each type of reactive surface group, proton binding affinity and ionizable site concentrations are unique. Data obtained from acid-base titrations can be used to determine reactive site concentrations at certain pK_a values. This study uses linear programming to calculate reactive site concentrations at various pK_a values. A synthetic wastewater was used since characterization of surface reactive sites would lead to an improvement in wastewater treatment modeling. High solid titration data agreed with the model after the addition of two positively charged surface reactive sites to the pH modeling. The first positively charged site had a pK_a of around 8 while the second site had a pK_a around 10.2. The pK_a value of 8 agreed with pK_as found for hydrous ferric oxides in literature as well as the pK_a spectra calculated using titration data and discrete site analysis for the high solids system.

KEYWORDS

Acid Base Titrations, Waste Water, Surface Characterization, Reactive Sites

5.2 INTRODUCTION

Modeling or simulating the various processes in nutrient removal has become a very important step in the design and optimization of a wastewater treatment plant. Simulation of a wastewater treatment process, for example chemically mediated phosphorus removal, can help to determine optimal ferric dosage, the level of mixing and/or the pH of the system. Simulation of pH is very important for almost all wastewater treatment processes. In biological removal, pH influences the biological activity of the microorganisms which have an optimal pH range. Outside of this pH range, biological activities are severely limited and may lead to organism death (Takács et al., 2010). In chemical removal, pH affects the rates of chemical precipitation reactions; the optimal pH range for chemical phosphorus removal was found to be between 3 and 5 (Fairlamb et al., 2003; Takács et al., 2010).

In the past, changes in alkalinity were used as a gauge to monitor potential problems with pH stability; alkalinity is the difference between the concentrations of strong anions and strong cations. Alkalinity was used because directly simulating pH was difficult due to the complexity of the underlying reactions and constituents (Fairlamb et al., 2003). Using alkalinity to indicate problems with pH had many disadvantages. One disadvantage is that this method makes the assumption that pH is in a range where it does not affect biological activity and that pH remains relatively constant. The second disadvantage is that precipitation and chemical reactions cannot be modeled using

alkalinity (Takács et al., 2010). Due to these limitations, pH simulation has been the focus of several studies. One of the most applicable models was developed by Fairlamb et al. (2003) for use in the wastewater treatment processes. The model takes into account equilibrium reactions of the major wastewater species, activity coefficients corrected for ionic strength, gas-liquid transfer and it includes compounds which effect biological activity.

The first proposal of an equilibrium/kinetic mixed approach to model pH was made by a group calculating pH for an aerobic digestor (Batstone el al., 2002). To simulate pH using the equilibrium/kinetic based model, the factors that affect pH are divided into two groups based on reaction rate constants (Takács et al., 2010). Processes which are classified into the first group have reaction rates that are fast enough to be considered to be at "equilibrium"; this first group is considered to be the equilibrium group. The reactions in the second group, the kinetic group, have rates that are much slower. The main difference between the two groups is how they are incorporated into the model. The equilibrium group only needs to take into account the total concentrations of the species while the kinetic group must have variables that take into account both reactants and products (Takács et al., 2010).

There are still areas in pH simulation in need of development. The CAMBI system, a high solids system that utilizes heat to break down organic waste material, specifically requires an adjusted pH model that takes into account the surface reactive sites of the suspended solids (Neyens and Baeyens, 2003). Current modeling determines pH based on the concentrations of strong base cations, strong acid anions, weak acids and ammonia. This causes an overestimation of $[H^+]$ because the modeling does not take into

account positively charged surface reactive sites in wastewater solids and proteinacious material. In high solid systems this problem is intensified by the addition of many surface reactive sites. Characterization of positively charged wastewater surface reactive sites will help correct the underestimation of pH in wastewater treatment modeling.

Surface reactivity is the result of deprotonation of acidic functional groups on the surface as the surface pH increases. For each reactive site type, proton binding affinities are unique and are dependent on the type and concentration of reactive surface group (Martinez et al., 2002). Acid-base titrations are a useful method to investigate surface reactivity by determining pK_a values and proton binding capacities (Smith et al., 2003).

The acid dissociation constant (K_a) is defined as the equilibrium constant for the reaction of the acid with water (Harris, 2003). A general acid dissociation reaction is shown in Equation (5.1).

$$HA \xleftrightarrow{Ka} H^+ + A^- \tag{5.1}$$

The equation using concentrations for K_a is shown in Equation (5.2). Concentration of a species is indicated by square brackets.

$$K_a = \frac{[H^+][A^-]}{[HA]} \tag{5.2}$$

The relationship between K_a and pK_a is shown in Equation (5.3).

$$pK_a = -\log K_a \tag{5.3}$$

In a thermodynamically correct equilibrium expression, activities are used instead of concentrations (Harris, 2003).

For a titration, stepwise data can be used to calculate charge excess; charge excess (b) is the negative charge required for electroneutrality and is calculated using Equation (5.4) (Sokolov et al., 2001).

$$b = C_b - C_a + [H^+] - [OH^-] \quad (5.4)$$

Concentrations of acid (C_a) and base (C_b) are known volumes of standardized titrants added, $[H^+]$ is determined by a glass electrode while $[OH^-]$ is calculated using the autoprolysis equilibrium expression rearranged to solve for $[OH^-]$, shown in Equation (5.5).

$$[OH^-] = K_w / [H^+] \quad (5.5)$$

Titration data can be expressed in charge excess versus pH. Charge excess data due to deprotonation of sorption sites is modeled using Discrete Site Analysis (DISI) to determine pK_a values and site densities for binding sites (Smith and Kramer, 1999). The DISI method uses linear programming to solve for the reactive site concentrations; linear programming optimizes a linear objective function that is subjected to linear equality and inequality constraints (Brassard et al., 1990). Linear programming is used because it gives a simple model to describe the data; a simple model is a good starting point for future advancement. The idea of the work completed in this chapter is to determine the pK_a values for high solids systems and implement them into a pH prediction model.

Acid-base titrations have been used in a number of studies to examine the characteristics of surface reactivity. Wang et al. (1998) investigated the chemical characteristics of dissolved organic matter (DOM) in wastewater by the use of both acidimetric and alkalimetric titrations. The group wanted to explore the chemical

characteristics in hopes to determine heavy metal uptake into the DOM. Wang et al. (1998) discovered that pH and the total suspended solids significantly affected dissolution of the DOM from the sludge. DOM was studied from primary, secondary and tertiary wastewater treatments; all DOM was found to have pK_as of 5.3 and 9.5 which were believed to consist of carboxylic and amino functional groups, respectively (Wang et al., 1998).

A study conducted by Smith and Ferris (2001) used acid-base titrations to examine proton binding by hydrous ferric oxide surfaces. The study found that binding sites in the HFO surface are consistent with the theoretical binding sites in the crystalline iron oxides. The research presented in this chapter aims to used acid-base titrations of a simple synthetic wastewater to test a pH simulation model based on electroneutrality. The chapter will also explore any impact the addition of solids to the synthetic wastewater has on the pH model and, if necessary, develop a revised pH simulation model that takes solids into account.

5.3 METHODOLOGY

5.3.1 Synthetic Wastewater

A synthetic wastewater solution was prepared containing 96 mg/L ammonium chloride (NH_4Cl) (BDH, West Chester, PA), 17 mg/L potassium phosphate monobasic (KH_2PO_4) (BDH, West Chester, PA), 24 mg/L magnesium sulfate heptahydrate ($MgSO_4 \cdot 7H_2O$) (Sigma Aldrich, St. Louis, MO), 2.4 mg/L calcium chloride dihydrate ($CaCl_2 \cdot 2H_2O$) (Fisher Scientific, New Jersey, NY) and 820.3 mg/L sodium acetate

(CH_3COONa) (EMD Chemicals, Gibstown, NJ). All reagents were ACS grade or higher. The synthetic wastewater used in this study was modified from Jung et al. (2005).

5.3.2 Acid-base Titrations

Acid-base titrations were completed using the 848 Titrino plus automatic titration unit (Metrohm Ion Anaylsis, Switzerland). Before initiating the titration, the pH of 50mL synthetic wastewater was adjusted to below a pH 5 using standardized HNO_3 (1.0 N, Aldrich, St. Louis, MO). After an equilibration period, the sample was titrated with a CO_2-free standardized 0.0975 M NaOH solution. Before initiating the titration, the sample was blanketed with argon to prevent contamination of the sample with CO_2 (Smith and Kramer, 1999). Titrations were complete when the pH of the sample exceeded a pH of 12.

The titrations were also performed on synthetic wastewater with the addition of 8000 mg/L iron (III) oxide (Fe_2O_3) (< 5 µm, Sigma Aldrich, St. Louis, MO) as a simple proxy to a high solid wastewater system. The iron (III) oxide was added to the synthetic wastewater and the pH was adjusted to below 5. The sample was then allowed to equilibrate for 12 hours. After equilibration, the pH of the solution was checked again and followed by titration.

5.3.3 Calculation of Total [H+] Using Tableau Notation

The pH throughout the titration was determined through the use of MATLAB™ and the Tableau method (Morel and Hering, 1993). Figure 5.1 shows the soluble synthetic wastewater species shown in tableau notation. The MATLAB™ code used to solve for the pH is located in Appendix B1. Reactants are given as components along the

top of the table and the species are listed in the first column. The second row is the charge of each reactive species. All log K values have been corrected for an ionic strength of the synthetic wastewater; this was completed by interpolation using several log K values measured at different ionic strengths; log K values were obtained from NIST (Martell and Smith, 2001). The deprotonation reaction of NH_4^+ can be used as an example of how to read the tableau. It is necessary to combine 1 H^+ and 1 NH_3 to produce NH_4^+, this is shown in reaction Equation 5.6. The log K for the reaction is shown in Figure 5.1 as -log K_{NH3}.

$$NH_4^+ \rightarrow NH_3 + H^+ \tag{5.6}$$

A lot of information can be gained from using tableau notation. As explained above, each row (with the exception of the charge row) can be described as a reaction equation and when you multiply across the row species concentration can be calculated. For example, $[NH_4^+]$ is calculated by multiplying by each species across the tableau raised to their corresponding stoichiometric coefficient. This can be seen in Equation 5.7.

$$[NH_4^+] = [H^+]^1 \times [NH_3]^1 \times [Ac^-]^0 \times [PO_4^{3-}]^0 \times [SO_4^{2-}]^0 \times [Ca^{2+}]^0 \times [Mg^{2+}]^0 \times [Na^+]^0 \times [K^+]^0 \times [Cl^-]^0 \times 10^{-\log K_{NH3}} \tag{5.7}$$

Equation 5.7 can be simplified since concentrations raised to the exponent of zero are equal to one. The simplified equation is shown in Equation 5.8.

$$[NH_4^+] = [H^+]\,[NH_3]\,(K_{NH3})^{-1} \tag{5.8}$$

To verify the method of the tableau, another way to calculate component concentration is to look at the reaction and its equilibrium expression. For example, Equation 5.9 is the equilibrium expression for the deprotonation expression shown in Equation 5.6.

Species	H^+	NH_3	Ac^-	PO_4^{3-}	SO_4^{2-}	Ca^{2+}	Mg^{2+}	Na^+	K^+	Cl^-	log K
Charge	+1	0	-1	-3	-2	+2	+2	+1	+1	-1	0
H^+	1	0	0	0	0	0	0	0	0	0	0
NH_3	0	1	0	0	0	0	0	0	0	0	0
Ac^-	0	0	1	0	0	0	0	0	0	0	0
PO_4^{3-}	0	0	0	1	0	0	0	0	0	0	0
SO_4^{2-}	0	0	0	0	1	0	0	0	0	0	0
Ca^{2+}	0	0	0	0	0	1	0	0	0	0	0
Mg^{2+}	0	0	0	0	0	0	1	0	0	0	0
Na^+	0	0	0	0	0	0	0	1	0	0	0
K^+	0	0	0	0	0	0	0	0	1	0	0
Cl^-	0	0	0	0	0	0	0	0	0	1	0
OH^-	-1	0	0	0	0	0	0	0	0	0	log Kw
NH_4^+	1	1	0	0	0	0	0	0	0	0	$-\log K_{NH3}$
HAc	1	0	1	0	0	0	0	0	0	0	$-\log K_{ac}$
HPO_4^{2-}	1	0	0	1	0	0	0	0	0	0	$-\log K_{HPO4}$
$H_2PO_4^-$	2	0	0	1	0	0	0	0	0	0	$-\log K_{H2PO4}$ $-\log K_{HPO4}$
H_3PO_4	3	0	0	1	0	0	0	0	0	0	$-\log K_{H3PO4}-\log K_{H2PO4}$ $-\log K_{HPO4}$
HSO_4^-	1	0	0	0	1	0	0	0	0	0	$-\log K_{HSO4}$
$CaOH^+$	-1	0	0	0	0	1	0	0	0	0	$\log Ks_{CaOH} + \log Kw$
$MgOH^+$	-1	0	0	0	0	0	1	0	0	0	$\log Ks_{MgOH} + \log Kw$

Figure 5.1: Tableau used for solving pH for the simulations of the synthetic wastewater titration.

$$K_{NH_3} = \frac{[NH_3][H^+]}{[NH_4^+]} \tag{5.9}$$

This equation can be rearranged to solve for $[NH_4^+]$; this is shown in Equation 5.10.

$$[NH_4^+] = [NH_3][H^+](K_{NH3})^{-1} \tag{5.10}$$

Equation 5.10 is the same as Equation 5.8; thus, the two methods are calculating the same species.

The mass balance of each reactive species can be determined by the summation of a column. For example, total ammonia concentration is the sum of its column. When the

coefficient of a species is zero, their concentration is zero. Therefore, NH_{3T} is a sum of the NH_3 and NH_4^+ species, shown in Equation 5.11. Tableau notation solves for the total concentration of each component while satisfying log K. Subscript T denotes that it is the total of the species.

$$NH_{3T} = [NH_3] + [NH_4^+] \tag{5.11}$$

Finally, electroneutrality can be determined from the sum of the mass balance for each component column. Electroneutrality is a simple concept that is based on the fact that the overall charge of a solution must be zero; the sum of the concentrations of the positively charged species must equal the sum of the concentrations of the negatively charged species (Takács et al., 2010). The pH of a system can be determined from rearranging the electroneutrality expression to solve for $[H^+]$. Total H^+ concentration, the first column of the tableau, can also be used to calculate pH; however, it must be determined. Total H^+ is a difficult concept to define and calculate from solution composition; however, it can be determined from the concepts of mass balance and electroneutrality. Total H^+ can be calculated using a linear combination of the electroneutrality and component charges. A simple definition of total H^+ is that it is equal to the sum of all the acids minus all the bases (Morel and Hering, 1993). For the tableau given in Figure 5.1, total H^+ is determined using Equation 5.12. The derivation of Equation 5.12 is described using a simple example in Appendix E.

$$H^+_T = Ac_T + 3PO_{4T} + 2SO_{4T} - 2Ca_T - 2Mg_T - Na_T - K_T + Cl_T \tag{5.12}$$

5.3.4 Reactive Site Concentration

Reactive site concentrations at different pK_a values were determined using linear programming as described by Brassard et al. (1990). As mentioned previously, linear programming is a method of optimizing a function that is subjected to linear equality and inequality constraints (Brassard et al., 1990).

To determine a pK_a spectrum, the pK_a values are defined on a fixed range, 5 to 10, at fixed step size of 0.2. Concentrations then need to be assigned to each site where a concentration of zero is possible. As explained above, the K_a is the equilibrium constant which describes the acid dissociation reaction of a species. The mass balance of a species, also explained above, is the sum of the concentrations of the protonated and deprotonated species (an example is shown in Equation 5.11). To calculate reactive site concentration $[L_i^-]$, the expression for the equilibrium constant and the mass balance must be combined. Equation 5.13 is a combination between the mass balance of a reactive site, rearranged to isolate $[L^-]$, and the acid dissociation expression, rearranged for [HL] and substituted into the mass balance.

$$[L^-] = C_L \left(\frac{Ka}{Ka+[H^+]}\right) \tag{5.13}$$

In Equation 5.13, C_L represents the total concentration of the species. However, this equation will only solve for one surface reactive site at one pK_a and one pH. To solve for a number of pH and pK_a values, a matrix of size *n* x *m* must be used; *n* is the number of steps in the titration, while *m* is the number of pK_a values. The term used in the matrix is dubbed alpha and is defined in Equation (5.14).

$$\alpha_{ij} = \left(\frac{K_{aj}}{K_{aj}+[H_i^+]}\right) \tag{5.14}$$

This is the bracketed term in Equation 5.13 with the addition of *i* and *j* terms which are the steps in the equation; $i = 1, \ldots, n$ and $j = 1, \ldots, m$. To calculate for different reactive sites, the data will be described by Equation (5.15) where charge excess (b) is equal to the sum of the product of site concentration (C_j) and alpha minus the term C_{anc}.

$$b = \sum C_{Lj}\alpha_{ij} - C_{anc} \tag{5.15}$$

C_{anc} is the initial acid neutralizing capacity (ANC) of the sample. ANC is defined as the difference between the sum of the concentrations of cations of strong bases and the sum of the concentrations of anions of strong acids (Brassard et al., 1990). Stability constants (K_j) are defined for each monoprotic site using the appropriate dissociation reactions (Smith and Ferris, 2003). Equation 5.15 can be simplified to matrix Equation 5.16

$$\mathbf{b}_{calc} = \mathbf{A}\boldsymbol{x} \tag{5.16}$$

where $\mathbf{b}_{calc}$ is the charge excess from the titration data and **x** is a vector of site concentration (C_{Lj}) of size (m + 1) x 1. The vector has an extra term (m + 1) which is for the C_{anc} constant; this is added to take into account any effects caused by ANC (Brassard et al., 1990). To solve for reactive site concentration, Equation (5.16) is rearranged to Equation (5.17), this is referred to as the PRIMAL solution (Brassard et al., 1990).

$$\mathbf{x} = \mathbf{b}_{calc}/\mathbf{A} \tag{5.17}$$

The PRIMAL solution can be quite complex to solve. Therefore, the DUAL problem is solved. In the Duality theorem, the dual solution of the dual problem returns the primal solution. The dual problem transposes the matrix, **A**. Solving for the dual problem is used because it is easier to solve than the primal solution; the dual problem minimizes the size of the matrix and the calculation gains speed and precision (Brassard et al., 1990).

5.4 RESULTS

Data for the synthetic wastewater titrations were collected in the form of pH measured for total volume NaOH added. The data were plotted as a titration curve for each trial. Figure 5.2 shows four trials of synthetic wastewater titrated with standardized NaOH; measured data is shown as data points. Figure 5.2 shows the predicted pH, depicted as a black line, calculated using tableau notation for each trial.

Data for the synthetic wastewater titrations with the addition of Fe_2O_3 was collected and were plotted as a titration curve for each trial. Figure 5.3 shows four trials

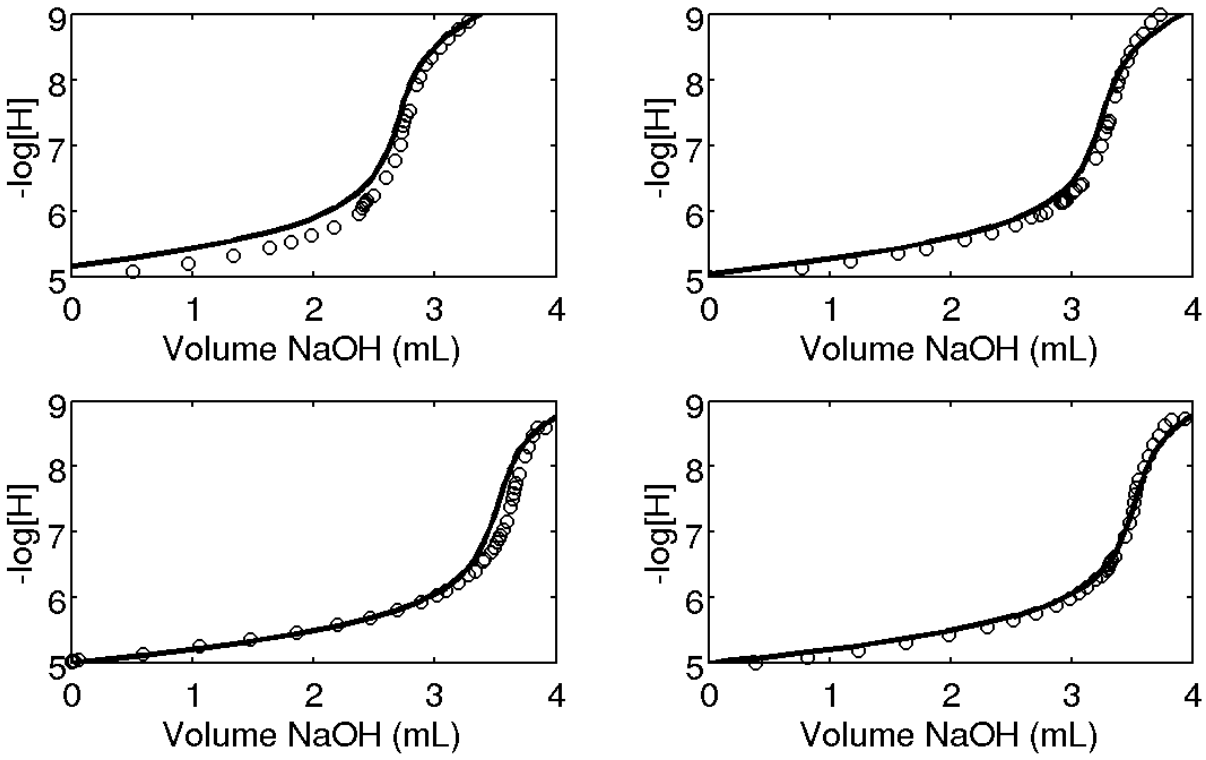

Figure 5.2: Titration curves for measured (data points) and calculated (line) titrations of 50 mL synthetic wastewater titrated with 0.0975 M NaOH. Each subplot represents a separate trial. No data points were observed between pH 9 and 10.

of synthetic wastewater with Fe_2O_3 which were titrated with standardized NaOH; measured data is shown as open-faced data points. Figure 5.3 also shows the predicted pH, depicted as a black line, calculated using tableau notation for each trial. Raw data from both synthetic titration sets (with and without ferric oxide) were used to calculate charge excess and, in turn, reactive site concentration.

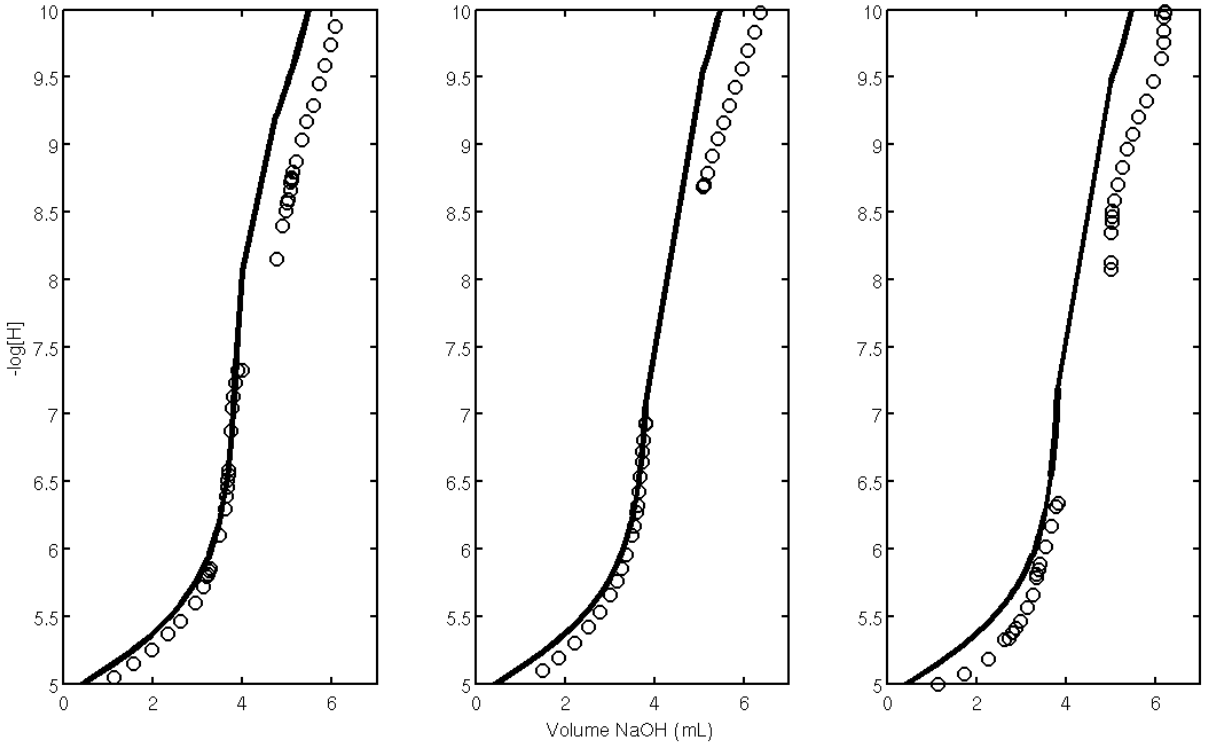

Figure 5.3: Titration curves for measured (data points) and calculated (line) titrations of 50 mL synthetic wastewater and 400 mg Fe_2O_3 titrated with 0.0975 M NaOH. Titrations were completed in triplicate.

5.5 DISCUSSION

5.5.1 Synthetic Wastewater

Although each sample was titrated until pH 12, the pH range most relevant for wastewater treatment is circumneutral. For this reason, as well as the fact that NH_3 degasses above pH 10, the pH range of interest is be between pH 5 and 10. For ease of comparison, pH measured throughout the titration was plotted with pH calculated using tableau notation. Figure 5.4 is a comparison between measured versus modeled pH for the synthetic wastewater trials plotted with a one-to-one line (shown in black). Each shape corresponds to a different trial. Measured data agreed with the calculated model very well, especially between pH 5 and 7 and pH 8.5 and 9.5. This shows that for the soluble system, the model produced by Fairlamb et al. (2003) is quite accurate.

From the titration data, the charge excess (b) was calculated for the synthetic wastewater for each trial. The results of the charge excess calculation for the four trials are plotted against pH in Figure 5.5. As pH increases, charge excess becomes more positive. Through the steps of the titration, pH increases causing the species in solution to become more negatively charged. This change causes the charge necessary for electroneutrality to decrease (Sokolov et al., 2001). From this data, reactive site concentrations were calculated using the DISI program at various pK_as; the results of pK_a spectra are shown in Figure 5.6. Figure 5.6 shows reactive site concentration (in mmol/L) on the y-axis and pK_a values are displayed on the x-axis. The four spectra shown are for each synthetic wastewater trial. The pK_a spectra for all trials share the same two peaks at pK_a 5 and at around pK_a 9.4 with reactive site concentrations of around 6.5 and 5.25 nM, respectively.

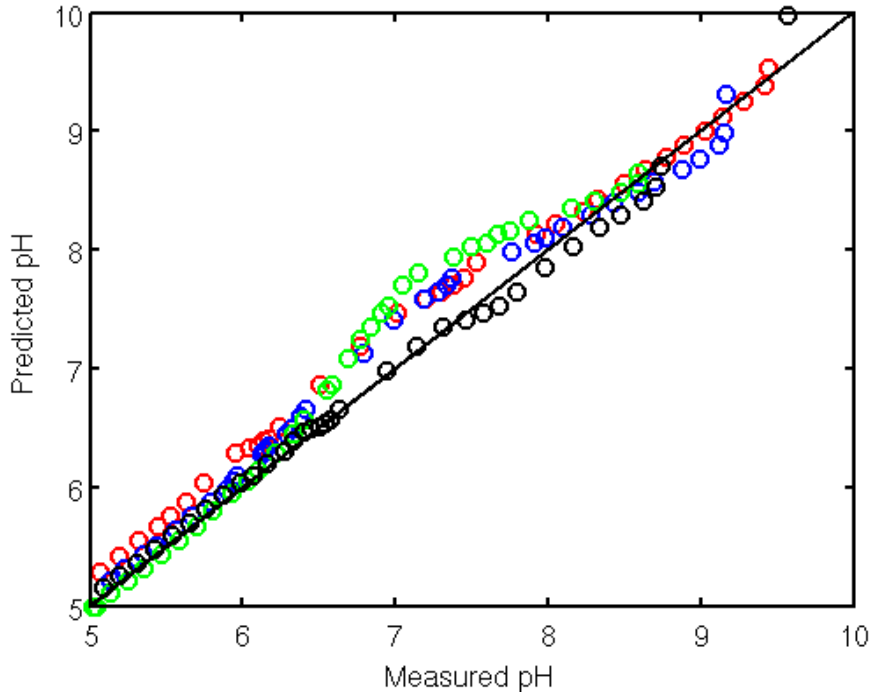

Figure 5.4: A comparison of measured and predicted pH for the synthetic wastewater titrations. Predicted pH was calculated using the tableau method. Different colours depict different trials.

These peaks may correspond to carboxylic and amine reactive surface sites. The synthetic wastewater was prepared with 10 mM acetate; this concentration is over 1.5 times higher than the calculated concentration at pKa 5. This would confirm the carboxylic reactive site a pH 5 due to the fact that acetic acid has a pKa of around 4.7. The synthetic wastewater also contained ammonia with a concentration of 2 mM, 62% lower than the calculated reactive site concentration. Ammonia has a pKa of around 9.3, after correcting for the ionic strength of the synthetic wastewater, which confirms the presence of the amine reactive groups in solution. Shifts in the pKa spectra could be contributed to the effect of alkalinity, or acid neutralizing capacity (ANC).

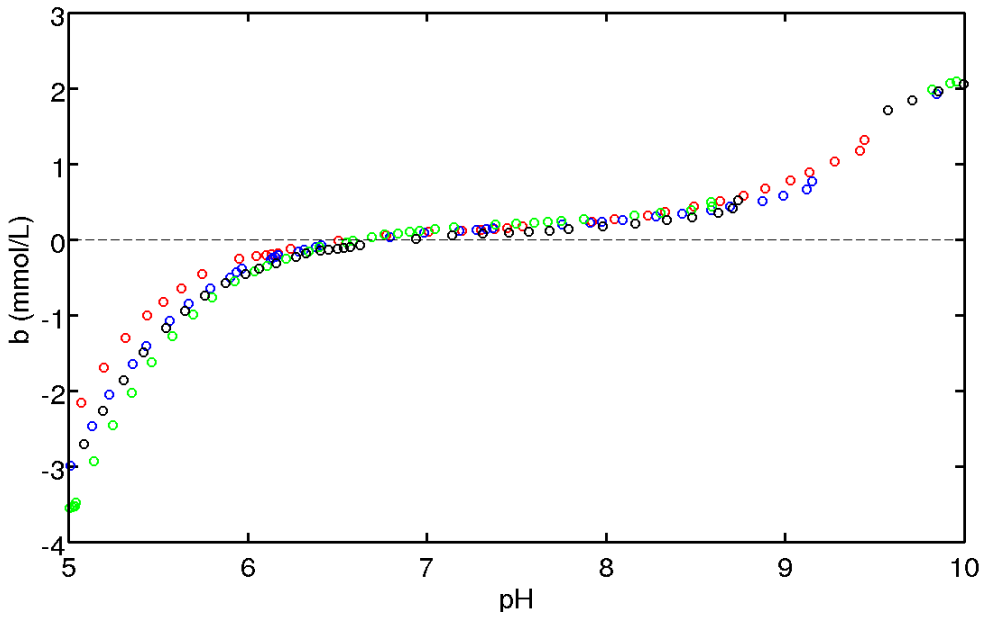

Figure 5.5: Charge excess (b) curve calculated for the titration of 50 mL synthetic wastewater with 0.0975 M NaOH. Charge excess (in mmol/L) is shown on the y-axis and pH is shown on the x-axis. Each colour corresponds to a different trial.

Removing the effect of ANC causes a shift in charge excess to become more negative. It should be noted that the calculated site concentrations at the various pK_a values are dependent on the shape of the charge excess curve and not the exact position (Brassard et al., 1990). Discrepancies between reactive site concentrations and concentrations present at extreme pH values (5 and 10) in the synthetic wastewater solution could be due to increasing uncertainty in measured charge excess. The lack of charge excess inflection within the titration range prevents accurate quantification of concentration (Smith et al., 1999).

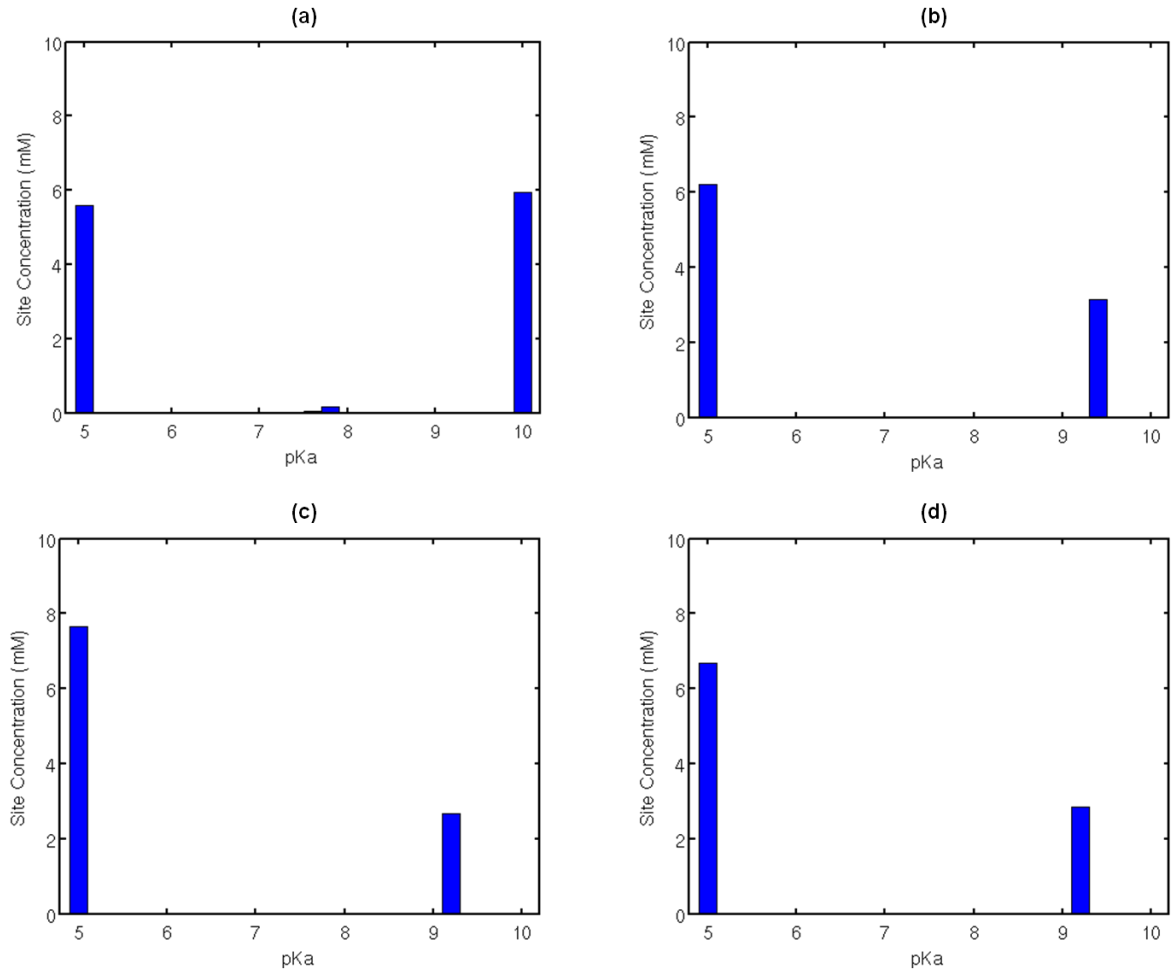

Figure 5.6: pKa spectra with site concentrations (in mM) determined for synthetic wastewater titration. Site concentrations determined using DISI method.

5.5.2 Synthetic Wastewater with Ferric Oxide

Figure 5.7 compares the measured pH and the predicted pH for the synthetic wastewater titration with ferric oxide. The model used to simulate pH for the system is the same model used to calculate theoretical pH for the synthetic wastewater simple system. In Figure 5.7, measured pH is on the x-axis while simulated pH is on the y-axis. A 1:1 line is also plotted for ease of comparison between the measured and modeled. Notably, the measured titration data does not agree with the modeled data. This can be

observed in both Figures 5.3 and 5.7. In Figure 5.3, the measured data falls below the simulation data consistently for all three trials. The difference is easier to see in Figure 5.7. The simulated titration continuously underestimates proton concentration, ergo causing an overestimation of pH. The underestimation is present in small amounts over the pH range of 5 to 7; however, it is most obvious above pH 7.

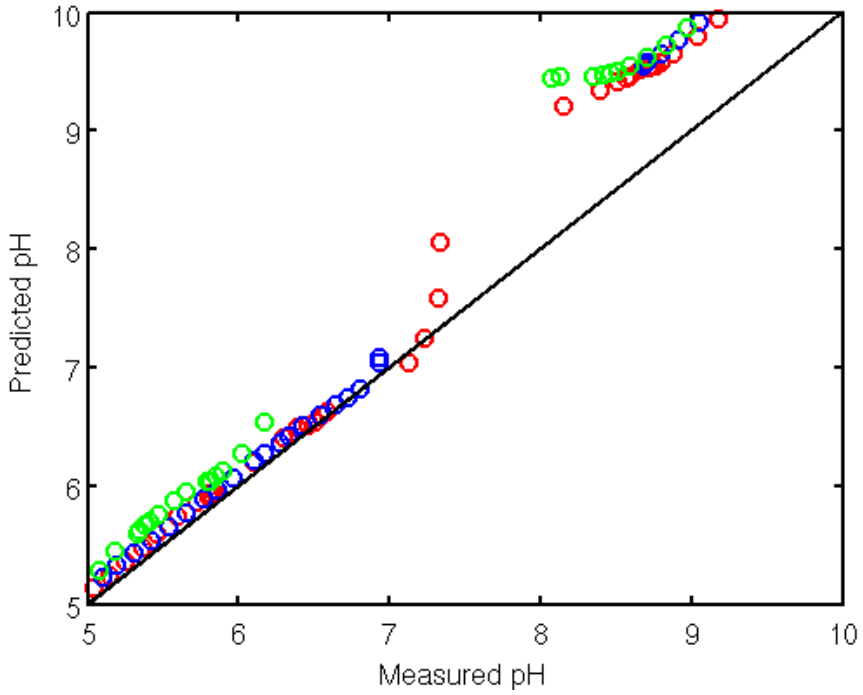

Figure 5.7: A comparison of measured and predicted pH for the synthetic wastewater titrations with Fe_2O_3. Predicted pH was calculated using the tableau method. Different colours correspond to different trials.

This trend, the overestimation of pH, was the opposite of what was expected to occur. An underestimation of pH was expected to be seen because the simple wastewater pH simulation does not take into account positively charged reactive sites which can be found on the surface of solid species. This can be seen in the electroneutrality of the

wastewater-solids system that has been rearranged for proton concentration shown in Equation 5.16

$$[H^+] = \sum[SAA] - \sum[SBC] + \sum[WAA] - \sum[PSS] \quad (5.16)$$

where SAA stands for strong acid anions, SBC is strong base cations, WAA is weak acid anions and PSS is positive surface sites. Since the underestimation of pH was not observed after the addition of the iron oxide, it was obvious that the model required more than the addition of the positively charged surface reactive sites; a negatively charged surface reactive site was also necessary to characterize the reactive sites available on the iron oxide surface.

5.5.3 Tableau Method for Wastewater System with Solids

In the first attempt to adjust the model, a negatively charged surface reactive site was added. This reactive site was treated as a spectator ion, much like Cl^-, in that it does not protonate during the titration. This reactive site was added due to the reasoning that there are surface oxygens that remain negatively charged throughout the 5 to 10 pH range. A study by Hiemstra et al. (1996) supports this claim. Hiemstra et al. (1996) studied the proton affinity of individual surface groups in goethite (α-FeOOH). Goethite is an iron hydroxide with triply coordinated oxygens; the oxygen atoms are bonded with three iron atoms. An asymmetrical configuration forms between two neighboring surface oxygen atoms when one of the oxygens is protonated. When the one oxygen is protonated a hydrogen bond forms between the hydrogen and the second oxygen atom (i.e. Fe_3OH – OFe_3). The formation of this hydrogen bond causes the protonation constant to be very low, with an estimated log K of +0.2. This means that when pH is less than pKa, in this

case less than 0.7, the second oxygen atom will be protonated; above pH 0.7 the oxygen atom will be deprotonated. Therefore the group will remain negatively charged across all pH values of 5 – 10.

After the addition of the permanently negatively charged reactive site, the pH of the simulated titration shifted to overestimate [H^+], the original trend expected to be observed. This shift can be seen in Figure 5.8 which, once again, plots measured versus simulated pH for the synthetic wastewater with Fe_2O_3. Since the model was now underestimating pH, the addition of positively charged surface reactive sites could be added to compensate. Two surface reactive sites were added to the tableau. The charge of these surface reactive sites is neutral until the sites are protonated which then give them a

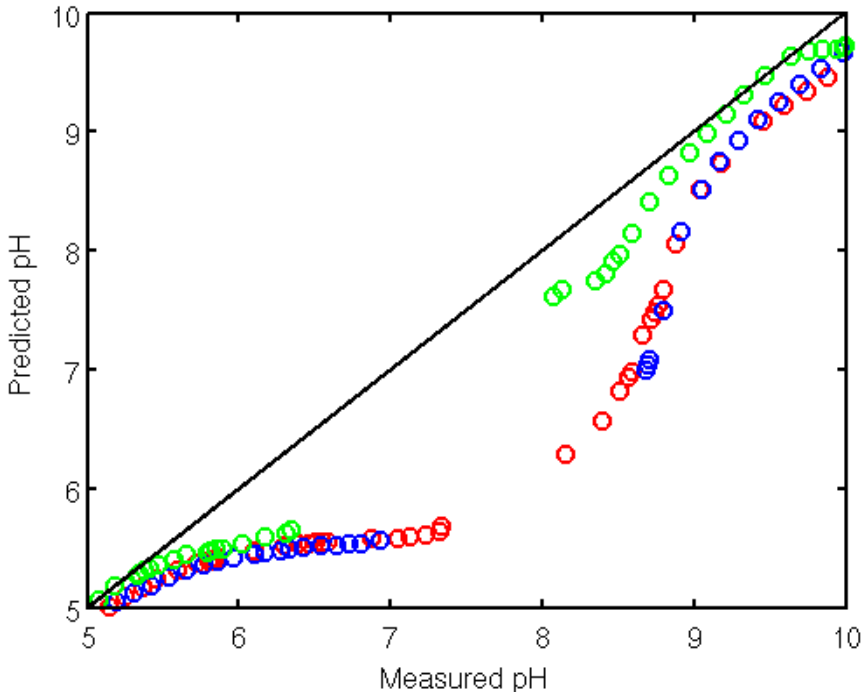

Figure 5.8: A comparison between predicted and measured pH for the synthetic wastewater with Fe_2O_3 titrations calculated using the tableau method with the addition of a permanently negatively charged surface reactive site. Different coloured data points represent different trials.

Species	H^+	NH_3	Ac^-	PO_4^{3-}	SO_4^{2-}	Ca^{2+}	Mg^{2+}	Na^+	K^+	Cl^-	S1	S2	S3	log K
Charge	+1	0	-1	-3	-4	+2	+2	+1	+1	-1	-1	+1	+1	0
H^+	1	0	0	0	0	0	0	0	0	0	0	0	0	0
NH_3	0	1	0	0	0	0	0	0	0	0	0	0	0	0
Ac^-	0	0	1	0	0	0	0	0	0	0	0	0	0	0
PO_4^{3-}	0	0	0	1	0	0	0	0	0	0	0	0	0	0
SO_4^{2-}	0	0	0	0	1	0	0	0	0	0	0	0	0	0
Ca^{2+}	0	0	0	0	0	1	0	0	0	0	0	0	0	0
Mg^{2+}	0	0	0	0	0	0	1	0	0	0	0	0	0	0
Na^+	0	0	0	0	0	0	0	1	0	0	0	0	0	0
K^+	0	0	0	0	0	0	0	0	1	0	0	0	0	0
Cl^-	0	0	0	0	0	0	0	0	0	1	0	0	0	0
S1	0	0	0	0	0	0	0	0	0	0	1	0	0	0
S2	0	0	0	0	0	0	0	0	0	0	0	1	0	0
S3	0	0	0	0	0	0	0	0	0	0	0	0	1	0
$S2H^+$	1	0	0	0	0	0	0	0	0	0	0	1	0	$-\log K_{1S2}$
$S3H^+$	1	0	0	0	0	0	0	0	0	0	0	0	1	$-\log K_{1S3}$
OH^-	-1	0	0	0	0	0	0	0	0	0	0	0	0	log Kw
NH_4^+	1	1	0	0	0	0	0	0	0	0	0	0	0	$-\log K_{NH3}$
HAc	1	0	1	0	0	0	0	0	0	0	0	0	0	$-\log K_{ac}$
HPO_4^{2-}	1	0	0	1	0	0	0	0	0	0	0	0	0	$-\log K_{HPO4}$
$H_2PO_4^-$	2	0	0	1	0	0	0	0	0	0	0	0	0	$-\log K_{H2PO4}$ $-\log K_{HPO4}$
H_3PO_4	3	0	0	1	0	0	0	0	0	0	0	0	0	$-\log K_{H3PO4}$ $-\log K_{H2PO4}$ $-\log K_{HPO4}$
HSO_4^-	1	0	0	0	1	0	0	0	0	0	0	0	0	$-\log K_{HSO4}$
$CaOH^+$	-1	0	0	0	0	1	0	0	0	0	0	0	0	$\log Ks_{CaOH} + \log Kw$
$MgOH^+$	-1	0	0	0	0	0	1	0	0	0	0	0	0	$\log Ks_{MgOH} + \log Kw$

Figure 5.9: Final tableau for synthetic wastewater with Fe_2O_3 surface reactive sites. Added species and log K values are shown in red.

charge of +1. An example of this is shown in the deprotonation reaction depicted in Equation 5.17.

$$\equiv SH^+ \rightarrow \equiv S + H^+ \qquad (5.17)$$

The equilibrium constant of this reaction is symbolically indicated as $\log K_{1S2}$. The third surface site 1S3 is represented by the same reaction shown in Equation 5.17; the equilibrium constant for 1S3 is $\log K_{1S3}$. These terms were added into the tableau

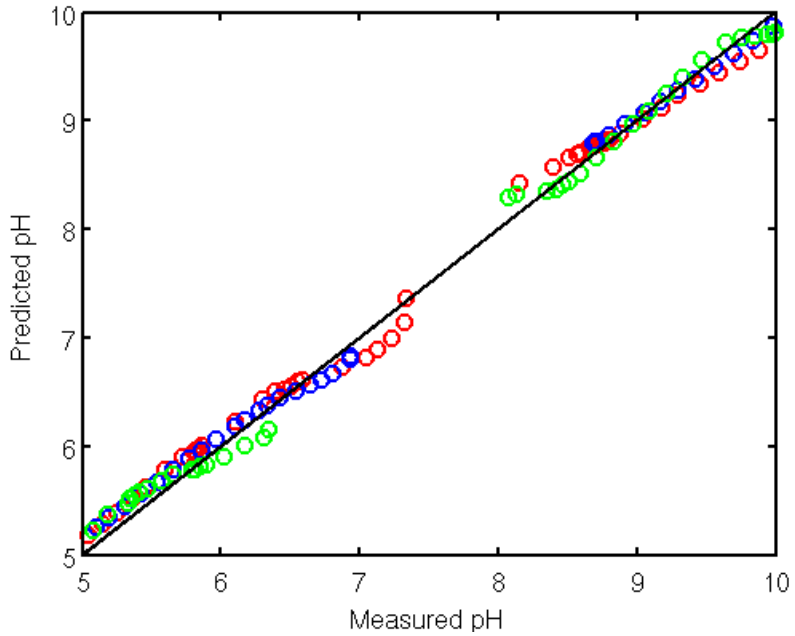

Figure 5.10: Predicted versus measured pH for the synthetic wastewater with Fe_2O_3 titrations using the tableau with positive surface reactive sites. Different colours depict the three trials.

modified for the presence of solids in the system. The modified tableau is shown in Figure 5.9; added species are shown in red. After the three surface reactive sites were added to the tableau, the parameters of the pH simulation were optimized to minimize the sum of squares of the error between the model and the measured data. The script used to solve for pH simulation for the synthetic wastewater with ferric oxide titration is shown in Appendix B2. Figure 5.10 compares the measured and simulated pH for the synthetic wastewater and Fe_2O_3 using the tableau method with additional surface reactive sites. With the addition of the three surface reactive sites, the simulated data now agrees quite well with the measured data. After the optimization of the parameters the first surface site (negatively charged) was found to have a total concentration of 1.27 mmol/L. The second and third reactive surface site (positively charged) were found to have total

concentrations of around 0.95 and 0.48 mmol/L and pKa values around 7.83 and 10.5, respectively. A summary of these results can be found in Table 5.1.

Table 5.1: Calculated pKa and reactive site concentrations for ferric oxide surface reactive sites. Literature values obtained from [a]Smith and Ferris (2001) and [b]Hiemstra et al. (1996).

Reactive Site	Concentration (mM)	pK_a	Literature pK_a Values
$S1^-$	1.27 ± 0.11	0.2[b]	N/A
$S2H^+$	0.95 ± 0.22	7.83 ± 0.62	8.12[a]
$S3H^+$	0.48 ± 0.42	10.54 ± 0.55	10.1[a]

5.5.4 pK_as and Reactive Site Concentrations for Synthetic Wastewater with Fe_2O_3

To compare between the wastewater system with and without iron oxide as well as the pK_as determined for the model compared to what can be calculated for the sample, charge excess and site concentrations were calculated for the synthetic wastewater with iron oxide. Charge excess was calculated using the raw titration data measured for the synthetic wastewater with ferric oxide. The resulting charge excess curves are shown in Figure 5.11. Charge excess, shown in mmol/L, is on the y-axis and pH is on the x-axis.

Reactive site concentration was calculated using pH vs. b; the pK_a spectra for the three trials are shown in Figure 5.12. The three spectra all contain reactive sites around the same three pK_a values. The reactive site around pK_a 5 has an average concentration of approximately 6.45 mmol/L. Reactive sites with pK_a values around 10 have highly varying concentrations ranging from 2 – 9 mmol/L. The last group of reactive sites to be discussed has pK_as around 8; these reactive sites have average concentrations around 2 mmol/L.

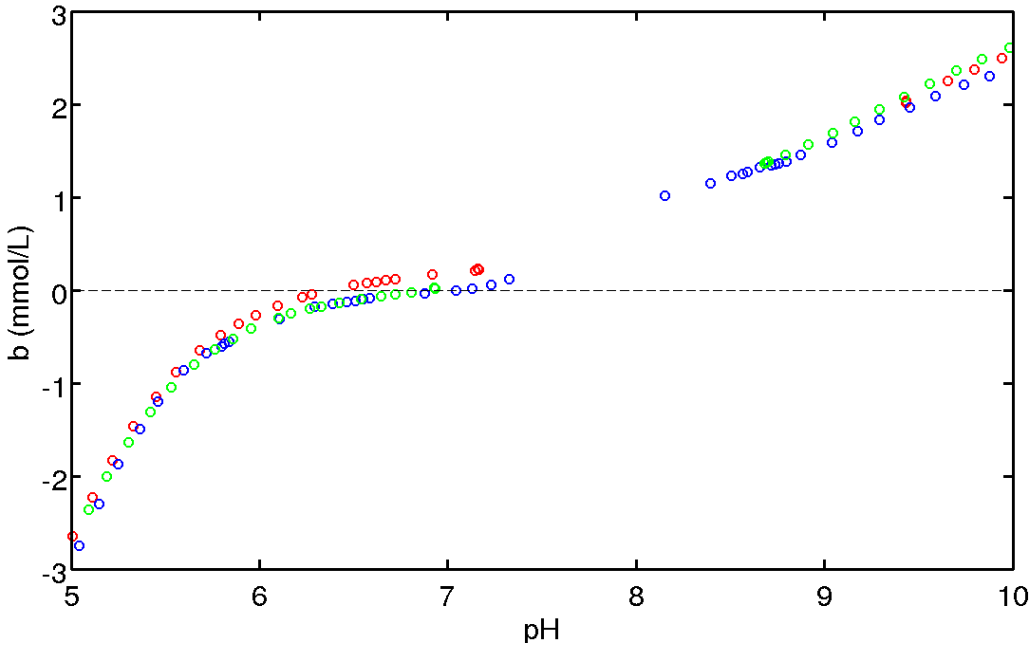

Figure 5.11: Charge excess (b) curve calculated for the titration of 50 mL high solid synthetic wastewater with 0.0975 M NaOH. Charge excess (in mmol/L) is shown on the y-axis and pH is shown on the x-axis. Each colour corresponds to a different trial.

Like the pK_a spectra obtained for the synthetic wastewater, the spectra for the synthetic wastewater with solids have pK_as of around 5 and 10 analogous to carboxylic (pK_a 4.7) and amine (pK_a 9.3) reactive surface sites. Reactive site concentrations for the sites with pK_a of 5 were found to be around 6.5 mmol/L. Reactive sites with a pK_a around 10 were found to have highly variable concentrations, in the range of 1.3 - 9.7 mmol/L; this was also similar to what was observed for the simple wastewater system. Unlike the synthetic wastewater, the pK_a spectra for the wastewater-solids system have the appearance of a new peak at pK_as around 8. This corresponds to the second surface reactive site added to the tableau which has a pK_a of 8.1. Also, the reactive site

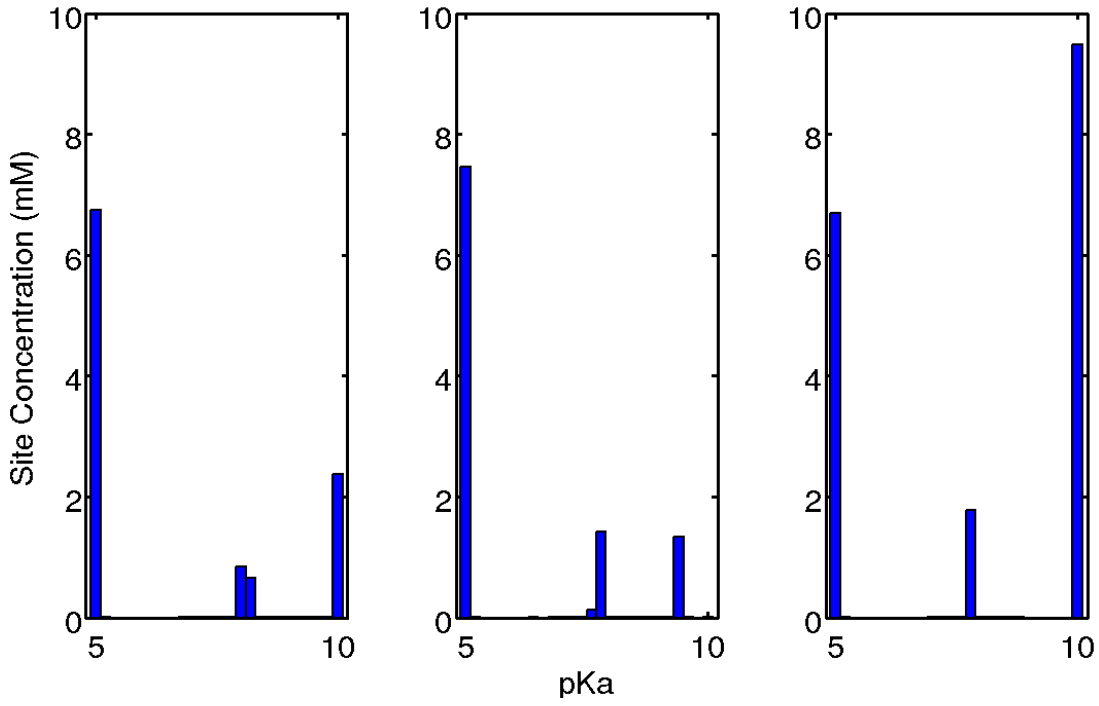

Figure 5.12: pKa spectra with site concentrations (in mM) determined for the high solid (Fe_3O_2) synthetic wastewater titration. Site concentrations determined using DISI method.

concentrations determined for the sites around pK_a of 8 were around 1.2 mmol/L, similar to the concentration (1.1 mmol/L) determined by optimizing the tableau parameters. An increase in surface reactive site concentration was also observed at pK_a 10 for the high solids system; average pK_a 10 site concentration for the synthetic wastewater without solids was 0.65 times lower than the average site concentration for the wastewater with solids. This increase in reactive site concentration could be due to the contribution of reactive sites on the iron oxide surface.

Reactive sites around pK_a values of 8 and 10 have also been observed in acid-base titrations with hydrous ferric oxide. As previously discussed, Smith and Ferris (2001)

used acid-base titrations to explore proton binding by hydrous ferric oxide (HFO) surfaces. Smith and Ferris found a reactive site on the HFO with a pK_a of 8.12 and 10.2; these values agree with the reactive sites observed in the pK_a spectra of the synthetic wastewater with iron oxide solid as well as the pK_a determined through the optimization of the tableau.

5.6 CONCLUSION

Acid-base titrations were utilized to characterize surface reactive sites in two wastewater relevant systems; a simple soluble synthetic wastewater system and a synthetic wastewater system which includes ferric oxide solids. A model using the tableau method was used to simulate pH for the titration of both systems. The simple system agreed with the model very well; as expected the synthetic wastewater system with Fe_2O_3 did not agree with the model. Originally, the model overestimated the pH of the high solids system. This was an unexpected trend due to the fact that the model does not take into account positively charged reactive sites, a condition which would lead to the underestimation of pH. After the addition of a permanently charged surface reactive site on the iron oxide surface, the expected trend was observed. Measured titration data agreed with the model after the addition of two positively charged surface reactive sites to the tableau notation. The first positively charged site had a pK_a of around 8 while the second site had a pK_a around 10.2. Both pK_a values agreed with pK_as found for hydrous ferric oxides in literature as well as the pK_a spectra calculated using titration data and discrete site analysis for the high solids system.

5.7 REFERENCES

Altundoğan, S.H., and Tümen, F. (2001). Removal of phosphates from aqueous solutions by using bauxite. 1: Effect of pH on the adsorption of various phosphates. *Journal of Chemical Technology and Biotechnology*, **77**, 77-85.

Batstone, D. J., Keller, J., Angelidaki, I., Kalyuzhnyi, S. V., Pavlostathis, S. G., Rozzi, S. G. A., Sanders, W. T. M., Siegrist, H., Vavilin, V. A. (2002) Anaerobic Digestion Model No. 1, 1Wa Scientific and Technical Report No. 13; IWA Publishing: London, England, UK.

Brassard, P., Kramer, J. R. and Collins, P. V. (1990) Binding Site Analysis Using Linear Programming. *Environ. Sci. Technol.* **24**, 195 - 201.

Fairlamb, M., Jones, R., Takács, I. and Bye, C. (2003). Formulation of a general model for simulation of pH in wastewater treatment processes. In Conference proceedings, *76th annual water environmental federation technical exhibit and conference*, Los Angeles, CA, USA. Water Environment Federation: Alexandria, VA.

Harris, D.C. (2007) Quantitative Chemical Analysis. 7th ed. W. H. Freeman and Company, New York, USA.

Hiemstra, T., Venema, P. and Van Riemsdijk, W. H. (1996) Intrinsic Proton Affinity of Reactive Surface Groups of Metal (Hydr)oxides;: The Bond Valence Prinicple. *J. Coll. Interface Sci.* **184**, 680 - 692.

Jung, Y., Koh, H., Shin, W. and Sung, N. (2005) Wastewater treatment using combination of MBR equipped with non-woven fabric filter and oyster-zeolite column. *Environ. Eng. Res*. **10**, 247-256.

Martell, A and Smith, R. (2001) Critically selected stability constants of metal complexes, NIST database 46 version 6. NIST, Gaithersburg, MD 20899.

Martinez, R. E., Smith, D. S., Kulczycki, E. and Ferris, F. G. (2002) Determination of Intrinsic Bacterial Surface Acidity Constants using a Donnan Shell Model and a Continuous pKa Distribution Method. *J. Coll. Interface Sci.*, **253**, 130-139.

Morel, F. M. M. and Hering, J. G. (1993) Principles and applications of aquatic chemistry. Wiley-Interscience.

Neyens, E. and Baeyens, J. (2003) A review of thermal sludge pre-treatment processes to improve dewaterability. *J. of Hazardous Materials* **98**, 51-67.

Smith, D. S., and Ferris, F. G. (2001) Proton binding by hydrous ferric oxide and aluminum oxide surfaces interpreted using fully optimized continuous pK_a spectra. *Environ. Sci. Technol.* **35**, 4637-4642.

Smith, D. S. and Ferris, F. G. (2003). Specific surface chemical interactions between hydrous ferric oxide and iron-reducing bacteria determined using pKa spectra. *J. of Coll. Interface Sci.* **266**, 60 - 67.

Smith, D. S., Adams, N. W., and Kramer, J. R. (1999) Resolving uncertainty in chemical speciation determinations. *Geochim. Cosmochim. Acta* **63**, 3337-3347.

Smith, D. S. and Kramer, J. R. (1999). Multi-site proton interactions with natural organic matter. *Environment International* **25**, 307 - 314.

Smith, D. S., I. Takács, S. Murthy, G. Diagger, and A. Szabó (2008). Phosphate complexation model and its implications for chemical phosphorus removal. *Water Environ. Res.* **80**, 428–438.

Sokolov, I., Smith, D. S., Henderson, G. S., Gorby, Y. A. and Ferris, F. G. (2001) Cell Surface Electrochemical Heterogeneity of the Fe(III)-Reducing Bacteria *Shewanella putrefaciens*. *Environ. Sci. Technol.* **35**, 341 – 347.

Takács, I., Belia, E., Boltz, J. P., Comeau, Y., Dold, P., Jones, R., Morgenroth, E., Schraa, O., Shaw, A. and Wett, B. (2010) Structured Process Models for Nutrient Removal. In *Nutrient Removal: WEF Manual of Practice No. 34.*; Water Environment Federation® (2010). WEF Press. Alexandria, VA.

Wang, J., Huang, C. P., Allen, H. E., Takiyama, L. R., Poesponegoro, I., Poesponegoro, H and Pirestani, D. (1998) Acid characteristics of dissolved organic matter in wastewater. *Water Environ. Res.*, **70**, 1041–1048.

Chapter 6: Conclusions and Future Work

6.1 CONCLUSIONS AND FUTURE WORK

The following section is a brief summary of the concluding remarks from the experimental chapters of this thesis. In each section the original objectives of the chapters will be addressed and ideas for future work will be shared.

6.1.1 Chapter 3: Molecular variability in wastewater organic matter and implications for phosphorus removal across a range of treatment technologies

The purpose of the experiments in Chapter 3 was to investigate dissolved organic matter in wastewater in hopes of learning about the various wastewater treatment technologies.

Objective 1: to develop a "fingerprinting" technique to characterize dissolved organic matter in wastewater across wastewater treatment plants and their different treatment technologies.

The fluorescence contour plots collected for each sample were different for each sample; this showed that the wastewater samples were different at a molecular level. The fluorescence contour plot was each wastewater sample's unique identifier. Changes in DOM in wastewater throughout treatment were also observed through the use of fluorescence. Distinct trends were witnessed as the dissolved organic matter passed through treatment such as decreases in proteinatious fluorophores.

Objective 2: to relate dissolved organic matter to phosphorus removal and speciation.

Correlations between fluorophore concentrations (concentrations determined for the different classifications of fluorescent DOM) and non-reactive phosphorus were examined in hopes to discover implications for phosphorus removal. A correlation was found between snRP and Trp concentrations for secondary treatment (R^2 = .642, r =.801, p<.01) and for tertiary treatment with biological removal (R^2 = .810, r =.900, p<.01). A correlation was also found between snRP and Tyr concentrations for tertiary treatment with biological removal (R^2 = .857, r =.926, p<.01). Wastewater organic matter has variable fluorescent components; water varies in terms of input source as well as within treatment plants. This variability has implications for phosphorus removal. The so-called non-reactive phosphorus (nRP) is defined colorimetrically to include all non-orthophosphate phosphorus. This fraction of total phosphorus tends to be more difficult to remove than orthophosphate. Biological treatment technologies tend to remove nRP to low levels correlated with a decrease in the fluorescent component tryptophan.

Future sampling and measurement of the fluorescent fluorophores and phosphorus speciation could be useful in developing these correlations.

6.1.2 Chapter 4: Screening of bench top wastewater treatment technologies for phosphorus removal

Objective 3: to test advanced wastewater treatment methods for conversion from non-reactive phosphorus and/or decrease total phosphorus.

Objective three was the main goal of Chapter 4: to look into preexisting wastewater treatments for a cost effective and efficient method to breakdown refractory (organic) phosphorus. This chapter examined adsorption chemistry through the use of activated carbon and explored five different AOPs; hydrogen peroxide, ultraviolet photolysis, the combination of H_2O_2 and photolysis, ozone and ferrate.

Three of the six methods decreased non-reactive phosphorus or decreased total phosphorus. UV photolysis was found to decrease non-reactive phosphorus by approximately 26% percent. In the combined UV/H_2O_2 treatment, non-reactive phosphorus was decreased by 18%. Ferrate was found to decrease total phosphorus by approximately 35%. Ferrate treatment was intriguing in that it could be very useful due to it being a combination treatment; ferrate treatment combines oxidation and chemical precipitation.

While some methods were successful in liberating reactive phosphorus, other methods had some difficulty. Due to the method used to prepare the surface of activated carbon, activated carbon was deemed to be a source of phosphorus contamination and not an appropriate method for phosphorus removal. Ozone had no effect on non-reactive phosphorus, but was found to be oxidizing some labile form of organic matter that did not contain phosphorus. Complications with colour formation arose with use of hydrogen peroxide leading to reactive phosphorus liberation with the use of H_2O_2 hot acid digestion.

Future studies in bench top testing can go in many directions. Some studies could include determining optimal dosages for hydrogen peroxide in the individual and UV

combined treatments. Dose dependency could also be explored for the ferrate treatment. Other combined treatments could also be explored. The ozone and UV treatments had no effect on the RO brine in this study; however ozone in combination with UV has been known to enhance the generation of hydroxyl radicals and, in turn, increase oxidation rates (Gogate and Pandit, 2004).

6.1.3 Chapter 5: Characterization of surface reactive sites in high solids synthetic wastewater and implications for pH simulation

Objective 4: to test a pH prediction model based on electroneutrality for a simple synthetic wastewater.

The first objective of Chapter 5 was to test an electroneutrality based pH model on a simple synthetic wastewater; the simulated titration agreed very well with the measured titration data of the simple system.

Objective 5: to test the impacts of solids on the pH prediction of the pH model based on electroneutrality.

Difficulties arose upon implementation of the second objective, to test the impact of solids on the pH prediction of the model. When measured titration data of the synthetic wastewater with ferric oxide was compared to the pH model, there was a large amount of error.

Objective 6: If necessary, develop revised pH prediction model that will take the solids surface reactive sites into account.

In the beginning, the model overestimated the pH of the high solids system. This was an unexpected trend due to the fact that the model does not take into account positively charged reactive sites, a condition which would lead to the underestimation of pH. After the addition of a permanently charged surface reactive site on the iron oxide surface, the expected trend of pH underestimation was observed. Measured titration data agreed with the model after the addition of two positively charged surface reactive sites to the tableau notation. The first positively charged site had a pK_a of around 8 while the second site had a pK_a around 10.2. The pK_a value of 8 agreed with pK_as found for hydrous ferric oxides in literature as well as the pK_a spectra calculated using titration data and discrete site analysis for the high solids system.

Investigating the effects of a more complicated high solid synthetic wastewater would be an excellent experiment to move forward with this project. One component that could be added to the more complicated synthetic wastewater would be carbonate which is present in all wastewater. Another study that could lead to the advancement of pH modeling would be to use acid-base titrations to measure high solids samples. Investigating the surface reactive sites in high solids wastewater samples would have real world applications.

6.2 REFERENCES

Gogate, P. R. and Pandit, A. B. (2004) A review of imperative technologies for wastewater treatement II: hybrid methods. *Advances in Environmental Research* **8**, 553-597.

Appendix A: Supplementary Information for Chapter 3

Non-reactive phosphorus (and dissolved organic phosphorus) correlations with humic substances, tryptophan and tyrosine fluorophores

Table A1: A summary of the correlations between non-reactive phosphorus (nRP) and tryptophan (Trp) fluorophore concentrations. Asterisks denote statistical significance.

Treatment Technology	r^2	*r*	*p*
Overall	0.539	0.795	<0.01*
Secondary Treatment	0.642	0.801	<0.01*
Tertiary Treatment with Biological Removal	0.810	0.901	<0.01*
Tertiary Treatment without Biological Removal	0.019	-0.139	0.518

Table A2: A summary of the correlations between non-reactive phosphorus (DOP) and tryptophan (Trp) fluorophore concentrations. Asterisks denote statistical significance.

Treatment Technology	*r*	*p*
Secondary Treatment	0.790	0.011*
Tertiary Treatment with Biological Removal	0.950	0.01*
Tertiary Treatment without Biological Removal	-0.139	0.516

Table A3: A summary of the correlations between non-reactive phosphorus (nRP) and tyrosine (Tyr) fluorophore concentrations. Asterisks denote statistical significance.

Treatment Technology	r^2	*r*	*p*
Overall	0.633	0.734	<0.01*
Secondary Treatment	0.291	0.539	0.134
Tertiary Treatment with Biological Removal	0.857	0.926	<0.01*
Tertiary Treatment without Biological Removal	0.007	-0.084	0.697

Table A4: A summary of the correlations between non-reactive phosphorus (DOP) and tyrosine (Tyr) fluorophore concentrations. Asterisks denote statistical significance.

Treatment Technology	*r*	*p*
Secondary Treatment	0.535	0.138
Tertiary Treatment with Biological Removal	0.949	0.01*
Tertiary Treatment without Biological Removal	0.026	0.451

Table A5: A summary of the correlations between non-reactive phosphorus (nRP) and humic substances (HS) fluorophore concentrations. Asterisks denote statistical significance.

Treatment Technology	r^2	*r*	*p*
Overall	0.216	0.464	<0.01*
Secondary Treatment	0.271	0.521	>0.15
Tertiary Treatment with Biological Removal	0.304	0.552	>0.15
Tertiary Treatment without Biological Removal	0.065	0.256	>0.15

Table A6: A summary of the correlations between non-reactive phosphorus (DOP) and humic substances (HS) fluorophore concentrations. Asterisks denote statistical significance.

Treatment Technology	*r*	*p*
Secondary Treatment	0.486	0.185
Tertiary Treatment with Biological Removal	0.607	0.148
Tertiary Treatment without Biological Removal	0.344	0.100

Table A7: A summary of the correlations between non-reactive phosphorus (nRP) and humic substances (HS) fluorophore concentrations for the filtration and sedimentation processes in tertiary treatment without biological removal. Asterisks denote statistical significance.

Treatment Technology	r^2	r	p
Filtration	0.701	0.837	0.019*
Sedimentation	0.842	0.917	0.83

Table A8: A summary of the correlations between non-reactive phosphorus (DOP) and humic substances (HS) fluorophore concentrations for the filtration and sedimentation processes in tertiary treatment without biological removal. Asterisks denote statistical significance.

Treatment Technology	r^2	r	p
Filtration	0.587	0.766	0.027*
Sedimentation	0.882	0.939	0.018*

Table A9: A summary of the correlations between non-reactive phosphorus (nRP) and humic substances (HS) fluorophore concentrations for physical removal processes. Asterisks denote statistical significance.

Treatment Technology	r	p
Single Sedimentation	0.656	0.15
Single Filtration	0.175	0.825
Sedimentation + Filtration	0.201	0.665
Filtration + Filtration	0.779	0.068

Table A10: A summary of the correlations between non-reactive phosphorus (DOP) and humic substances (HS) fluorophore concentrations for physical removal processes. Asterisks denote statistical significance.

Treatment Technology	*r*	*p*
Single Sedimentation	0.944	0.005*
Single Filtration	-0.309	0.691
Sedimentation + Filtration	0.087	0.853
Filtration + Filtration	0.428	0.397

Appendix B: Supplementary Information for Chapter 5

B1. MATLAB™ script used to simulate pH for a simple synthetic wastewater titration.

```
function II=holly_test_model_titration(Na,Cl)

warning('off')

% define total concs and equilib constants
%%

% NH4Cl - 96.0mg/L ->1.795mM
% KH2PO4 - 17.4mg/L -> 0.125mM
% MgSO4 7H2O - 24.0mg/L -> 0.0974mM
% CaCl2 2H2O - 2.4mg/L -> 0.0163mM
% NaHCO3 - 300mg/L -> 3.5710mM
% NaAcetate - 10mM

NH3t=0.001795; SO4t=0.0000974; AceticTot=0.010; PO4t=0.000125; Cat=0.0000163;
Mgt=0.0000974;
ClT=NH3t+2*Cat+Cl; NaT=AceticTot+Na; KT=PO4t;

KiSO4=0.01023292992;
Kw =10^(-13.9620);
KiNH3 =10^(-9.2464);
KiAc =10^(-4.7254);
KP1 =10^(-2.0965);
KP2 =10^(-7.1093);
KP3 =10^(-12.2123);
ksCaOH1 =19.95262315;
ksMgOH1 =398.1071706;


%%

% define tableau (log base 10 not base e!)

%%
tableauandcharge=[...
    %H  NH3  Ac  PO4  SO4 Ca  Mg   Na   K  Cl logK
    +1  0    -1   -3  -2  +2  +2   +1  +1  -1  0  % NEW charge row
    1   0    0    0    0  0   0  0   0   0   0
    0   1    0    0    0  0   0  0   0   0   0
    0   0    1    0    0  0   0  0   0   0   0
    0   0    0    1    0  0   0  0   0   0   0
    0   0    0    0    1  0   0  0   0   0   0
    0   0    0    0    0  1   0  0   0   0   0
    0   0    0    0    0  0   1  0   0   0   0
    0   0    0    0    0  0   0  1   0   0   0 %Na
    0   0    0    0    0  0   0  0   1   0   0 %K
    0   0    0    0    0  0   0  0   0   1   0 %Cl
    -1  0    0    0    0  0   0  0   0   0   log10(Kw) %OH-
    1   1    0    0    0  0   0  0   0   0  -log10(KiNH3) %NH4+
    1   0    1    0    0  0   0  0   0   0  -log10(KiAc) %HAc
    1   0    0    1    0  0   0  0   0   0  -log10(KP3) %HPO4
```

```
    2   0    0    1    0  0   0  0   0   0  -log10(KP2)-log10(KP3)
                                                        %H2PO4
    3   0    0    1    0  0   0  0   0   0  -log10(KP1)-log10(KP2)-
                                                 log10(KP3) %H3PO4
    1   0    0    0    1  0   0  0   0   0  -log10(KiSO4) %HSO4
   -1   0    0    0    0  1   0  0   0   0  log10(ksCaOH1)+log10(Kw)
                                                         %CaOH
   -1   0    0    0    0  0   1  0   0   0  log10(ksMgOH1)+log10(Kw)
                                                         %MgOH
    ];
%%

[tableau,charge]=gettableau(tableauandcharge); % NEW function

% define other stuff

%%
SPECIESNAMES=strvcat('H','NH3','Ac','PO4','SO4','Ca','Mg','Na','K', ...
    'Cl','OH','NH4','HAc','HPO4','H2PO4','H3PO4','HCO3','H2CO3',...
    'HSO4','CaOH','MgOH');

masstotals=[NH3t  AceticTot  PO4t  SO4t  Cat  Mgt NaT KT ClT]; % NEW (modifed
just mass no TOTH)

totals=gettotals(masstotals,charge); % NEW function get totals include TOTH

recipe=eye(size(totals,2),size(totals,2));

iterations=10000; criteria=1e-16;
%%


% define species for algebraic method

%%
fH=@(pH)10^-pH;
fOH=@(pH)Kw/fH(pH);
fAc=@(pH)(AceticTot*KiAc)/(fH(pH) + KiAc);
fHAc=@(pH)(AceticTot*fH(pH))/(fH(pH) + KiAc);
fPO4=@(pH)(KP3*KP2*KP1*PO4t)/
                (fH(pH)^3+fH(pH)^2*KP1+fH(pH)*KP1*KP2+KP1*KP2*KP3);
fHPO4=@(pH)(fH(pH)*KP2*KP1*PO4t)/
                (fH(pH)^3+fH(pH)^2*KP1+fH(pH)*KP1*KP2+KP1*KP2*KP3);
fH2PO4=@(pH)(fH(pH)^2*KP1*PO4t)/
                (fH(pH)^3+fH(pH)^2*KP1+fH(pH)*KP1*KP2+KP1*KP2*KP3);
fH3PO4=@(pH)(fH(pH)^3*PO4t)/
                (fH(pH)^3+fH(pH)^2*KP1+fH(pH)*KP1*KP2+KP1*KP2*KP3);
fSO4=@(pH)(SO4t*KiSO4)/(fH(pH) + KiSO4);
fHSO4=@(pH)(fH(pH)*SO4t)/(fH(pH) + KiSO4);
fCa=@(pH)(Cat*fH(pH))/(fH(pH)+ksCaOH1*Kw);
fCaOH=@(pH)(Cat*ksCaOH1*Kw)/(fH(pH)+ksCaOH1*Kw);
fMg=@(pH)(Mgt*fH(pH))/(fH(pH)+ksMgOH1*Kw);
fMgOH=@(pH)(Mgt*ksMgOH1*Kw)/(fH(pH)+ksMgOH1*Kw);
fNH4=@(pH)(NH3t*fH(pH))/(fH(pH) + KiNH3);
fNH3=@(pH)(NH3t*KiNH3)/(fH(pH) + KiNH3);
fNa=@(pH)(NaT);
fK=@(pH)(KT);
fCl=@(pH)(ClT);
%%
```

```
% solve for pH using tableau

%%
pHguess=7;
guess=[fH(pHguess)  fNH4(pHguess)  fAc(pHguess)    fPO4(pHguess) ...
    fSO4(pHguess) fCa(pHguess)  fMg(pHguess) fNa(pHguess) fK(pHguess)
fCl(pHguess)];

%guess=[1e-7 TOTALS*10];

[species1,err1]=solve_tableau_recipe(tableau,recipe,totals,guess,iterations,cri
teria);

for i=1:size(species1,1)
    txt=[SPECIESNAMES(i,:),'=species1(i,:);']; eval(txt)
end

format short e; pHsolve=-log10(species1(1));

%%

II=pHsolve;

end



% function to solve for speciation in aqueous phase

function
[species,err]=solve_tableau_recipe(tableau,recipe,totals,guess,iterations,crite
ria)

% this is a function to make a speciation calculation
% using the newton-raphson method and tableau notation
% matlab version is function [II,G,
HH]=solve_tableau(tableau,guess,Imax,criteria)
% structure of tablea, the entries are the stoichimetric coeff for the species
% with each column a component except the last is the log10 of the stab
constant
% and the bottom row is the mass balances

[n,m]=size(tableau); X=guess';

K=tableau(1:n,m);
A=tableau(1:n,1:m-1);
T=recipe'*totals';

for II=1:iterations

       logC=(K)+A*log10(X); C=10.^(logC); % calc species
       R=A'*C-T; % calc residuals

       % calc the jacobian

       z=zeros(m-1,m-1);

       for i=1:size(A,1); % loop thru the species
              for j=1:size(A,2); % loop thru components
                     for k=1:size(A,2); % loop thru components
                            z(j,k)=z(j,k)+A(i,j)*A(i,k)*C(i)/X(k);
                     end
```

```
            end
        end

        deltaX=z\(-1*R);

        one_over_del=max([1, -1*deltaX'./(0.5*X')]);
        del=1/one_over_del;
    X=X+del*deltaX;

        %tst=max(abs(R));
    tst=sum(abs(R));
    %tst=sum(R.^2);
        if tst<=criteria; break; end

end

logC=(K)+A*log10(X); C=10.^(logC); % calc species
R=A'*C-T; % calc residuals

err=R;
species=C;

end

% alter existing tableau for a given fixed pH

function II=make_fixedpH_tableau(tableau,pH)

H=10.^(-1*pH);

[n,m]=size(tableau);

% just alter the stability constants

last_column=tableau(:,m);
first_column=tableau(:,1);

new_last_column=(H.*ones(size(first_column))).^(first_column).*(10.^(last_colum
n));
new_last_column=log10(new_last_column);

tableau=[tableau(:,2:m-1) new_last_column];

II=tableau;

end

function [II,GG]=gettableau(tableaupluscharge)
[n,m]=size(tableaupluscharge);
tableau=tableaupluscharge(2:n,1:m);
charge=tableaupluscharge(1,2:m-1); %  leave off H+ and the logK entry.  just
charge of species
II=tableau;
GG=charge;
end

function [II]=gettotals(masstotals,charge)
TOTH=sum(-1*masstotals.*charge); %
totals=[TOTH masstotals]; %
II=totals;
end
```

B2. MATLAB^{TM} script adjusted to simulate pH for a high solids synthetic wastewater titration.

```
function II=holly_test_model_titration_surfacemod(p,Na,Cl)

warning('off')


S1T=p(1); S2T=p(2); S3T=p(3); K1S2=p(4); K1S3=p(5);

% define total concs and equilib constants
%%

% NH4Cl - 96.0mg/L ->1.795mM
% KH2PO4 - 17.4mg/L -> 0.125mM
% MgSO4 7H2O - 24.0mg/L -> 0.0974mM
% CaCl2 2H2O - 2.4mg/L -> 0.0163mM
% NaHCO3 - 300mg/L -> 3.5710mM
% NaAcetate - 10mM

NH3t=0.001795; SO4t=0.0000974; AceticTot=0.010; PO4t=0.000125;
Ct=0.0000000001; Cat=0.0000163; Mgt=0.0000974;
ClT=NH3t+2*Cat+Cl; NaT=Ct+AceticTot+Na; KT=PO4t;

KiSO4=0.01023292992;
Kw =0.6867000000e-14;
KiNH3 =0.3966000000e-9;
KiAc =0.00001754000000;
KP1 =0.007452000000;
KP2 =0.6103000000e-7;
KP3 =0.9484000000e-12;
KC1 =0.4140000000e-6;
KC2 =0.4201000000e-10;
ksCaOH1 =19.95262315;
ksMgOH1 =398.1071706;

%%
%%
tableauandcharge=[...
    %H  NH3  Ac  PO4   CO3  SO4    Ca  Mg   Na   K  Cl S1 S2  S3  logK
    +1  0    -1   -3    -2  -2    +2  +2   +1  +1  -1 -1 0   0    0  % NEW charge row
    1   0    0    0     0    0     0   0  0   0   0   0  0   0    0
    0   1    0    0     0    0     0   0  0   0   0   0  0   0    0
    0   0    1    0     0    0     0   0  0   0   0   0  0   0    0
    0   0    0    1     0    0     0   0  0   0   0   0  0   0    0
    0   0    0    0     1    0     0   0  0   0   0   0  0   0    0
    0   0    0    0     0    1     0   0  0   0   0   0  0   0    0
    0   0    0    0     0    0     1   0  0   0   0   0  0   0    0
    0   0    0    0     0    0     0   1  0   0   0   0  0   0    0
    0   0    0    0     0    0     0   0  1   0   0   0  0   0    0 %Na
    0   0    0    0     0    0     0   0  0   1   0   0  0   0    0 %K
    0   0    0    0     0    0     0   0  0   0   1   0  0   0    0 %Cl
    0   0    0    0     0    0     0   0  0   0   0   1  0   0    0 %S1
    0   0    0    0     0    0     0   0  0   0   0   0  1   0    0 %S2
    0   0    0    0     0    0     0   0  0   0   0   0  0   1    0 %S3
    -1  0    0    0     0    0     0   0  0   0   0   0  0   0  log10(Kw)
                                                                  %OH-
    1   0    0    0     0    0     0   0  0   0   0   0  1   0 -log10(K1S2)
                                                                  %S2H
    1   0    0    0     0    0     0   0  0   0   0   0  0   1 -log10(K1S3)
                                                                  %S3H
    1   1    0    0     0    0     0   0  0   0   0   0  0   0 -log10(KiNH3)
                                                                  %NH4+
    1   0    1    0     0    0     0   0  0   0   0   0  0   0 -log10(KiAc)
                                                                  %HAc
    1   0    0    1     0    0     0   0  0   0   0   0  0   0 -log10(KP3)
```

```
                                                                    %HPO4
    2   0    0    1     0    0     0   0  0   0   0   0  0   0 -log10(KP2)-
                                                                  log10(KP3)
                                                                    %H2PO4
    3   0    0    1     0    0     0   0  0   0   0   0  0   0  -log10(KP1)-
                                                               log10(KP2)-log10(KP3)
                                                                    %H3PO4
    1   0    0    0     1    0     0   0  0   0   0   0  0   0  -log10(KC2)
                                                                    %HCO3
    2   0    0    0     1    0     0   0  0   0   0   0  0   0   -log10(KC2)-
                                                                 log10(KC1)  %H2CO3
    1   0    0    0     0    1     0   0  0   0   0   0  0   0  -log10(KiSO4)
                                                                    %HSO4
   -1   0    0    0     0    0     1   0  0   0   0   0  0   0  log10(ksCaOH1)
                                                                   +log10(Kw) %CaOH
   -1   0    0    0     0    0     0   1  0   0   0   0  0   0  log10(ksMgOH1)
                                                                   +log10(Kw) %MgOH
    ];
%%

[tableau,charge]=gettableau(tableauandcharge); % NEW function

% define other stuff

%%
SPECIESNAMES=strvcat('H','NH3','Ac','PO4','CO3','SO4','Ca','Mg','Na','K','Cl','S1', ...
'S2','S3','OH','S2H','S3H','NH4','HAc','HPO4','H2PO4','H3PO4','HCO3','H2CO3','HSO4',...
    'CaOH','MgOH');

masstotals=[NH3t  AceticTot  PO4t  Ct  SO4t  Cat  Mgt NaT KT ClT S1T S2T S3T]; % NEW
(modifed just mass no TOTH)

totals=gettotals(masstotals,charge); % NEW function get totals include TOTH

recipe=eye(size(totals,2),size(totals,2));

iterations=10000; criteria=1e-16;
%%

% define species for algebraic method

%%
fH=@(pH)10^-pH;
fOH=@(pH)Kw/fH(pH);
fS1=@(pH)(S1T);
fS2=@(pH)(S2T);
fS3=@(pH)(S3T);
fAc=@(pH)(AceticTot*KiAc)/(fH(pH) + KiAc);
fHAc=@(pH)(AceticTot*fH(pH))/(fH(pH) + KiAc);
fPO4=@(pH)(KP3*KP2*KP1*PO4t)/(fH(pH)^3+fH(pH)^2*KP1+fH(pH)*KP1*KP2+KP1*KP2*KP3);
fHPO4=@(pH)(fH(pH)*KP2*KP1*PO4t)/(fH(pH)^3+fH(pH)^2*KP1+fH(pH)*KP1*KP2+KP1*KP2*KP3);
fH2PO4=@(pH)(fH(pH)^2*KP1*PO4t)/(fH(pH)^3+fH(pH)^2*KP1+fH(pH)*KP1*KP2+KP1*KP2*KP3);
fH3PO4=@(pH)(fH(pH)^3*PO4t)/(fH(pH)^3+fH(pH)^2*KP1+fH(pH)*KP1*KP2+KP1*KP2*KP3);
fCO3=@(pH)(KC2*KC1*Ct)/(fH(pH)^2+fH(pH)*KC1+KC1*KC2);
fHCO3=@(pH)(fH(pH)*KC1*Ct)/(fH(pH)^2+fH(pH)*KC1+KC1*KC2);
fH2CO3=@(pH)(fH(pH)^2*Ct)/(fH(pH)^2+fH(pH)*KC1+KC1*KC2);
fSO4=@(pH)(SO4t*KiSO4)/(fH(pH) + KiSO4);
fHSO4=@(pH)(fH(pH)*SO4t)/(fH(pH) + KiSO4);
fCa=@(pH)(Cat*fH(pH))/(fH(pH)+ksCaOH1*Kw);
fCaOH=@(pH)(Cat*ksCaOH1*Kw)/(fH(pH)+ksCaOH1*Kw);
fMg=@(pH)(Mgt*fH(pH))/(fH(pH)+ksMgOH1*Kw);
fMgOH=@(pH)(Mgt*ksMgOH1*Kw)/(fH(pH)+ksMgOH1*Kw);
fNH4=@(pH)(NH3t*fH(pH))/(fH(pH) + KiNH3);
fNH3=@(pH)(NH3t*KiNH3)/(fH(pH) + KiNH3);
fNa=@(pH)(NaT);
fK=@(pH)(KT);
fCl=@(pH)(ClT);
%%
```

```
% solve for pH using tableau

%%
pHguess=7;
guess=[fH(pHguess)  fNH4(pHguess)  fAc(pHguess)    fPO4(pHguess)   fCO3(pHguess) ...
    fSO4(pHguess) fCa(pHguess)  fMg(pHguess) fNa(pHguess) fK(pHguess) fCl(pHguess) ...
    fS1(pHguess) fS2(pHguess) fS3(pHguess)];

%guess=[1e-7 TOTALS*10];

[species1,err1]=solve_tableau_recipe(tableau,recipe,totals,guess,iterations,criteria);

for i=1:size(species1,1)
    txt=[SPECIESNAMES(i,:),'=species1(i,:);']; eval(txt)
end

format short e; pHsolve=-log10(species1(1));

%%

II=pHsolve;

end

% function to solve for speciation in aqueous phase

function
[species,err]=solve_tableau_recipe(tableau,recipe,totals,guess,iterations,criteria)

% this is a function to make a speciation calculation
% using the newton-raphson method and tableau notation
% matlab version is function [II,G, HH]=solve_tableau(tableau,guess,Imax,criteria)
% structure of tablea, the entries are the stoichimetric coeff for the species
% with each column a component except the last is the log10 of the stab constant
% and the bottom row is the mass balances

[n,m]=size(tableau); X=guess';

K=tableau(1:n,m);
A=tableau(1:n,1:m-1);
T=recipe'*totals';

for II=1:iterations

        logC=(K)+A*log10(X); C=10.^(logC); % calc species
        R=A'*C-T; % calc residuals

        % calc the jacobian

        z=zeros(m-1,m-1);

        for i=1:size(A,1); % loop thru the species
                for j=1:size(A,2); % loop thru components
                        for k=1:size(A,2); % loop thru components
                                z(j,k)=z(j,k)+A(i,j)*A(i,k)*C(i)/X(k);
                        end
                end
        end

        deltaX=z\(-1*R);

        one_over_del=max([1, -1*deltaX'./(0.5*X')]);
        del=1/one_over_del;
    X=X+del*deltaX;

        %tst=max(abs(R));
    tst=sum(abs(R));
    %tst=sum(R.^2);
        if tst<=criteria; break; end
```

```
end

logC=(K)+A*log10(X); C=10.^(logC); % calc species
R=A'*C-T; % calc residuals

err=R;
species=C;

end

% alter existing tableau for a given fixed pH

function II=make_fixedpH_tableau(tableau,pH)

H=10.^(-1*pH);

[n,m]=size(tableau);

% just alter the stability constants

last_column=tableau(:,m);
first_column=tableau(:,1);

new_last_column=(H.*ones(size(first_column))).^(first_column).*(10.^(last_column));
new_last_column=log10(new_last_column);

tableau=[tableau(:,2:m-1) new_last_column];

II=tableau;

end

function [II,GG]=gettableau(tableaupluscharge)
[n,m]=size(tableaupluscharge);
tableau=tableaupluscharge(2:n,1:m);
charge=tableaupluscharge(1,2:m-1); %  leave off H+ and the logK entry.  just charge of
species
II=tableau;
GG=charge;
end

function [II]=gettotals(masstotals,charge)
TOTH=sum(-1*masstotals.*charge); %
totals=[TOTH masstotals]; %
II=totals;
end
```

B3. MATLAB™ script used to calculate reactive site concentrations (DISI – Discrete Site Analysis).

```
% this will take data and fit it to Lts given a fixed
% pKas distribution

function [II,G,H]=disi_new(b,pH,pKas,Kw);

H=10.^(-1*pH); OH=(Kw*ones(size(H)))./H;

% now a nested loop of size i and j to make matrix A of alphas
% and make vector b of values to be fit = charge excess

K=10.^(-1*pKas);

for i=1:size(pH,2)
```

```
        for j=1:size(pKas,2)
                A(i,j)=K(j)/(K(j)+H(i));
        end
end

%figure(1); plot(pH,b,'o'); figure(1); %pause

[m,n]=size(A);

% now setup the dual problem as in Kramer and Brassard 1992

Ad=[A' 0.5*diag(ones(1,n))];
Ad(size(Ad,1)+1,:)=[ones(1,size(A',2)) zeros(1,n)];

bd=0.5*sum(A); bd(size(bd,2)+1)=m/2;

fd=[-1*b' zeros(1,n)];

vlb=zeros(size(fd));  vub=2*ones(size(fd));
%vub=[];

N=length(bd);

Aeq=Ad(1:N,:); beq=bd(1:N); Ad=Ad(N+1:end,:); bd=bd(N+1:end,:);
OPTIONS=optimset('Display','final');

%[Xd,lambda]=lp(fd,Ad,bd,vlb,vub,[],length(bd));
[X,FVAL,EXITFLAG,OUTPUT,LAMBDA]=linprog(fd,Ad,bd,Aeq,beq,vlb,vub,[],OPTIONS);
%[Xd,lambda]=lp(fd,Ad,bd,vlb,vub,[],length(bd));

%vlb=zeros(size(fd)); % vub=2*ones(size(fd));
%vub=[];

%[Xd,fval,exitflag,output,lambda]=linprog(fd,Ad,bd,[],[],vlb,vub);

solv=LAMBDA.eqlin(1:N-1);
Canc=-1*LAMBDA.eqlin(N)

% also calculate error

bcalc=A*solv-Canc;
err=bcalc-b

%figure(1); plot(pH,bcalc,'o','markerfacecolor','b','markersize',12);
%hold on
%plot(pH,b,'k-','markersize',12);
%figure(2); bar(pKas,solv); axis([pKas(1) pKas(N-1) -max(solv) max(solv)]);
figure(2)

II=solv; G=Canc; H=err;
```

Appendix C: Ultrafiltration using Molecular Weight Cut Off Summary

Objectives

This research was implemented to characterize composition of total dissolved phosphorus based on molecular size. Ultrafiltration of the various fractions of nonreactive phosphorus will aid in the understanding of refractory phosphorus and if the phosphorus is found in a certain molecular size range.

C.1 METHODOLOGY

Molecular weight cut off (MWCO) centrifuge filters of cut off sizes 30 kDa and 10 kDa (VWR, modified polyethersulfone (PES)) with a 500 µl sample size were used. The MWCO Filters were rinsed to avoid contamination of the sample. The sample chamber was filled with 0.1N NaOH and spun in the centrifuge at 12 000g for 30 seconds. The sample chamber and the collection chamber were then rinsed with MilliQ water and tapped on a clean Kim Wipe (Kimberly-Clark Worldwide Inc., Mississauga, ON) to removed excess water. The sample chamber was then filled again with MilliQ water and spun at 12 000g for 30 seconds and tapped again to removed excess water. The filter was then rinsed with a small volume of sample and tapped on a clean Kim Wipe to remove any excess.

A small volume (520 µl) of sample is passed through the MWCO filter. The sample is centrifuged at 14 000g for 15 minutes and then 500 µl of filtrate is then diluted to 10ml. Colorimetric phosphorus determination was completed using the ascorbic acid method optimized by Gilmore et al. (2008) following the Standard Method (4500-P E.).

The concentration of the unknown samples will be determined through the use of a calibration curve. Soluble reactive phosphorus (sRP) is then measured directly from the sample or the sample is digested using an ammonium persulfate digestion from the Standard Methods to determine the total phosphorus in the filtrate (sTP). The sRP was measured for both the 30 kDa and the 10 kDa MWCO filtrates as a check for sample inconsistencies.

C.2 RESULTS

Through the use of ultrafiltration and colorimetric methods, several molecular weight fractions of total dissolved phosphate (sTP) have been measured for samples of the BNR process at the WWTP-A. The summary of these results are presented in Table D.1. Total phosphorus decreases through the BNR process from 1.164 mg P/L in the influent to 0.224 mg P/L in the effluent.

The fraction with the largest amount of nonreactive phosphorus for both the BNR influent and effluent samples was the 0.45 μm to 30 kDa fraction (high molecular weight phosphorus). The influent had a nonreactive phosphorus concentration of 0.158 mg P/L, while the effluent had a concentration of 0.114 mg P/L. The sample fraction below 10 kDa had nonreactive phosphorus concentrations of 0.072 and 0.024 mg P/L for the BNR influent and effluent, respectively. These results are shown in Table D.2.

Sample Location	sRP 0.45µm	sTP 0.45µm	sTP 30kDa	sTP 10kDa
Las Vegas Water Pollution Control Facility				
BNR Influent	0.882	1.164	1.006	0.954
BNR Effluent	0.089	0.224	0.110	0.113

Table C.1: Summary of total dissolved phosphorus (sTP) and soluble reactive phosphorus (sRP) concentration (mg P/L) for BNR influent and effluent of the Las Vegas WPCF.

As seen in Figure D.1, there is a noticeable difference in the change of total dissolved phosphorus concentrations in the 30 kDa and 10 kDa fractions between the BNR influent and effluent. Nonreactive phosphorus decreases in each of the molecular weight fractions through the BNR process. There is a 27% decrease in the fraction of total dissolved phosphorus for species above 30 kDa and ~60% decrease in the fraction of less than 10kDa. The fraction between 10 and 30 kDa was completely lost through the BNR process. This could mean that the phosphorus found in the 10-30 kDa fraction is more bioavailable than the phosphorus of the other fractions.

Sample Location	30kDa< nRP< 0.45µm	10kDa<nRP<30kDa	nRP<10kDa
Las Vegas Water Pollution Control Facility			
BNR Influent	0.158	0.042	0.072
BNR Effluent	0.114	N/D	0.024

Table C.2: **Concentrations (mg P/L) of nonreactive phosphorus (nRP) for various size fractions measured in BNR influent and effluent samples (N/D- not detectable).**

Progress has halted on this experiment due to changes in the speciation of the wastewater samples from storage and/or age and possible contamination of the MWCO spin filters. Although the MWCO spin filters were tested for orthophosphate contamination, the filters were not tested for any other form of phosphorus contamination. While working with other forms of filters (membrane filters), it was found that there was phosphorus contamination when a blank was measured for total phosphorus. This may have also been the case for the MWCO spin filters.

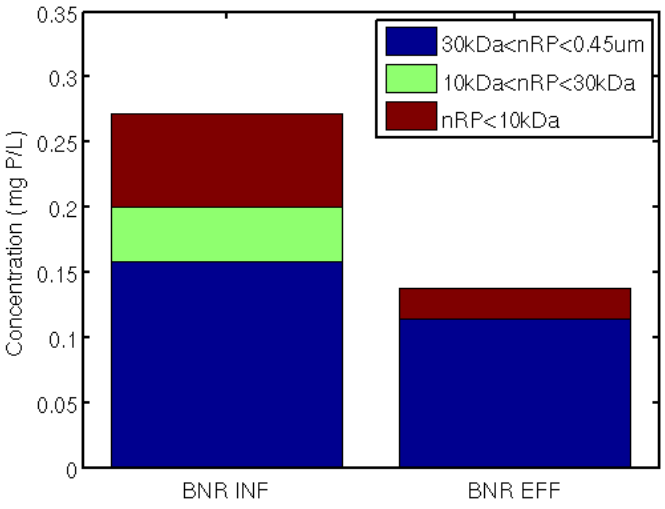

Figure C.1: Concentrations (mg P/L) of nonreactive phosphorus (nRP) for various size fractions measured in BNR influent and effluent samples.

Appendix D: Solving for Total [H^+]

This appendix will solve for the expression of H+T using a simple system; the system is described by the tableau in Figure E.1

Species	H^+	NH_3	Ac^-	PO_4^{3-}	log K
Charge	+1	0	-1	-3	0
H^+	1	0	0	0	0
NH_3	0	1	0	0	0
Ac^-	0	0	1	0	0
$PO4^{3-}$	0	0	0	1	0
OH^-	-1	0	0	0	$\log K_w$
NH_4^+	1	1	0	0	$-\log K_{NH3}$
HAc	1	0	1	0	$-\log K_{Ac}$
HPO_4^{2-}	1	0	0	1	$-\log K_{PO4}$
$H_2PO_4^-$	2	0	0	1	$-\log K_{HPO4} -\log K_{PO4}$
H_3PO_4	3	0	0	1	$-\log K_{H2PO4}-\log K_{HPO4}-\log K_{PO4}$

Figure E.1: Tableau for simple system.

H^+_T can be calculated by using a linear combination of electroneutrality and species charge; species charge is given in row 2 of the tableau in Figure E.1. In this example, H^+_T can be calculated from the tableau as a function of NH_{3T}, Ac_T and PO_{4T}. The electroneutrality (E_{NEUT}) expression of the system is determined through the summation of the total concentrations of each species which has been multiplied by the charge of the species. This expression is shown in Equation E.1

$$E_{NEUT} = +1H^{+}_{T} + 0NH_3 - 1Ac_T - 3PO_{4T} \quad \text{(E.1)}$$

Equation E.1 can be simplified (Equation E.2) and rearranged to solve for H^{+}_{T} (Equation E.3)

$$0 = +1H^{+}_{T} + 0 - 1Ac_T - 3PO_{4T} \quad \text{(E.2)}$$

$$H^{+}_{T} = Ac_T + 3PO_{4T} \quad \text{(E.3)}$$

To see if electroneutrality is satisfied, the vector for the charge of each component can be added to Equation E.3; if it holds true, the solution of the vector equation will return the vector of H^{+}_{T} stoichiometric coefficients. This is shown in Equation E.4 below; the solution returns the H^{+}_{T} vector (final vector on far right).

$$\begin{pmatrix} 1 \\ 0 \\ 0 \\ 0 \\ -1 \\ 1 \\ 1 \\ 1 \\ 2 \\ 3 \end{pmatrix} = \begin{pmatrix} 1 \\ 0 \\ -1 \\ -3 \\ -1 \\ 1 \\ 0 \\ -2 \\ -1 \\ 0 \end{pmatrix} + 0 \begin{pmatrix} 0 \\ 1 \\ 0 \\ 0 \\ 1 \\ 0 \\ 0 \\ 0 \\ 0 \\ 0 \end{pmatrix} + \begin{pmatrix} 0 \\ 0 \\ 1 \\ 0 \\ 0 \\ 0 \\ 1 \\ 0 \\ 0 \\ 0 \end{pmatrix} + 3 \begin{pmatrix} 0 \\ 0 \\ 0 \\ 1 \\ 0 \\ 0 \\ 0 \\ 1 \\ 1 \\ 1 \end{pmatrix} = \begin{pmatrix} 1 \\ 0 \\ 0 \\ 0 \\ -1 \\ 1 \\ 1 \\ 1 \\ 2 \\ 3 \end{pmatrix} \quad \text{(E.4)}$$

Appendix E: Supplementary Information for Manuscript

E.1 METHODOLOGY

Samples were measured in a 1cm quartz cuvette using a Varian Cary Eclipse Fluorescence Spectrometer. The spectrometer scans simultaneously across excitation wavelengths (220–600 nm, 10 nm increments) and emission wavelengths (250 – 600 nm, 1 nm increments). Absorbance spectra were also measured in the same 1cm quartz cuvette using a Varian Cary 50 Conc UV-Visible Spectrophotometer. Absorbance spectra were used to correct fluorescence data (corrections explained in further detail below).

A fluorescence standard of known composition (5.093 mgC/L, 2.4 µmol Tyr/L and 1.0 µmol Trp/L) was made daily using reagent grade stock solutions of L-tryptophan, L-tyrosine and Luther Marsh organic matter. Luther Marsh is a terrestrial reverse osmosis organic matter isolate. The standard was also measured daily and was used to determine relative component concentrations using PARAFAC (PARAlell FACtor analysis) (Stedman and Bro, 2008).

MATLAB^{TM} was used to create 3D fluorescence emission-excitation matrices (FEEMs) from the fluorescence data. Scattered light was removed from the FEEMs during preprocessing to prevent errors during data analysis. Also using MATLAB, fluorescence data was corrected for inner-filtering using Equation C.1 (Larsson et al., 2007). Equation C.1 was applied to each intensity data point in each sample FEEM and the new corrected matrix was renamed and saved.

$$F = F_o(10^{-b(Aex+Aem)}) \qquad C.1$$

where

F = corrected fluorescence intensity

F_o = fluorescence observed

b = assumed path length

Aex = absorbance at the excitation wavelength

Aem = absorbance at the emission wavelength

In processing of the data using PARAFAC, the system was weighted to three components; one humic-like and two proteinateous components. Spectra from pure tryptophan and tyrosine were used as spectral-shape calibration standards. The relative concentrations of the three components were determined using a linear calibration curve and the resolved component concentrations.

E.2 REFERENCES

Larsson, T., Wedborg, M. and Turner, D. (2007). Correction of inner-filter effect in fluorescence excitation-emission matrix spectrometry using Raman scatter. *Analytica Chimica Acta*, **583**, 357-363.

Stedman, C. A. and Bro, R. (2008). Characterizing dissolved organic matter fluorescence with parallel factor analysis: a tutorial. *Limnol. Oceanogr. Methods*, **6**, 572-579.

Table E.1: Uncorrected and corrected fluorescence fluorophore intensities and relative concentrations. Fluorophores include Humic Substances (HS) in mg C/L, Tyrosine (Tyr) in µmol/L and Tryptophan in µmol/L.

		Fluorophores			(Uncorrected) Concentrations			Corrected Fluorophores			Corrected Concentrations		
		HS	Tyr	Trp	HS	Tyr	Trp	HS	Tyr	Trp	HS (mg C/L)	Tyr (µM)	Trp (µM)
Standard		2.206	3.594	2.230	5.093	2.400	1.000	0.309	0.331	0.523	5.093	2.400	1.000
Sample 1	North Durham Hydrophobic	6.763	0.774	0.893	15.613	0.517	0.401	0.836	0.121	0.070	13.761	0.876	0.134
Sample 2	North Durham Hydrophilic	2.343	0.000	0.042	5.408	0.000	0.019	0.334	0.046	0.087	5.490	0.333	0.166
Sample 3	South Durham Hydrophobic	4.823	0.796	0.887	11.134	0.532	0.398	0.579	0.111	0.069	9.526	0.806	0.132
Sample 4	South Durham Hydrophilic	2.172	0.000	0.032	5.013	0.000	0.014	0.302	0.041	0.080	4.974	0.298	0.153
Standard		2.246	3.635	2.257	5.093	2.400	1.000	0.317	0.331	0.530	5.093	2.400	1.000
Sample 5	Rivanna Hydrophobic	4.778	0.656	0.953	10.832	0.433	0.422	0.584	0.132	0.067	9.379	0.956	0.126
Sample 6	Rivanna Hydrophilic	2.911	0.000	0.135	6.599	0.000	0.060	0.374	0.061	0.074	6.012	0.445	0.139
Sample 7	Nansemond Hydrophobic	5.644	0.989	0.995	12.795	0.653	0.441	0.678	0.131	0.084	10.898	0.948	0.158
Sample 8	Neuse Hydrophobic	6.864	1.428	1.241	15.561	0.942	0.550	0.844	0.1745	0.141	13.563	1.267	0.266
Sample 11	Parkway Hydrophobic	8.024	1.181	1.131	18.193	0.780	0.501	1.009	0.1754	0.124	16.218	1.274	0.233

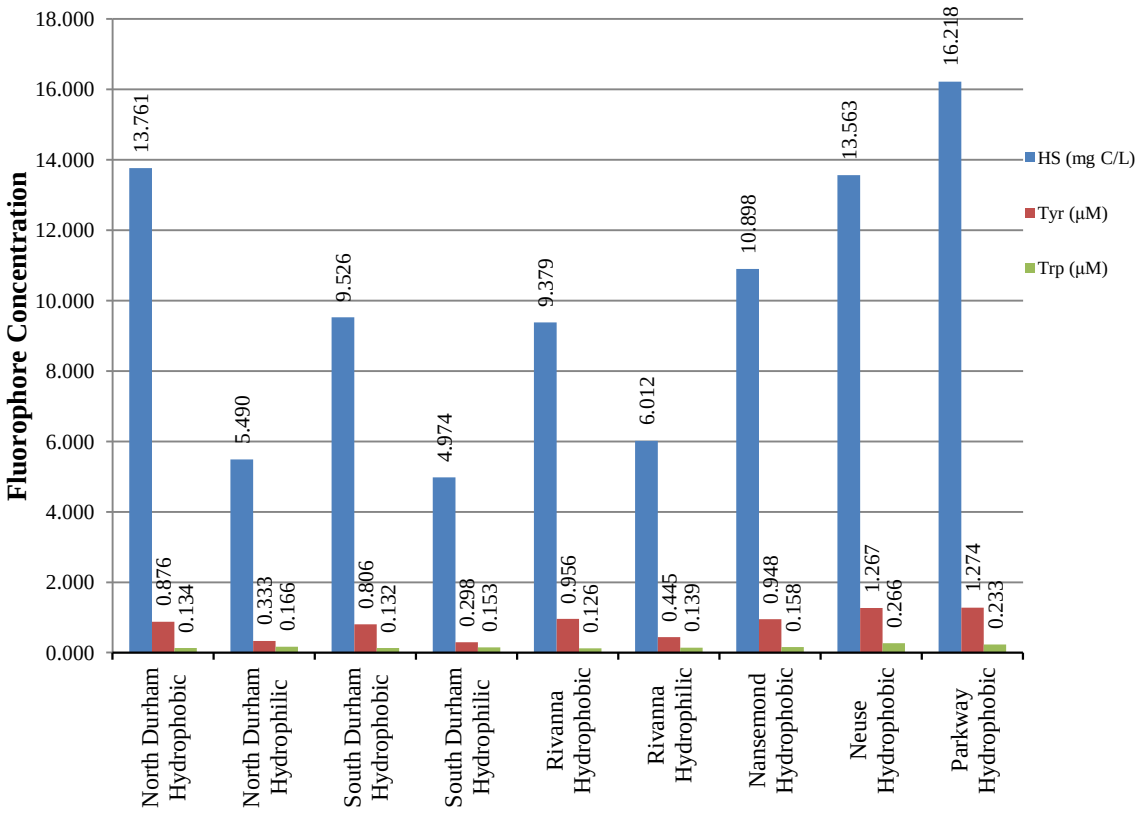

Figure C.1: Relative component concentrations for the three fluorophores. Fluorophores include HS concentration expressed in mg C/L, Tyr and Trp concentrations expressed in µmol/L.

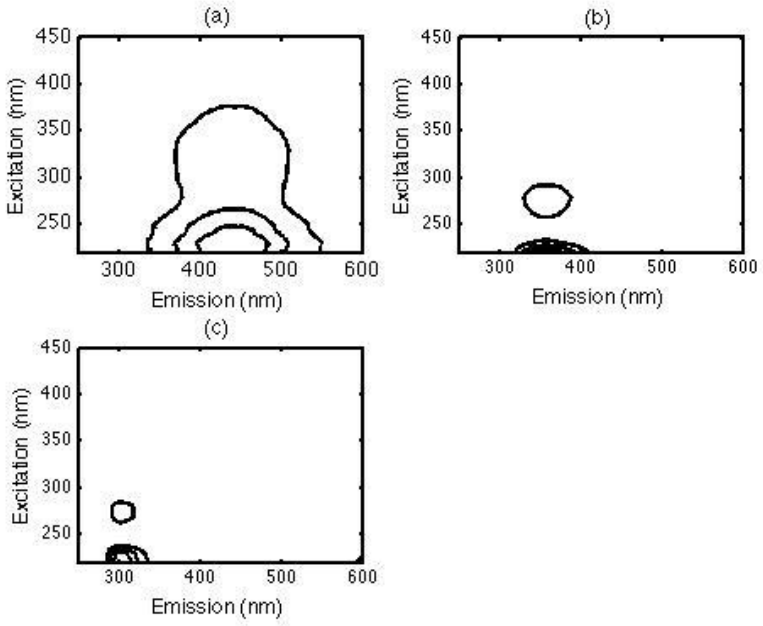

Figure C.2: Resolved spectra of the three components used to describe the fluorescent dissolved organic matter in the samples. Spectra correspond to (a) HS, (b) Trp and (c) Tyr.

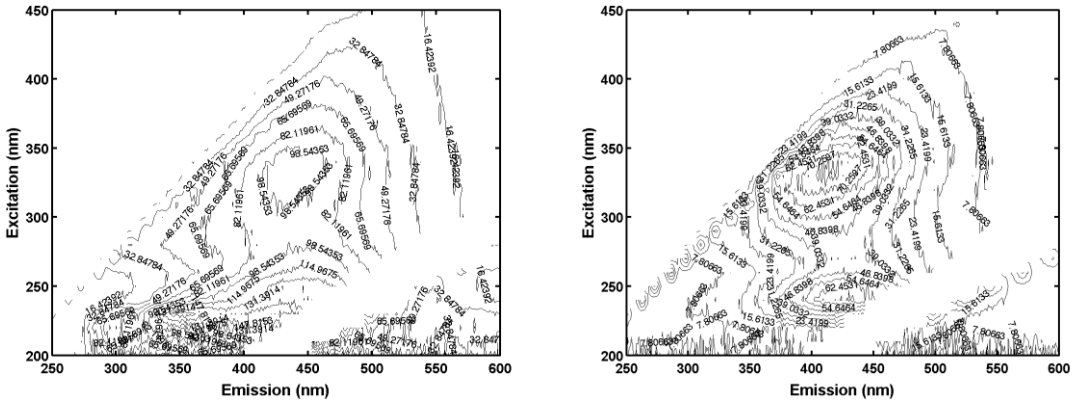

Figure C.3: Example of uncorrected fluorescence excitation-emission contour plots. Sample spectra include South Durham Hydrophobic (left) and South Durham Hydrophilic (right).

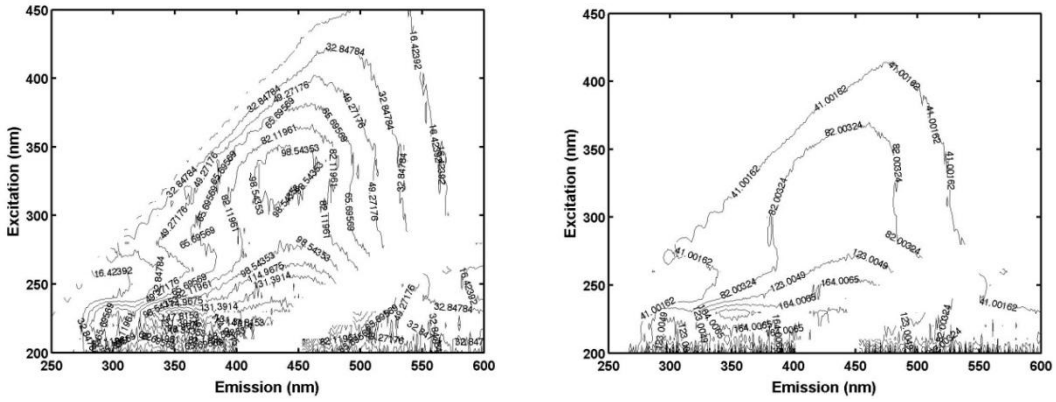

Figure C.4: Sample spectra include uncorrected South Durham Hydrophobic (left) and corrected South Durham Hydrophobic (right).

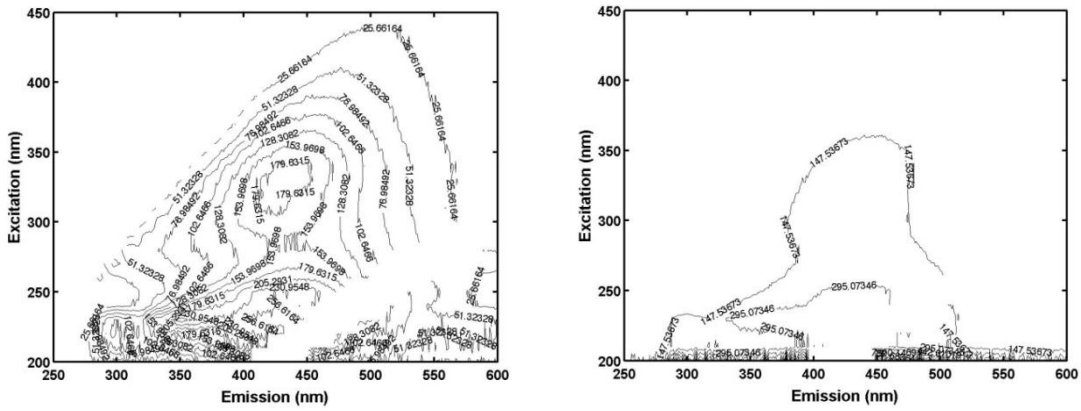

Figure C.5: Sample spectra include uncorrected South Parkway Hydrophobic (left) and corrected South Parkway Hydrophobic (right).

Appendix F: Algal Uptake of Hydrophobic and Hydrophilic Dissolved Organic Nitrogen in Effluent from Biological Nutrient Removal Municipal Wastewater Treatment Systems

The author of this thesis contributed to the following journal article by measuring fluorescence and PARAFAC data analysis on various samples.

Environmental Science & Technology

Article

pubs.acs.org/est

Algal Uptake of Hydrophobic and Hydrophilic Dissolved Organic Nitrogen in Effluent from Biological Nutrient Removal Municipal Wastewater Treatment Systems

Haizhou Liu,[†] Joonseon Jeong,[†,§] Holly Gray,[‡] Scott Smith,[‡] and David L. Sedlak*[,†]

[†]Department of Civil and Environmental Engineering, University of California at Berkeley, Berkeley, California 94720, United States

[‡]Department of Chemistry, Wilfrid Laurier University, 75 University Avenue West Waterloo, Ontario, N2L 3C5 Canada

Supporting Information

ABSTRACT: Dissolved organic nitrogen (DON) accounts for a large fraction of the total nitrogen discharged to surface waters by municipal wastewater treatment plants designed for biological nutrient removal (BNR). Previous research indicates that some but not all of the DON in wastewater effluent is available to bacteria and algae over time scales that are relevant to rivers and estuaries. To separate bioavailable DON from nitrate and less reactive DON species, an XAD-8 resin coupled with an anion exchange treatment was employed prior to chemical analysis and algal bioassays. Analysis of effluent samples from a range of municipal BNR plants (total DON concentrations ranging from 0.7 to 1.8 mg N/L) employing a range of technologies indicated that hydrophilic DON, which typically accounted for approximately 80% of the total DON, stimulated algal growth, whereas hydrophobic DON, which accounted for the remaining DON, remained at nearly constant concentrations and had little or no effect on algal growth during a 14-day incubation period. The hydrophobic DON exhibits characteristics of humic substances, and is likely to persist for long periods in the aquatic environment. The distinct differences between these two classes of DON may provide a basis for considering them separately in water quality models and effluent discharge regulations.

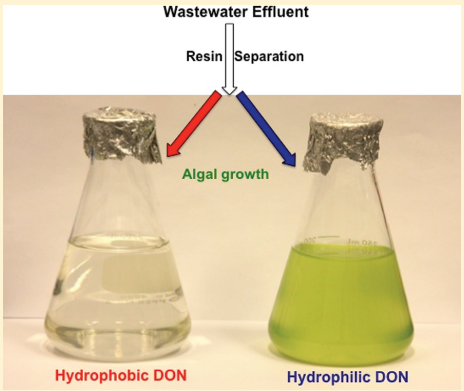

INTRODUCTION

The discharge of municipal wastewater effluent is an important source of anthropogenic nitrogen loading to surface waters, especially in urbanized estuaries and effluent-dominated rivers.[1] To control cultural eutrophication, many utilities have installed biological nutrient removal systems that lower concentrations of inorganic nitrogen species. As a result, the majority of the effluent nitrogen discharged to certain sensitive surface waters consists of dissolved organic nitrogen (DON).[2]

In many locations, regulations and effluent-control strategies target total nitrogen concentrations without differentiating between inorganic and organic forms of nitrogen despite research suggesting differences in the behavior of these two forms of nitrogen.[3] While NO_3^- is readily utilized by heterotrophic bacteria and phytoplankton,[4] the macromolecular forms of DON in wastewater effluent must be transformed before they can stimulate algal growth.[3]

A considerable fraction of effluent DON consists of combined amino acids, soluble microbial products, and other biomolecules.[3,5−7] These macromolecular nitrogen-containing organic compounds are produced during biological wastewater treatment processes, as proteins are metabolized and microbial products are released by bacteria.[8] Humic substances, derived from source water [5,9] and introduced with wastes during biological wastewater treatment,[10,11] account for another form of effluent DON. This form of macromolecular DON tends to be more recalcitrant than DON derived from proteins and soluble microbial products with respect to microbial transformation.[12]

Previous research suggests that the chemical composition of DON affects the bioavailability of DON to bacteria and algae. Compounds derived from proteins and soluble microbial products are bioavailable while humic substances tend to be resistant to biodegradation.[9,13−16] These findings suggest that the DON species in wastewater effluent may behave differently in surface waters, with proteins and soluble microbial products undergoing faster release and biological uptake by bacteria and algae while DON exhibiting humic substance-like properties undergo much slower cycling.[17]

Received: September 2, 2011
Revised: December 1, 2011
Accepted: December 7, 2011
Published: December 29, 2011

Table 1. Wastewater Effluent Samples and Concentrations of Nitrogen Species

wastewater treatment facility	abbreviation	site location	nitrogen species concentration (mg N/L) DON	NO_3^-	NH_4^+	NO_2^-
Truckee Meadows Water Reclamation Facility	TMWRF	Reno, NV	1.01 ± 0.02	n.d.[a]	n.d.[a]	n.d.[a]
HRSD King William Wastewater Treatment Plant	KWWTP	King William, VA	1.01 ± 0.23	0.20 ± 0.02	n.d.[a]	n.d.[a]
Broad Run Water Reclamation Facility	BRWRF	Loudoun County, VA	0.66 ± 0.04	5.83 ± 0.10	n.d.[a]	n.d.[a]
San Jose Wastewater Treatment Plant	SJWTP	San Jose, CA	0.94 ± 0.65	11.18 ± 0.25	0.10 ± 0.01	n.d.[a]
North Durham Water Reclamation Facilities	NDWRF	Durham, NC	1.25 ± 0.01	10.67 ± 0.21	0.27 ± 0.01	n.d.[a]
South Durham Water Reclamation Facilities	SDWRF	Durham, NC	1.17 ± 0.19	8.85 ± 0.14	0.02 ± 0.01	n.d.[a]
RWSA Moores Creek Wastewater Treatment Plant	RVWTP	Charlottesville, VA	1.83 ± 0.18	6.68 ± 0.04	0.98 ± 0.01	0.79 ± 0.1
HRSD Nansemond Wastewater Treatment Plant	NAWTP	Suffolk, VA	1.02 ± 0.10	1.66 ± 0.12	0.15 ± 0.01	n.d.[a]

[a]n.d.= not detected.

To test the hypothesis that DON species in wastewater effluent exhibits different rates of release and algal update, a resin separation method was used to separate DON on the basis of hydrophobicity. Following separation, the effluent DON fractions from eight wastewater treatment plants were characterized and subjected to an algal growth bioassay. Reference materials, controls, and quantitative analyses of nitrogen fate were used to provide a basis for employing this approach to assess the contribution of effluent DON to algal growth in surface waters.

MATERIALS AND METHODS

Sample Collection. Effluent samples were collected from eight municipal wastewater treatment plants equipped with some form of biological nutrient removal (Tables 1 and S1 of the Supporting Information, SI). Composite effluent samples with low suspended solids were collected over a 24-h period after disinfection (either UV or chlorination/dechlorination depending on the site). After collection, samples were placed in 2.5 L polyethylene bottles and shipped overnight in a cooler with ice packs to the lab. Immediately upon receipt, samples were sequentially filtered though 1.0 and 0.22 μm Millipore filters (glass fiber and hydrophilic polyvinylidene fluoride PVDF membrane filters, respectively) to remove suspended solids and residual bacteria. All samples were stored at 3 °C until initiation of resin separation and bioassays, which occurred within 7 days. In addition, two reference samples, Suwannee River humic acid (purchased from International Society of Humic Substances, product no. 2S101H) and glutamic acid (prepared from its salt monosodium glutamate, Sigma-Aldrich Inc.) solutions were evaluated.

Resin Separation Protocol. To separate hydrophobic and hydrophilic DON, wastewater samples were first extracted with Amberite XAD-8 resin (now called Supelite DAX-8 resin, Sigma-Aldrich, Inc.). The resin was chosen because it has long been used as a standard material for the extraction of humic substances.[18] Prior to use, the XAD-8 resin was cleaned following procedures developed previously [18−20] (See SI for details).

To fractionate DON, 5 g of cleaned resin was packed in a borosilicate glass column (1.0 cm diameter, 10 cm length, Thomas Scientific, Swedesboro, NJ). A 400-mL portion of 0.22 μm-filtered wastewater effluent was first acidified to pH 2.0 with concentrated HCl and then pumped through the column at a flow rate of 1 mL/min. Hydrophilic DON passing through the column was collected in a 500 mL glass bottle. The column was then eluted in the reverse direction with 100 mL of 0.1 M NaOH at a flow rate of 1 mL/min to yield hydrophobic DON. Due to the differences in the extraction and elution volumes, the hydrophobic DON was concentrated by a factor of 4 relative to the untreated effluent sample.

To remove nitrate from the sample that had passed through the XAD-8 resin, the sample was reacidified to pH 2.0 and passed through an anion exchange resin (Dowex 1 × 8 chloride form resin, Sigma-Aldrich Inc.). After the ion exchange treatment, the concentration of nitrate in the sample was less than 0.05 mg N/L. Details related to optimization of the ion exchange treatment are included in the SI.

Algal Bioassay. To assess the potential for different DON fractions to stimulate algal growth, the filtered wastewater effluent sample, XAD-8 extract and two fractions of the sample passing through the resin (i.e., before and after ion exchange treatment) were evaluated in an algal bioassay. *Selenastrum capricornutum* (obtained from the center of culture collection of algae at University of Texas Austin) was selected as the test algal species because it has been used as a standard test organism for algal growth studies.[21,22] Details on algal inoculum preparation are included in the SI. Because bacteria often enhance the uptake of DON,[23] a bacterial inoculum was added to the samples. Specifically, a 1-L aliquot of mixed liquor from each treatment facility was filtered through a 1-μm glass fiber filter to remove large particles and then through a 0.2-μm PVDF filter. Particles collected on the 0.2 μm filter were resuspended in 100 mL of 0.2 μm-filtered wastewater effluent as a site-specific bacterial inoculum.

One-hundred milliliter aliquots of each resin extract were transferred to a 250-mL sterilized Erlenmeyer flask, adjusted to pH 7.0 by dropwise addition of 1 M HCl or NaOH solution. The samples were amended with all essential algal nutrients except for NO_3^-.[22] Final concentrations of nutrients are included in SI. Sufficient K_2HPO_4 was added to each sample to yield a N:P molar ratio of 11.[23] To start the bioassay, 1.5 mL of algal inoculum and 1 mL of bacterial inoculum were added to the 100 mL sample. Each bioassay was incubated on a shaker at 25 ± 2 °C using a 12-h light/dark cycle with a growth light source (Xtrasun 1000W 240 V halide lamp, Hydrofarm Inc., Petaluma, CA). Each sample was tested in triplicate, along with a negative control consisting of deionized water and positive controls with reference materials of known hydrophobicity,

specifically, Suwannee River humic acid (SRHA) and glutamic acid. The fate of background DON introduced by inoculation, typically around 0.2 mg N/L, was evaluated with the deionized water control. Algal growth was continuously monitored for 2 weeks with in vivo chlorophyll-a measured by a TD-700 fluorometer (Turner Instruments, Sunnyvale, CA).

Chemical Analysis. Dissolved organic carbon (DOC) was measured using a Shimadzu 5000-A TOC analyzer (Shimadzu Corp., Kyoto, Japan).

The concentration of DON was calculated as the difference between total nitrogen and the sum of inorganic nitrogen species (i.e., NO_3^-, NH_4^+, and NO_2^-). NO_3^- and NO_2^- were measured by ion chromatography (Dionex DX-120) with conductivity detection and a 4 × 250 mm IonPac AS14 anion column with AG14A guard column (Dionex Corp., Sunnyvale, CA). NH_4^+ was measured using the phenate colorimetric method[5] with a Lambda-14 UV spectrophotometer (Perkin-Elmer Inc., Waltham, MA). To measure total nitrogen, samples were oxidized to NO_3^- using persulfate digestion.[24] The NO_3^- concentration in the digested solution was then quantified by ion chromatography. Detection limits for all nitrogen species in effluent samples and resin extracts were below 0.05 mg N/L.

Fluorescence analyses of hydrophobic and hydrophilic fractions were conducted with a Varian Cary Eclipse Fluorescence Spectrometer. The spectrometer was set to scan across excitation wavelengths (220 to 600 nm, 10 nm increments) and emission wavelengths (250 to 600 nm, 1 nm increments). Absorbance spectra were measured using a Varian Cary 50 UV−visible Spectrophotometer to correct fluorescence data.[25] Relative fluorophore concentrations were determined using PARAFAC (PARAlell FACtor) analysis[26] and the absorbance-corrected excitation−emission fluorescence matrices. Additional details on the measurement and data processing techniques are available elsewhere.[27,28]

RESULTS

Characterization of Wastewater Effluent Samples. The concentration and speciation of nitrogen varied among the 8 treatment plants. The total nitrogen concentration ranged from 0.9 to 12.3 mg N/L. The concentration of DON ranged from 0.7 to 1.8 mg N/L. NO_3^- was the predominant inorganic nitrogen species for most of the plants, accounting for over 80% of the inorganic nitrogen (Table 1). The contribution of DON to total nitrogen showed an inverse relationship with total nitrogen concentration (Figure 1). DON was the predominant nitrogen species in samples with total nitrogen concentrations below 2 mg N/L.

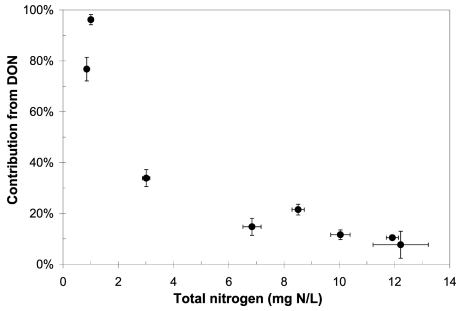

Figure 1. Contribution of dissolved organic nitrogen (DON) to the total nitrogen concentration of wastewater effluent samples.

XAD-8 resin treatment resulted in separation of DON into hydrophobic and hydrophilic fractions. The sum of DON concentrations measured in the two extracts was not different from the DON concentration measured in the untreated, filtered sample (Figure 2A). The same behavior was observed for DOC concentrations (Figure S1 of the SI). These results indicate negligible loss of DON and DOC (3% ± 2%) during XAD-8 resin treatment. The hydrophobic DON accounted for an average of 21% ± 7% of the total DON (Figure 2A). The hydrophobic fraction exhibited a higher C:N ratio than the hydrophilic counterpart (average ratio of 16 ± 3 vs. 6 ±2) (Figure 2B).

Passing the hydrophilic fraction through the ion-exchange resin reduced the concentration of NO_3^- below 0.05 mg N/L. Despite acidification, some DON was retained on the ion-exchange resin. An average of 88% ± 11% of DON and 85% ± 7% of DOC were recovered after passing the hydrophilic extract through the ion-exchange resin (Figure S2 of the SI). The modest loss of DON removal was most likely attributable to interactions of DON with the high surface area of the ion-exchange resin.

DON Bioavailability in Fractionated Samples. To assess DON bioavailability, filtered wastewater effluent samples, hydrophobic and hydrophilic fractions were evaluated in algal bioassay tests. Differences in the behavior of the hydrophobic and hydrophilic fractions were clearly evident in the sample from Truckee Meadows Water Reclamation Facility (TMWRF). The initial hydrophobic DON concentration in the bioassay was four times higher than that detected in the effluent sample because the XAD-8 extraction process concentrated the DON. For the hydrophobic fraction (Figure 3A), the DON concentration decreased by approximately 0.2 mg N/L. This amount was attributable to DON introduced by the algal and bacterial inocula. A similar decrease was observed in the deionized water control (square-solid line in Figure 3A). In both the hydrophobic fraction and the deionized water control, the DON from inoculum resulted in approximately 65 μg/L of chlorophyll-a after 14 days (Figure 3A). After the inoculum DON disappeared, the concentration of DON in the hydrophobic fraction was approximately constant at 0.9 to 1.0 mg N/L (Figure 3A).

In contrast to the hydrophobic fraction, the hydrophilic fraction exhibited a large decrease in DON from 0.8 to 0.3 mg N/L accompanied by an increase in chlorophyll-a to 220 μg/L after 14 days (Figure 3B). The decrease of DON was faster during the first 7 days and chlorophyll-a production was faster during the second 7 days of the bioassay. The untreated sample exhibited a similar trend with respect to chlorophyll-a production, suggesting all of the bioavailable DON was present in the hydrophilic fraction. The slightly higher concentration of DON in the untreated sample was approximately equal to the concentration of hydrophobic DON in the sample.

A similar behavior was observed in bioassays conducted in effluent samples with other concentrations of inorganic nitrogen. For instance, in a sample from King William Wastewater Treatment Plant (KWWTP) where the NO_3^- concentration was approximately 6 mg N/L, the hydrophobic fraction only exhibited 70 μg/L of chlorophyll-a production, which was nearly identical to the deionized water control and the concentration of DON remained approximately constant after the DON from the inoculum disappeared (Figure S3-A of the SI). The hydrophilic fraction in the KWWTP sample, which had been passed through

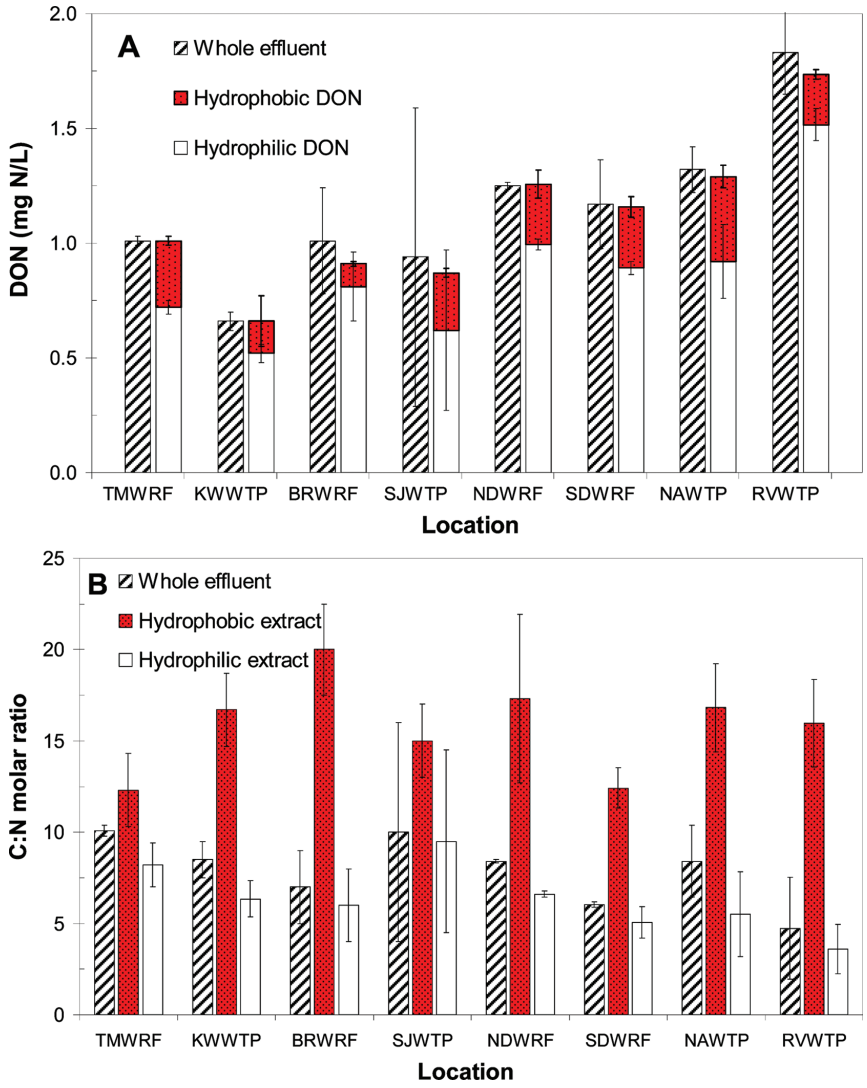

Figure 2. Speciation of DON and carbon-to-nitrogen ratio in wastewater effluent extracts. (A) DON speciation and (B) C:N molar ratio.

the ion-exchange resin, produced 200 μg/L chlorophyll-a and the DON concentration decreased by approximately 0.4 mg N/L (Figure S3-B). Chlorophyll-a production increased to approximately 1200 μg/L in the untreated sample, due to the effect of NO_3^- (Figure S3-B of the SI).

In all eight wastewater effluent samples, the DON concentration in the hydrophilic extracts decreased by 0.4 to 1.0 mg N/L, after subtracting out DON contributed by the bacterial inoculum (Figure 4). This decrease in DON was accompanied by an increase in chlorophyll-a of 120 to 290 μg/L. For the hydrophobic fractions, DON concentration decreased by an average of 0.03 mg N/L during the 14-day incubation after subtracting out the effect of the inoculum (Figure 4).

Controls and Reference Materials. An additional bioassay for each sample was carried out with the hydrophobic fraction amended with NO_3^-. Addition of NO_3^- substantially increased algal growth. For example, the TMWRF hydrophobic fraction amended with 0.7 mg N/L NO_3^- (i.e., a concentration equal to the hydrophilic DON in the effluent) resulted in nearly the same chlorophyll-a production as observed in the hydrophilic fraction (Figure S4 of the SI).

In positive controls with reference materials, nearly all of the SRHA was retained on the XAD-8 resin as expected. This hydrophobic fraction and the untreated SRHA did not promote algal growth, and like the hydrophobic DON in the wastewater effluent, the DON concentration in the extract was not affected by inoculation with algae and bacteria (Figure 5A). In contrast,

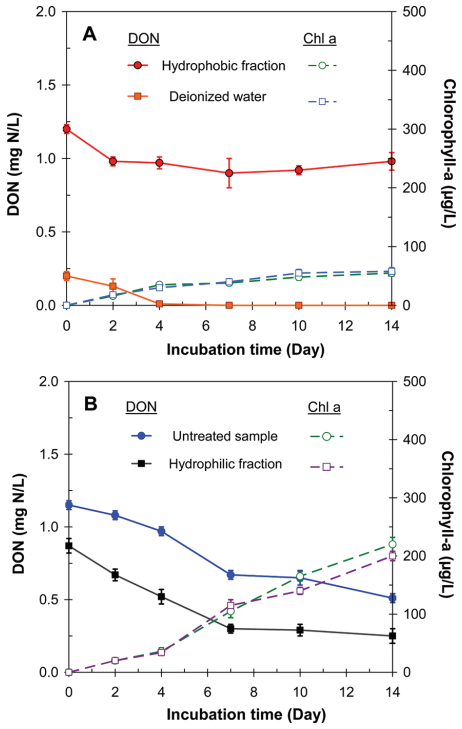

Figure 3. Bioavailability of XAD-8 resin extracts of TMWRF effluent in 14-day algal bioassay experiments: (A) Hydrophobic fraction and negative control with deionized water. The initial hydrophobic DON concentration in the bioassay was 4 times higher than that detected in effluent sample because the XAD-8 resin extraction concentrated the DON; (B) Hydrophilic fraction and the untreated sample.

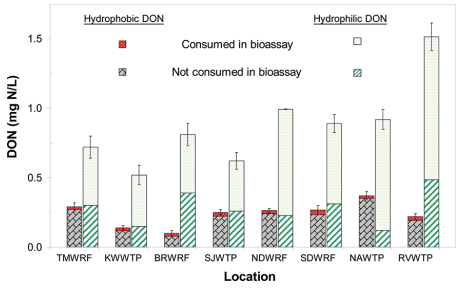

Figure 4. Changes of both hydrophobic and hydrophilic DON from all wastewater effluent samples during algal bioassays.

all of the glutamic acid was recovered in the hydrophilic fraction. Both the hydrophilic DON and the untreated glutamic acid solution were consumed rapidly in the bioassay and produced approximately 400 μg/L chlorophyll-a (Figure 5B).

Fluorescence Characterization. Fluorescence excitation–emission maps were consistent with wastewater samples[28] (Figure S5 of the SI). Peaks corresponding to protenacious materials (i.e., tyrosine and tryptophan-like fluorophores) were observed at emissions wavelength of approximately 300 and 350 nm,

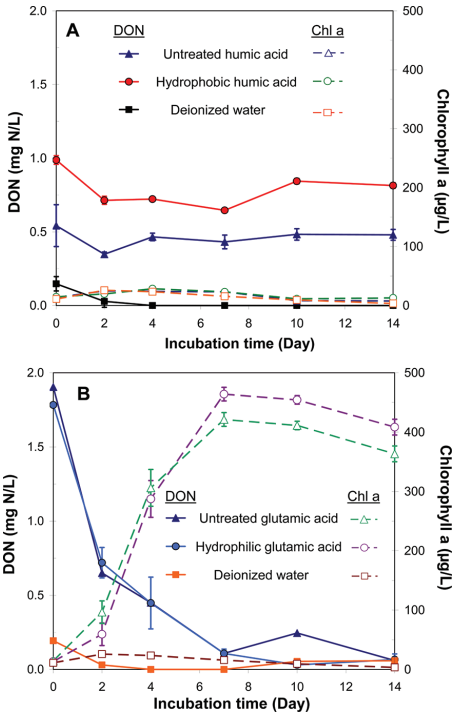

Figure 5. Bioavailability of XAD-8 resin extracts of two reference materials in bioassay experiments. Bacterial inoculum in the bioassay was obtained from RVWTP. (A) Suwannee River humic acid (SRHA). Initial hydrophobic humic acid concentration in the bioassay was concentrated by a factor of 4; (B) Glutamic acid.

respectively, with excitation wavelengths of around 240 and 280 nm. Longer wavelegnth fluorescence (440 nm emission and 240 to 340 nm excitation) corresponding to humic-like fluorophores were also observed. The relative contributions of tyrosine, tryptophan and humic-like fluorophores varied in hydrophobic and hydrophilic fractions, but these three components accounted for over 96% of the total variability of the measured fluorescence according to the PARAFAC analysis (Table S2 of the SI).

DISCUSSION

The inverse relationship between the percentage of nitrogen accounted for by DON and the total nitrogen concentration in wastewater effluents (Figure 1) is consistent with previous observations[2] and highlights the increasing importance that DON will play in point source discharges of nitrogen as more treatment plants install biological nutrient removal systems. As indicated by the absence of a correlation between inorganic nitrogen and DON concentrations, nutrient removal systems that rely on physical processes, such as nanofiltration and activated carbon adsorption, or a combination of different types of biological treatment would be needed to minimize effluent DON.[11] Such treatment methods would have a smaller-than-expected impact on primary productivity if a portion of the effluent DON does not stimulate algal growth.

Data from the resin separation indicate substantial differences between hydrophobic and hydrophilic DON. Hydrophilic

DON stimulated algal growth almost as quickly as glutamic acid with 40% to 85% consumed during the 14-day bioassay whereas hydrophobic DON was unable to stimulate algal growth and remained at nearly constant concentrations during the entire test. The distinct differences between these two classes of DON and the relative simplicity of the resin separation technique may provide a basis for considering these two fractions separately in water quality models.

To assess the merits of this premise, it is appropriate to examine the results from the bioassays conducted on these two fractions. Measurements of chlorophyll-a production in the bioassays conducted with the hydrophobic fraction and the deionized water control were nearly identical (Figures 3A and S3-A of the SI). In contrast, bioassays conducted with the hydrophilic extract after ion exchange treatment always showed substantial chlorophyll-a production (Figures 3B and S3-B of the SI). For the TMWRF sample, which contained a negligible concentration of inorganic nitrogen (Table 1), chlorophyll-a production in the hydrophilic fraction was nearly identical to that observed in the untreated sample, indicating that all of the bioavailable DON was present in the hydrophilic fraction. The hydrophilic fractions for the remaining sites stimulated less algal growth than the untreated samples due to the presence of relatively high concentration of inorganic nitrogen.

During the bioassay of the hydrophobic DON extract, the concentration always decreased by approximately 0.2 mg N/L during the first two days due to the addition of labile DON in the bacterial inoculum. After the initial decrease, the concentration of DON remained nearly constant (Figure 3 and S3). However, in several samples, a small but measurable decrease in the concentration of hydrophobic DON occurred after Day 2 (Figure S3 of the SI). It is possible that a small amount of low molecule weight but bioavailable DON was associated with the hydrophobic DON as is sometimes observed in marine systems.[29,30] Nevertheless, this small decrease in hydrophobic DON does not impact the observation that nearly all of the hydrophobic DON was not bioavailable.

The concentrations of hydrophilic DON decreased by 40% to 85% in different samples during the bioassay (Figures 4 and S6 of the SI). The incomplete removal of DON might due to the release of DON from senescent algal cells at the end of their life cycle, which has been observed in previous studies.[17,23] There could also be slowly released species in the hydrophilic DON that were not completely transformed during the 14-day bioassay. A similar behavior has been observed in the biochemical oxygen demand test[31] and other microcosm studies,[32] where a slowly biodegradable carbonaceous fraction persist for over a week.

In terms of the mass of algae produced per milligram of DON taken up during the algal bioassay, the stoichiometry should be approximately consistent with the Redfield ratio:[33−35]

$$106CO_2 + 16NO_3^- + HPO_4^{2-} + 122H_2O + 18H^+ \rightarrow (C_{106}H_{263}O_{110}N_{16}P)_{algae} + 138O_2 \quad (1)$$

Reaction 1 predicts that each mg of nitrogen incorporated into algal biomass will produce 46 mg of algae. While it was impractical to measure the mass of algae produced during the bioassays, previous research indicates that the chlorophyll-to-carbon ratio in algal biomass typically ranges from 10 to 110 mg chlorophyll/g C.[35,36] Combining these two parameters gives a theoretical value of algal biomass yield in the range of 0.06 to 0.63 g chlorophyll/g N.

Using data from the bioassays to convert chlorophyll to algal biomass gives algal biomass yields with respect to hydrophobic and hydrophilic DON and reference materials (Figure 6). All

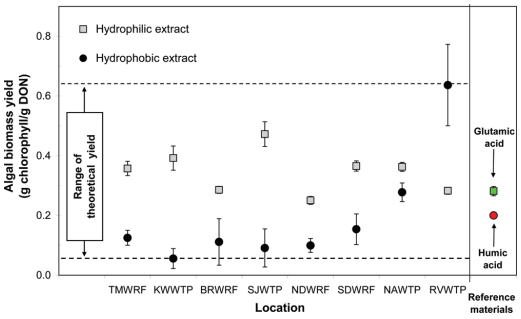

Figure 6. Biomass yields for algae from the hydrophobic and hydrophilic DON fractions in wastewater effluent samples.

experimental data were within the expected range, with the hydrophobic extracts exhibiting lower biomass yields (mean = 0.13 g chlorophyll/g N) than the hydrophilic extracts (mean = 0.36 g chlorophyll/g N). This difference could have been due to competition between bacteria and algae for nitrogen during the bioassays in the hydrophobic extracts. Alternatively, algae could have produced less chlorophyll under nitrogen-limited conditions.

The source of the bacterial inoculum used in the bioassay could have affected the rate and extent of DON release.[3−5] It was a pragmatic decision to only include bacteria collected from the mixed liquor of the wastewater treatment plant, because the large mass and high diversity of the medium made the method more reproducible. Surface water bacteria, especially those in nitrogen-limited systems might be better able to release labile nitrogen from DON.[17,21]

Resin separation, pH adjustment, and elution also could alter the DON or introduce substances that could inhibit algal growth. For example, increases in ionic strength, especially accompanied by increases in the concentrations of Ca^{2+} and Mg^{2+} can inhibit primary production or activity of amino-peptidase enzymes, reducing the rate of hydrolysis of DON and lowering algal growth.[17,37] When the wastewater effluent sample was fractionated using the XAD-8 resin with 0.01 M HCl or 0.1 M NaOH for pH adjustment, the ionic strength of hydrophobic and hydrophilic extracts increased from approximately 0.01 to 0.02 M and 0.1 M, respectively. Additional bioassay controls in which NO_3^- was added to the hydrophobic fraction resulted in nearly the same chlorophyll-a production as the hydrophilic fraction and untreated sample (Figure S4 of the SI), suggesting that the absence of algal growth in the hydrophobic fraction was not a result of toxicity or slower algal growth under higher ionic strength conditions employed in the experiments.

Ion exchange treatment to remove NO_3^- resulted in a loss of 10 ± 5% of the hydrophilic DON (Figure S2 of the SI). However, the behavior of the remaining DON was not affected by ion exchange treatment, as indicated by the slight difference between the untreated and ion exchange treated samples from TMWRF (Figure 3B). Given the simplicity of ion exchange method relative to other approaches for nitrate removal such as dialysis,[38] it is appropriate to use this approach.

Most previous studies on the bioavailability of DON have been focused on marine systems,[5] where DON is often the largest reservoir of fixed nitrogen.[17,29,30] Studies have demonstrated that marine DON includes two pools with distinct bioavailability: a biodegradation-resistant pool mostly made up of high molecular weight compounds with amide functional groups [39,40] and a labile fraction that includes urea, combined amino acids and nucleic acids.[17,41] Like marine DON, wastewater effluent DON has a diverse chemical composition that determines its bioavailability. Wastewater originates from treated drinking water that typically contains 0.05 to 0.2 mg N/L of DON.[38] Additional DON is added with wastes when nitrogen-containing organic compounds are transformed during biological wastewater treatment. Therefore, the chemical composition of wastewater effluent DON is impacted by both the drinking water source and the biological treatment process.[12] DON in drinking water is often derived from terrestrial lignaceous materials with high aromaticity and complex molecular structures.[21,29] This group of compounds typically have a C:N molar ratio ranging from 15 to 30[42] and a concentration of 0.3 to 0.5 mg N/L in source water.[43−45] Water treatment typically removes 20% to 50% of source water DON, yielding approximately 0.1 to 0.2 mg N/L of humic-like DON in treated drinking water.[46] When human activities add nitrogen and organic matter to the treated drinking water as it is used and sent to the wastewater treatment plant, the concentration of hydrophilic and labile DON increase. During biological wastewater treatment, much of the labile materials are converted into inorganic forms.[8,11] In addition, protein-like soluble microbial products are produced by bacteria during the biological treatment processes. These biopolymers and proteinaceous forms of DON typically exhibit a C:N ratio of 3 to 6.[29,43]

Previous research suggests that C:N ratio can act as an indicator for the source of organic matter.[21,29,43−46] Specifically, a high C:N ratio suggests allochthonous humic-like DON and a low C:N ratio is characteristic of proteinaceous DON. Because the complex molecular structure with a high C:N ratio makes it difficult for microbes to extract nitrogen, the humic-like substances tend to be resistant to biodegradation over time scales relevant to most surface waters.[42] Simultaneous measurements of DON and DOC in this study also indicate a consistent pattern of higher C:N ratio in the hydrophobic extract than the hydrophilic extract (Figure 2B), which is consistent with expectations about the bioavailability of the compounds.

Fluorescence spectroscopy confirms these observations about the nature of the DON fractions. The fluorescence ratio of tryptophan to humic substance was higher in the hydrophilic fractions (mean = 0.24) than the hydrophobic fractions (mean = 0.10) (Figure 7) indicating that the low C:N hydrophilic fractions were more proteinaceous than the high C:N hydrophobic fractions. The ranges of the fluorescence ratio of tryptophan to humic substance for marine water of allochthonous and autochthonous origin, are 0.18 to 0.23 and 0.01 to 0.10, respectively.[27]

The resin separation method indicates that municipal wastewater effluent from facilities employing various biological nutrient removal technologies usually contains 0.1 to 0.4 mg N/L in a hydrophobic form (Figure 4) that is not converted into species that are available to algae in two weeks.[2,21,23] The remaining 0.4 to 1.0 mg N/L is available to algae when bacteria are present to facilitate the conversion into low molecular weight forms. At treatment plants where the removal of inorganic nitrogen is incomplete, hydrophobic DON will usually account for a very small fraction of the overall nitrogen loading.

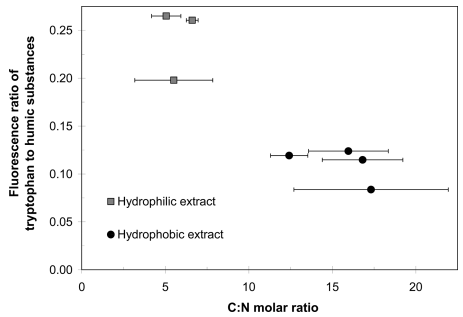

Figure 7. The fluorescence ratio of tryptophan to humic substances versus C:N molar ratio for hydrophobic and hydrophilic extracts of wastewater effluents. The fluorescence ratio was calculated from PARAFAC-resolved fluorescence.

However, at BNR treatment plants with enhanced nitrogen removal, the contribution of hydrophobic DON to the total nitrogen load can be significant.

As water quality criteria for nutrient are becoming more stringent, permits are likely to include requirements for lower concentration of nitrogen species in wastewater effluent. The current regulations typically include limitations on effluent TN levels without differentiating the bioavailability of the DON. If the hydrophobic DON behaves similarly in surface water to the bioassays, it might be appropriate to exclude the hydrophobic DON from effluent TN regulations, particularly if the objective of control is protection of waters immediately downstream of the outfall of the wastewater treatment plant. While a large fraction of effluent DON consists of hydrophilic forms in facilities with different BNR processes (Figure 2), using alternative biological treatment systems such as membrane biological reactors or employing physical removal processes such as reverse osmosis might reduce the concentration of hydrophilic DON.[11]

Like DON, dissolved organic phosphorus (DOP) also could be present in a hydrophobic form. Using previously published N:P ratios,[43] we estimate that humic-associated organic phosphorus could contribute approximately 1 to 4 μg P/L to effluent DOP. For comparison, effluent DOP typically ranges from 3 to 8 μg P/L.[47] DOP can originate from biological-derived phospholipids and terrestrial-associated humic substances.[48] Previous research indicates that DOP associated with humic acids[49] is more difficult to remove during wastewater treatment.[28] Future research will employ the XAD-8 extraction approach to examine the bioavailability of organic phosphorus in hydrophobic and hydrophilic extracts.

■ ASSOCIATED CONTENT

Supporting Information

Additional description of ion-exchange resin separation and bioassay protocol, additional data on optimization of resin separation, and figures showing the bioavailability of DON extracts are provided in the Supporting Information section. This material is available free of charge via the Internet at http://pubs.acs.org.

■ AUTHOR INFORMATION

Corresponding Author

*Phone: (510) 643-0256we; e-mail: sedlak@berkeley.edu.

Present Address

[§]Samsung Advanced Institute of Technology, Mt. 14, Nongseo-Dong, Giheung-Gu, Yongin-Si, Gyeonggi-Do, 446−712, South Korea.

■ ACKNOWLEDGMENTS

This study was supported by the Water Environmental Research Foundation (Project No. 07-013). We thank Yan Nusinovich and Laura Weiden (UC Berkeley) for assisting with algal bioassay tests. We also appreciate inputs from David Stensel (University of Washington) and JB Neethling (HDR Engineering), and the help of Paul Pitt, Christopher White, and Hazen and Sawyer personnel in collecting and shipping wastewater effluent samples.

■ REFERENCES

(1) Howarth, R. W. Human acceleration of the nitrogen cycle: drivers, consequences, and steps towards solutions. *Water Sci. Technol.* **2004**, *49* (5−6), 7−13.

(2) Pagilla, K. R.; Urgun-Demirtas, M.; Ramani, R. Low effluent nutrient technologies for wastewater treatment. *Water Sci. Technol.* **2006**, *53* (3), 165−172.

(3) Pehlivanoglu-Mantas, E.; Sedlak, D. L. Wastewater-derived dissolved organic nitrogen: analytical methods, characterization and effects−A review. *Crit. Rev. in Environ. Sci. Technol.* **2006**, *36* (3), 261−285.

(4) Bronk, D. A. Dynamics of DON. Chapter 5 in *Biogeochemistry of Marine Dissolved Organic Matter*; Academic Press: San Diego. 2002, 153−249.

(5) Pehlivanoglu-Mantas, E.; Sedlak, D. L. Measurement of dissolved organic nitrogen forms in wastewater effluents: concentrations, size distribution and NDMA formation potential. *Water Res.* **2008**, *42* (14), 3890−3898.

(6) Holbrook, R. D.; Love, N. G.; Novak, J. T. Sorption of 17 β-estradiol and 17 α-ethinylestradiol by colloidal organic carbon derived from biological wastewater treatment systems. *Environ. Sci. Technol.* **2004**, *38* (14), 3890−3898.

(7) Dignac, M. F.; Ginestet, P.; Ryback, D.; Bruchet, A.; Urbain, V.; Scribe, P. Fate of wastewater organic pollution during activated sludge treatment: Nature of residual organic matter. *Water Res.* **2000**, *34* (17), 4185−4194.

(8) Westgate, P. J.; Park, C. Evaluation of proteins and organic nitrogen in wastewater treatment effluents. *Environ. Sci. Technol.* **2004**, *38* (14), 3890−3898.

(9) Leenheer, J. A.; Croue, J. P. Characterizing dissolved aquatic organic matter. *Environ. Sci. Technol.* **2003**, *37* (1), 18A−26A.

(10) Holbrook, R. D.; Breidenich, J.; Derose, P. C. Impact of reclaimed water on selected organic matter properties of a receiving stream-fluorescence and perylene sorption behavior. *Environ. Sci. Technol.* **2005**, *39* (17), 6453−6460.

(11) Krasner, S. W.; Westerhoff, P.; Chen, B.; Rittmann, B. E.; Nam, S.; Amy, G. Impact of wastewater treatment processes on organic carbon, organic nitrogen and DBP precursors in effluent organic matter. *Environ. Sci. Technol.* **2009**, *43* (8), 2911−2918.

(12) Drewes, J. E.; Fox, P. Effect of drinking water sources in reclaimed water quality in water reuse systems. *Water Environ. Res.* **2000**, *72* (3), 353−362.

(13) Pace, M. J.; Cole, J. J. Synchronous variation of dissolved organic carbon and color in lakes. *Limnol. Oceanogr.* **2002**, *47* (2), 333−342.

(14) Barker, D. J.; Stuckey, D. C. A review of soluble microbial products (SMP) in wastewater treatment systems. *Water Res.* **1999**, *33* (14), 3063−3082.

(15) Parkin, G. F.; McCarty, P. L. Sources of soluble organic nitrogen in activated sludge treatment. *J. Water Pollut. Control Fed.* **1987**, *53* (1), 89−98.

(16) Parkin, G. F.; McCarty, P. L. Production of soluble organic nitrogen during activated sludge treatment. *J. Water Pollut. Control Fed.* **1987**, *53* (1), 99−112.

(17) Bronk, D. A.; See, J. H.; Killberg, L. DON as a source of bioavailable nitrogen for phytoplankton. *Biogeosciences* **2007**, *4* (3), 283−296.

(18) Eaton, A. D.; Clesceri, L. S.; Greenberg, A. E. Section 5510 C: Aquatic humic substances/XAD method. *Standard Methods for the Examination of Water and Wastewater*, 19th ed.; American Public Health Association: Washington, DC., 1995.

(19) Leenheer, J. A. Comprehensive approach to preparative isolation and fractionation of dissolved organic carbon from natural waters and wastewaters. *Environ. Sci. Technol.* **1981**, *15* (5), 578−587.

(20) Thurman, E. M.; Malcolm, R. L. Preparative isolation of aquatic humic substances. *Environ. Sci. Technol.* **1981**, *15* (4), 463−466.

(21) Urgun-Demirtas, M.; Sattayatewa, C.; Pagilla, K. R. Bioavailability of dissolved organic nitrogen in treated effluents. *Water Environ. Res.* **2008**, *80* (5), 397−406.

(22) United States Environmental Protection Agency. Method 1003.0 in *Short-Term Methods for Estimating the Chronic Toxicity of Effluents and Receiving Waters to Freshwater Organisms*, 4th ed.; U.S. EPA; Washington DC. 2002.

(23) Pehlivanoglu, E.; Sedlak, D. L. Bioavailability of wastewater-derived organic nitrogen to the alga *Selenastrum capricornutum*. *Water Res.* **2004**, *38* (14−15), 3189−3196.

(24) Patton, C. J.; Kryskalla, J. R. Evaluation of alkaline persulfate digestion as an alternative to Kjeldahl digestion for determination of total and dissolved nitrogen and phosphorus in water. Water-Resources Investigations Report 03-4174; U.S. Geological Survey: Denver, CO, 2003.

(25) Larsson, T.; Wedborg, M.; Turner, D. Correction of inner-filter effect in fluorescence excitation-emission matrix spectrometry using Raman scatter. *Anal. Chim. Acta* **2007**, *583* (2), 357−363.

(26) Stedman, C. A.; Bro, R. Characterizing dissolved organic matter fluorescence with parallel factor analysis: a tutorial. *Limnol. Oceanogr.: Methods.* **2008**, *6*, 572−579.

(27) DePalma, S. G. S.; Arnold, W. R.; McGeer, J. C.; Dixon, D. G.; Smith, D. S. Variability in dissolved organic matter fluorescence & reduced sulphur concentration in coastal marine & estuarine environments. *Appl. Geochem.* **2011**, *26* (3), 394−404.

(28) Gray, H.; Gu, A.; Houweling, D.; Smith, D. S. Molecular variability in wastewater organic matter and implications for phosphorus removal across a range of treatment technologies. In *Proceedings of the Nutrient Recovery and Management Conference*; Water Environment Federation, WEF: Miami, FL, 2011; pp 129−149.

(29) Stepanauskas, R.; Edling, H.; Tranvik, L. J. Differential dissolved organic nitrogen availability and bacterial aminopeptidase activity in limnic and marine waters. *Microb. Ecol.* **1999**, *38* (3), 264−272.

(30) Berman, T.; Bronk, D. A. Dissolved organic nitrogen: A dynamic participant in aquatic ecosystems. *Aquat. Microb. Ecol.* **2003**, *31* (3), 279−305.

(31) Tchobanoglous, G.; Burton, F. L.; Stensel, H. D. *Wastewater Engineering, Treatment and Reuse*, 4th ed.; McGraw Hill Inc.: New York, 2002; pp 81−90.

(32) Lim, M. H.; Snyder, S. A.; Sedlak, D. L. Use of biodegradable dissolved organic carbon (BDOC) to assess the potential for transformation of wastewater-derived contaminants in surface waters. *Water Res.* **2008**, *42* (12), 2943−2952.

(33) Redfield, A. C.; Ketchun, B. H.; Rechards, F. A. The influence of organisms on the composition of seawater. in *The Sea*. Wiley-Interscience: New York, 1963; pp 26−77.

(34) Stumm, W.; Morgan, J. J. Aquatic chemistry: Chemical equilibria and rates in natural waters. John Wiley & Sons, Inc.: New York, 1996; pp 886−890.

(35) Chapra, S. C. *Surface Water-Quality Modeling*; Waveland Press, Inc.: Long Grove, IL., 2008; pp 527−528.

(36) Bowie, G. L.; Milles, W. B.; Porcella, D. B.; Campbell, C. L.; Pagenkopf, J. R.; Rupp, G. L.; Johnson, K. M.; Chan, P. W.; Gherini, S.

A.; Chamberlin, C. E. Rates, constants, and kinetic formulations in surface water quality modeling. pp 316.
(37) Keil, R. G.; Kirchman, D. L. Abiotic transformations of labile protein to refractory protein in sea water. *Mar. Chem.* **1994**, *45* (3), 187−196.
(38) Lee, W.; Westerhoff, P. Dissolved organic nitrogen measurement using dialysis pretreatment. *Environ. Sci. Technol.* **2005**, *39* (3), 879−884.
(39) McCarthy, M. D.; Pratum, T.; Hedges, J.; Benner, R. Chemical composition of dissolved organic nitrogen in the ocean. *Nature* **1997**, *390* (6656), 150−154.
(40) Aluwihare, L. I.; Repeta, D. J.; Pantoja, S.; Johnson, C. G. Two chemically distinct pools of organic nitrogen accumulate in the ocean. *Science* **2005**, *308* (5724), 1007−1010.
(41) Bronk, D. A.; Roberts, Q. N.; Sanderson, M. P.; Canuel, E. A.; Hatcher, P. G.; Mesfioul, R.; Filippino, K. C.; Mulholland, M. R.; Love, N. G. Effluent organic nitrogen (EON): Bioavailability and photochemical and salinity-mediated release. *Environ. Sci. Technol.* **2010**, *44* (15), 5830−5835.
(42) Leenheer, J. A.; Dotson, A.; Westerhoff, P. Dissolved organic nitrogen fractionation. *Ann. Environ. Sci.* **2007**, *1* (1), 45−56.
(43) Westerhoff, P.; Marsh, H. Dissolved organic nitrogen in drinking water supplies: a review. *J. Water Supply: Res. Technol.-AQUA.* **2002**, *51* (8), 415−448.
(44) Alberts, J. J.; Takacs, M. Importance of humic substances for carbon and nitrogen transport into southeastern United Sates estuaries. *Org. Geochem.* **1999**, *30* (6), 335−343.
(45) Arheimer, B.; Anderson, L.; Lepisto, A. Variation of nitrogen concentration in forest stream, influences of flow, seasonality and catchment characteristics. *J. Hydrol.* **1996**, *179* (1−4), 281−304.
(46) Lee, W.; Westerhoff, P.; Esparza-soto, M. Occurrence and removal of dissolved organic nitrogen in US water treatment plants. *J. Am. Water Work Assoc.* **2006**, *98* (10), 102−110.
(47) Gu, A. Z.; Liu, L.; Neethling, J. B.; Stensel, H. D.; Murthy, S. Treatability and fate of various phosphorous fractions in different wastewater treatment processes. *Water Sci. Technol.* **2011**, *63* (4), 804−810.
(48) Brookes, P. C.; Powlson, D. S.; Jenkinson, D. S. Phosphorus in the soil microbial biomass. *Soil Biol. Biochem.* **1984**, *16* (2), 169−175.
(49) Reynolds, C. S.; Davies, P. S. Sources and bioavailability of phosphorus fractions in freshwaters: A British perspective. *Biol. Rev.* **2001**, *76* (1), 27−64.